Distributed Distant-Downstream Controller Design for Large-Scale Irrigation Channels

Laven Soltanian

Submitted in partial fulfilment of the requirements of the degree of

Doctor of Philosophy
(with coursework component)

December 2014

Department of Electrical and Electronic Engineering
THE UNIVERSITY OF MELBOURNE

Produced on archival quality paper.

Abstract

IRRIGATION networks of open-water channels are widely used to distribute water for agricultural purposes under the power of gravity alone. These channels are of low efficiency when operated manually in open-loop under a supply-based logic. Water sustainability concerns, arising from food security and climate change issues, translate into the need to improve the operation of irrigation channel networks. Modernisation projects around the world are leading to the installation of a sensor, actuator, and communications infrastructure that can facilitate automatic control. So-called distant-downstream controllers lead to demand-driven release of water from upstream storage. The spatial stability properties of such automatic control schemes is the focus of this thesis.

Within a network, each open-water channel is divided into sections called pools, which are linked by gates that locally set the flow. Automatic control involves the use of on-line measurements to dynamically determine the setting for operational variables. The automation objectives for each pool are to provide (i) steady-state matching between water in-flow and out-flow including the local offtakes to farms or secondary channels and the downstream flow load and (ii) tight regulation of the water-level at the downstream end of pools, which corresponds to the capacity to supply flow at the off-take points and downstream. Therefore, water-level regulation is an important aspect of large-scale irrigation network automation.

Distributed distant-downstream feedback control structures can yield operational benefits and scope for the development of scalable controller design procedures. Under this control architecture, propagation of water-level and flow transients are confined to the upstream direction, which is desirable in that it corresponds to demand-driven water release from primary sources, while achieving the aforementioned local objectives for step changes in water-level references and off-take loads. For the distributed distant-downstream controllers available in the literature, transient

flow peaks are amplified as they propagate when the channel is a homogeneous cascade of pool dynamics. In view of the limited authority of the control gates, which saturate in terms of the flow delivered when in the fully open or fully closed position, the spatial propagation of transients under such feedback control structures is of interest.

A scalable approach to achieve string-stability (spatially stable transient propagation) under distributed distant-downstream control is proposed. The approach is underpinned by a new controller architecture, inspired by headway scheme in vehicle platoons, and it accommodates heterogenous pool dynamics. In particular, focusing on the flow interactions between pools, the new scheme involves the augmentation of each decentralised local feedback with a feedforward path from the downstream flow to the controller input. This translates to adjustment of the local water-level reference on the basis of downstream flow. The feedforward compensation is designed to satisfy a decentralised condition on the flow-to-flow interaction, which ensures non-amplification of flow peaks as these propagate. The improvement in spatial stability comes at the expense of steady-state error in the water-level for a step change in flow demand. The robustness of the string-stability property to model parameter uncertainty is of practical concern and this is investigated via LMI based analysis conditions. While the application of these sufficient conditions does not confirm robustness of the string-stability property, the bounds obtained for a benchmark channel show that the degree to which the robustness property is violated remains mild in the face of substantial uncertainty.

Finally, motivated by the two-dimensional nature of the dynamics of channels under distributed distant-downstream control, a 2-D Roesser model is introduced for automated irrigation channels. The model reflects the directed information flow in both temporal and spatial dimensions and it applies within the context of heterogenous channel and local control dynamics. Lyapunov function based analysis of the 2-D Roesser model ultimately yields decentralised string-stability certificates that are weaker than the non-amplification condition applied in the approach described above. Collectively, these certificates imply uniformly bounded flow interactions between the locally controlled pool dynamics without uniformly requiring non-amplification of transient peaks. Various illustrative simulation examples are discussed throughout the thesis.

Declaration

This is to certify that

1. the thesis comprises only my original work towards the PhD except where indicated in the Preface,
2. due acknowledgement has been made in the text to all other material used,
3. the thesis is less than 100,000 words in length, exclusive of tables, maps, bibliographies and appendices.

Laven Soltanian, December 2014

This page intentionally left blank.

Preface

Unless otherwise stated below, the material presented in this thesis, submitted for the degree of Doctor of Philosophy, is a result of collaboration between my supervisors and myself during my postgraduate study undertaken at the University of Melbourne, Australia.

The following is a list of publication done during the course of research.

1. L. Soltanian, A.R, Neshastehriz, and M. Cantoni, "Validating an approach to distributed controller synthesis for irrigation channels via simulation with a PDE model", in *Proceedings of the Australian Control Conference, Melbourne, Australia*, 2011, [1].

2. L. Soltanian and M. Cantoni, "A 2-D Roesser model for automated irrigation channels and tools for practical stability and performance analysis", in *Proceedings of the Australian Control Conference, Sydney, Australia*, 2012, [2].

3. L. Soltanian and M. Cantoni, "Achieving string stability in irrigation channels under distributed distant-downstream control", in *Proceedings of the IEEE Conference on Decision and Control, Florence, Italy,* 2013, [3].

4. L. Soltanian and M. Cantoni, " Robustness analysis of a nominally string-stable irrigation channel control system", *in the 21st International Symposium on Mathematical Theory of Networks and Systems, Gronigen, Netherlands*, 2014, [4].

This page intentionally left blank.

Acknowledgements

My Ph.D. journey has been rewarding and challenging at the same time. I have gained much more than what has been reflected in my thesis or papers. I would like to express my special appreciation and thanks, first and foremost, to my supervisor Professor Michael Cantoni who has provided me with guidance and insight each step of the way. I wish to thank my committee members A/Professor Erik Weyer and A/Professor Peter Dower for their support during my studies.

I would like to take this time to thank Rubicon Water for supporting my research financially and providing us with data and a field trip.

I am grateful to A/Professor Margreta Kuijper for giving me the opportunity to experience lab demonstration. I would also like to thank Nasrin Hashemi for her advice and being there for me when I needed to talk to someone. A very big thank goes to Dr. Nadia Bedjaoui for her kindness, true friendship, and also being a passionate mentor.

My thanks goes to my office mates Senaka, Merid, Arash, Michelle, Mohmmad, Omid, Adel, Shabnam, Saeed, Roghieh, Keith, Lu who have been a source of happiness, and good friends both in and out of the office. Also, the office would have not been fun without our cheerful visitors Alessandro and Luca who completely transformed the ambiance of our office and elevated our spirits. I am also grateful to my friends Atefeh, Azara, Parisa, Toktam, Pouya, and Nasim for their understanding and making my life exceptionally enjoyable.

I am ever thankful and indebted to my parents whom I greatly admire. They have supported and loved me unconditionally. Thanks to my lovely sister who is a great joy of my life even when I was and am far from home. My PhD would not have been possible without my loving husband Amir. Thank you for your continued and unfailing affection.

This page intentionally left blank.

To my love Amir, my caring parents, and lovely sister.

This page intentionally left blank.

Contents

List of Figures

List of Tables

This page intentionally left blank.

Chapter 1
Introduction

An introduction to irrigation channels as water distribution networks along with the motivation for their automation is presented. Different control structures and the merits of so-called distant-downstream controllers are reviewed in this chapter. Moreover, different aspects of distant-downstream controller design including spatial propagation of transients and scalability of design procedure are considered. This thesis is focused on the development of a new so-called distributed distant-downstream control architecture and scalable design procedures for achieving spatially stable behaviour of an automated irrigation channel. An outline of the thesis is also provided here.

1.1 Sustainable Water Distribution For Irrigation

Water is a source of life. It is used for municipal, agricultural, and industrial purposes, where irrigated agriculture's share is about 70% [5, 6]. Irrigation networks have low efficiency when operated manually and only around 60% of the amount of water dedicated to irrigation is used consumptively [5, 6]. Although 20% of the world's cultivated land is irrigated, this portion accounts for 40% of global crop production [5, 7]. The growing need for food worldwide and higher water consumption due to population growth translates to an increase in water demand globally [7, 8]. Thus, improving the operation of the irrigation channel networks used to distribute fresh water for agriculture is important from a sustainability point of view [7, 8].

Irrigation networks of open water channels, natural or man-made, are utilised to distribute water from reservoirs such as lakes, to supply points, mainly onto farms. Flume gates are installed along the channel that can locally impose flow, see Figure 1.1. A channel's bedding has a slope, from reservoirs towards the consumers, facilitating gravity-powered water transportation without

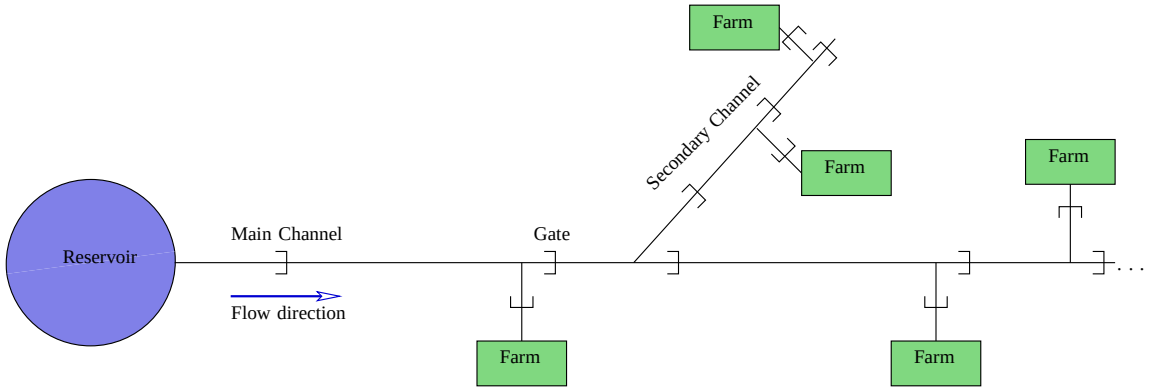

Figure 1.1: Structure of a typical irrigation network

utilising any other source of energy. Thus, water-levels along the channel reflect the capacity to supply flow to farms and further downstream [7, 9, 10].

A channel comprises an interconnection of pools which are separated by the flume gates. The gates controlling water flow into (out of) a pool are considered as upstream (downstream) gates of the pool. The side-view of a pool is illustrated in Figure 1.2. Pools are indexed from downstream towards upstream, with the bottom and top pools indexed by 0, and N, respectively. Let h_i and h_{i-1} (m) denote the head of water over upstream and downstream gates of pool i, respectively, y_i (m) the downstream water-level of the pool measured from the Datum, and d_i offtake load at downstream end of pool i.

The operation of channels requires command over the water-level along the channel. In gravity-powered networks, offtake points for the supply of water to farms or secondary channels are located at the downstream end of pools, where the water-level reflects the capacity to supply flow. Therefore, command over the downstream water-level of each pool is an important objective. Command of the water-level must be achieved in a way that leads to steady-state matching of flow supply to the demand. Automation of irrigation channels, as part of modernising irrigation networks, aims at achieving the aforementioned operational objectives of the channels by translating them to standard automatic control problems that can be expressed in terms of water-level regulation and flow load disturbance rejection.

In this chapter, common existing models for irrigation channels and the one more suitable for identification and control synthesis purposes are introduced. Different control mechanisms to

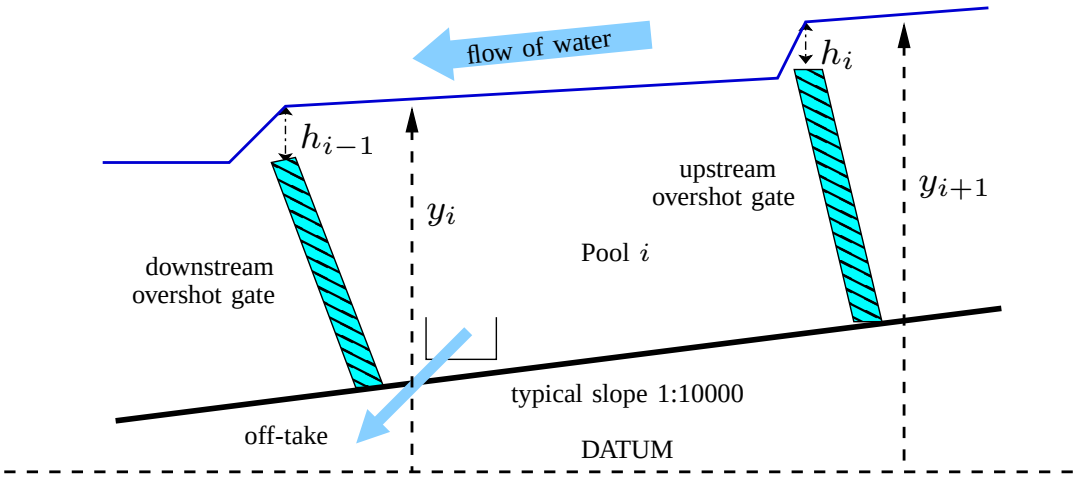

Figure 1.2: A typical pool with over-shot gates. Off-takes are usually drawn from downstream end (to the left).

achieve control objectives for an irrigation channel are discussed. Various possible control structures and design approaches for distant-downstream feedback control which leads to demand-driven release of water from primary sources are considered. Spatial behaviour of the transient flows and scalability of design which are both practically important are evaluated for an automated channel running under such controllers. Spatial instability properties of the existing control structures motivates the introduction of a new distributed distant-downstream control architecture which can, by contrast, be exploited to achieve spatially stable propagation of transients flow peaks as pursued in this thesis.

1.2 Modeling Irrigation Channels

1.2.1 Saint-Venant Equations

A model which is conventionally used to describe an open water channel dynamics is the so-called Saint-Venant equations based model [11, 12]. For a pool, let $A(x,t)$ with units m^2 denote the wetted surface, defined to be the portion of the channel cross-section occupied with water at position x and time t. Furthermore, let $Q(x,t)$ denote the corresponding flow rate or discharge in m^3/s. With gravitational acceleration, the bottom width, the per unit length longitudinal bottom

slope and friction slope, denoted respectively by g, B, S_0 and

$$S_f = \frac{n^2 Q^2}{A^2 R^{4/3}}, \tag{1.1}$$

where n is Manning's constant and R is the hydraulic radius (ratio of wetted surface to wetted perimeter), the dynamics of a pool modeled using the Saint-Venant equations is given by

$$\frac{\partial A}{\partial t} + \frac{\partial Q}{\partial x} = 0 \tag{1.2}$$

$$\frac{\partial Q}{\partial t} + (\frac{gA}{B} - \frac{Q^2}{A^2})\frac{\partial A}{\partial x} + 2\frac{Q}{A}\frac{\partial Q}{\partial x} + gA(S_f - S_0) = 0, \tag{1.3}$$

for $t \geq 0$ and $x \in [0, L]$, where L is the length of the pool and $x = 0$ is the upstream end, subject to the boundary conditions

$$Q(L,t) = Q_L(t), \qquad Q(0,t) = Q_0(t),$$
$$Q(x,0) = \bar{Q}, \qquad A(x,0) = \bar{A}(x),$$

where $Q_L(t)$ and $Q_0(t)$ are the flows over the downstream and upstream gates with units m^3/sec, respectively, $\bar{Q} = Q_L(0) = Q_0(0)$ is an initial *equilibrium* flow and $\bar{A}(x)$ is the corresponding initial *equilibrium* wetted surface, which satisfies

$$\frac{d\bar{A}}{dx} = \frac{g\bar{A}(\bar{S}_f - S_0)}{g\frac{\bar{A}}{B} - \frac{\bar{Q}^2}{\bar{A}^2}},$$

with boundary condition $\bar{A}(L) = \tilde{A}$, where $\tilde{A}$ is the initial downstream wetted area and $\bar{S}_f$ denotes the friction slope as defined in (1.1) with $Q = \bar{Q}$ and $A = \bar{A}$.

Equation (1.2) represents mass balance, the so-called continuity equation, and equation (1.3) conservation of momentum in a given pool. This model captures the dynamics of a large-scale open water channel [13] and accounts for the water-level along the entire length via the wetted cross-section variable. There are other variations of Saint-Venant equations; see e.g. [14]. Irrespective of the model form, to simulate such dynamics a suitable temporal and spatial discretisation is required. There are different methods for approximately solving the St-Venant equations, e.g. an implicit finite difference scheme known as the Preissmann scheme which proves to be

consistent, convergent and stable [15].

However, due to complexity of these equations, it is not a suitable model for the purpose of system identification and closed-loop analysis and design [16, 17]. Rational approximation of the linearized Saint-Venant equations are proposed in Chapter 4 of [7]. In addition, based on physical properties of a pool, a grey box first or third order model are introduced [16]. The third order model captures both mass balance and wave dynamics oscillatory behaviour. However, the simpler first order integrator-delay model which does not captur wave dynamics can be used for control purposes as long as proper care is taken into account for high frequency uncertainties.

1.2.2 Integrator-Delay Model

The nonlinear model based on the Saint-Venant equations is not useful for analysis and controller synthesis purposes. Other simpler models such as linearised version of this nonlinear PDE model are used to represent the dynamical characteristics of channels [7, 18]. Also, a simpler model derived based on physical properties of a channel, including mass balance and water transportation delay, which is tractable and suitable for identification, control analysis and design purposes is used in [16, 19, 20]. It is a grey box first order integrator-delay model used to represent a pool's dynamics [16]. Although such a model may not capture all of the dynamics such as waves at high frequencies, the use of feedback control can yield robustness to modeling errors, provided the nature of such mismatches are properly taken into account in the design process. With reference to the side-view of a pool shown in Figure 1.2 where pools are enumerated from downstream to upstream, note that

- $h_{i-1}(m)$ is a function of y_i and the position of the upstream gate of pool i
- the flow over the upstream gate of pool i is proportional to $h_i^{\frac{3}{2}}$, i.e. $u_i = \gamma_i h_i^{\frac{3}{2}} (\mathrm{m}^3/\mathrm{min})$.

This integrator-delay model that captures mass balance along a pool results from approximating the volume of water towards the downstream end of a pool by a constant times the downstream water-level [16, 19, 20]. The model is given by

$$\dot{y}_i(t) = \frac{1}{\alpha_i}[\gamma_i h_i^{\frac{3}{2}}(t-\tau_i) - \gamma_{i-1}(h_{i-1}^{\frac{3}{2}}(t) + d_{h,i}(t))], \tag{1.4}$$

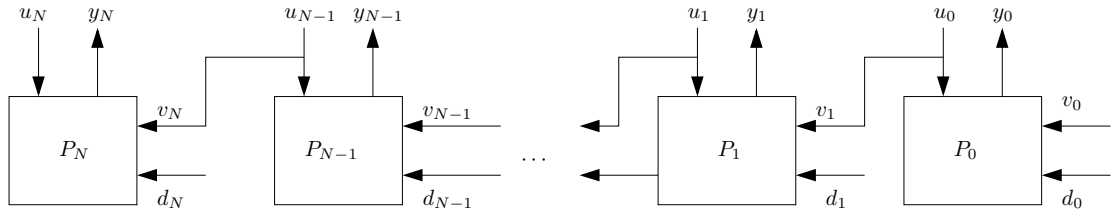

Figure 1.3: Irrigation channel modeled by string of pools

where τ_i (min) accounts for the delay associated with the transport of water from the upstream end to the downstream end of the pool, α_i is a measure of pool surface area and $d_{h,i}$ ($\mathrm{m}^{3/2}$/min) models water offtake in pool i due to load disturbance onto farms or into secondary channels. Define the parameters $c_{\text{in},i} := \frac{\gamma_i}{\alpha_i}$ and $c_{\text{out},i} := \frac{\gamma_{i-1}}{\alpha_i}$ ($\mathrm{m}^{-1/2}/\mathrm{min}$). Then model (1.4) becomes

$$\dot{y}_i(t) = c_{\text{in},i} h_i^{\frac{3}{2}}(t-\tau_i) - c_{\text{out},i}(h_{i-1}^{\frac{3}{2}}(t) + d_{h,i}(t)). \tag{1.5}$$

Parameters $c_{\text{in},i}$, $c_{\text{out},i}$, τ_i, and α_i can be obtained via system identification techniques using data generated from field test or simulations of the Saint-Venant PDE model [13, 16]. Linearising (1.4) and (1.5) via the change of variables $u_i = \gamma_i h_i^{\frac{3}{2}}$ ($\mathrm{m}^3/\mathrm{min}$), $v_i = \gamma_{i-1} h_{i-1}^{\frac{3}{2}}$($\mathrm{m}^3/\mathrm{min}$), $d_i = \gamma_{i-1} d_{h,i}(t)$($\mathrm{m}^3/\mathrm{min}$), $u_{h,i} = h_i^{\frac{3}{2}}$ ($\mathrm{m}^{3/2}$), and $v_{h,i} = h_{i-1}^{\frac{3}{2}}$ ($\mathrm{m}^{3/2}$) leads to integrator-delay models

$$\dot{y}_i(t) = \frac{1}{\alpha_i}[u_i(t-\tau_i) - (v_i(t) + d_i(t))], \tag{1.6}$$

and

$$\dot{y}_i(t) = c_{\text{in},i} u_{h,i}(t-\tau_i) - c_{\text{out},i}(v_{h,i}(t) + d_{h,i}(t)), \tag{1.7}$$

for pool i, respectively. Note that models (1.6) and (1.7) are interchangeable by a change of variable.

The model for a channel is then obtained by interconnecting integrator-delay models via $v_i(t) = u_{i-1}(t)$ or $v_{h,i}(t) = u_{h,i-1}(t)$, see Figure 1.3 . Taking the Laplace transform of (1.6) assuming $y(0) = 0$, yields

$$Y_i(s) = \frac{1}{\alpha_i s}[U_i(s)e^{-\tau_i s} - (U_{i-1}(s) + D_i(s))], \tag{1.8}$$

which is used later for controller design purposes. This simple integrator-delay model is used for both analysis and synthesis purposes throughout this thesis.

1.3 Irrigation Channel Automation

Traditionally, the channels are operated manually [7, 10]. In this case, water distribution involves manual adjustment of the gates [17]. In particular, water-levels are maintained to ensure sufficient flow rates at offtakes [10]. Manual distribution of water in the channels, may lead to water losses mainly due to oversupply, which can result in spillage along the channels and also irrecoverable outflow at the end of the channels [21]. Modernisation of irrigation channels, such as those of Goulburn-Murray Irrigation District, Australia, Canal de Provence in Sourthern France, or Central Arizona Project, USA, can be exploited to achieve improved operation of irrigation channels and water distribution management in the networks [7, 22], via a shift from manual to automatic control, as underpinned by advancement in sensor and actuator technology. The large scale and networked nature of irrigation automation calls for the layered application of model based and optimisation based techniques in a hierarchy of control as seen in the operation of other complex infrastructures, [23, 24]. Automatic control typically involves the use of on-line measurements to dynamically determine the settings for operational variable via the use of feedback. This can provide robustness to modeling uncertainties that inevitably arise in the design process or unknown demand, by contrast with open-loop approaches that try to set flow on the basis of demand forecast. At the same time, the performance achievable with feedback alone, a purely reactive approach, can be limited and conservative. Recall that, in gravity-powered networks, the water-level at downstream end of each pool reflects the capacity to supply flow from that point, either off-channel or further downstream. As such, the control of these water-levels across the network is operationally important in terms of meeting demand. The water-levels of the pools in a channel are mainly determined by the flows over the gates along the channel. The local control objectives in each pool are the following:

- matching water in-flow and out-flow including the local offtakes to farms or secondary channels and the downstream flow load in steady-state; and
- tight regulation of the water-level at the downstream end of pools.

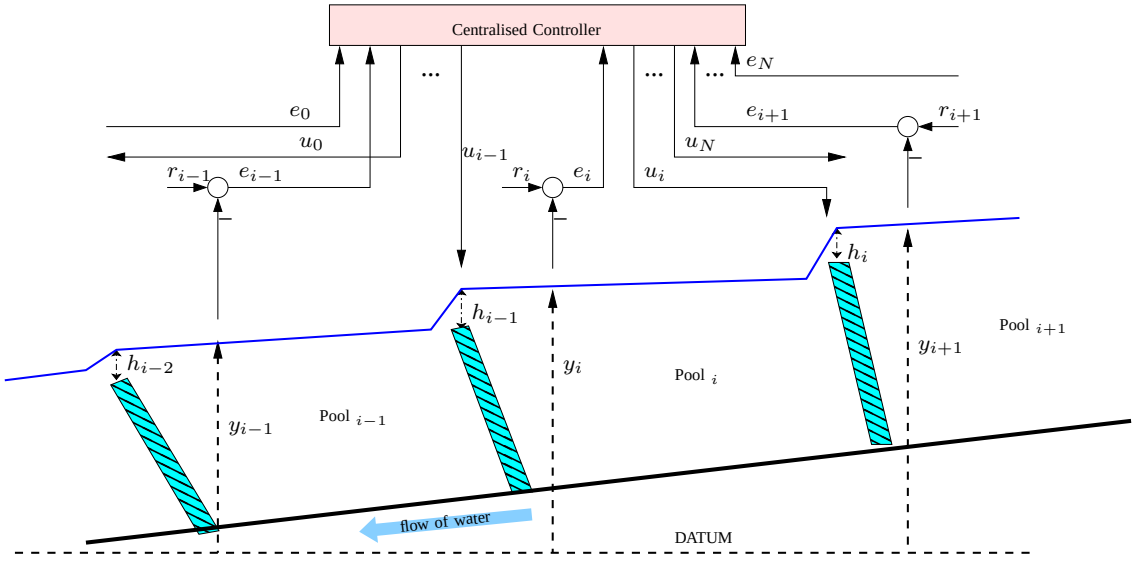

Figure 1.4: Centralised control scheme of an irrigation channel.

These can be achieved with different control architectures such as the ones described in the sequel.

1.3.1 Centralised Feedback Control

A centralised multi-input multi-output (MIMO) feedback control is a mechanism for achieving the aforementioned control objectives. A centralised controller for a channel of N pools is shown in Figure 1.4. With this structure, all gates positions can be utilised in order to regulate a measured water-level error received as input of the controller [25,26], and to satisfy local control objectives. Simulations of a channel running under a centralised controller can be found in [25, 27]. As can be seen, in the absence of any structure for the controller, a centralised controller results in bidirectional propagation of transients, i.e. an offtake drawn from a pool can affect all the pools along the channel. Note that downstream propagation of transients relies on downstream storage, which is always limited, to the extent that excess water may need to be spilled at the end in an irrecoverable fashion. However, effect of an offtake drawn from one pool is smaller in the other pools, see [27, page 53]. Moreover, the communication burden increases with the number of pools and this may lead to delays in information transmission for large number of pools [25,28].

There are different possible control strategies to synthesise a centralised controller, for instance linear quadratic (LQ) control is used in [26,28–31] for controller design. H_∞ loop-shaping control

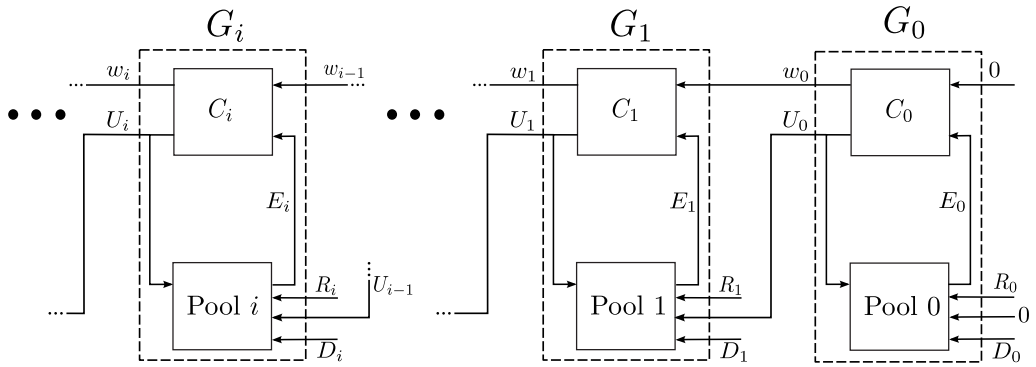

Figure 1.5: An irrigation channel running under distributed distant-downstream control modeled as a cascade.

scheme is also used to design a centralised controller for open water channels, [25, 32]. The centralised controller design procedure can involve selecting the weights used in LQ cost functions or local loop-shaping weights in the H_∞ scheme on a pool by pool basis using each pool's information alone. Synthesis of such centralised controllers involves the solution of a channel-wide optimisation problem. This stage is not scalable and has to be repeated if an update is necessary due to local changes of dynamics or operating regime of a pool for instance.

1.3.2 Distant-Downstream Feedback Control

In order to reduce water wastage at the end of the channel, the so-called distant-downstream control strategy, as considered in [21] can be used, whereby the gates positioned upstream relative to flow load are manipulated on the basis of water-level measurements. This is in contrast with so-called upstream control, where water-levels are regulated via immediate downstream gate, [7, 10, 18]. In this case, the overall water wastage increases since such control structure relies on downstream storage, which is limited [33]. The distant-downstream feedback control is the special case of a centralised controller with triangular structure for the multi input-multi output transfer function. This way the propagation of flow transients are confined to the upstream direction, which is desirable in view of the demand-driven water release from primary sources. Communication burden can still be large with such control architecture, as for the pools close to the downstream end of the channel, data has to be communicated to all upstream pools. Moreover, design of a general distant-downstream controller can involve using all pools information. This is undesirable

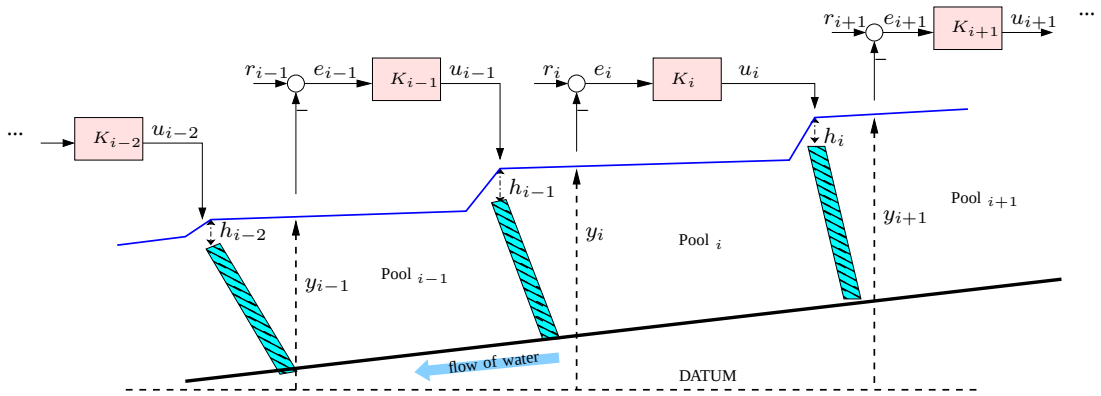

Figure 1.6: Decentralised control scheme of an irrigation channel.

since all components of the controller may have to change due to a change in dynamics or operational conditions of a small section of the channel when optimal control approaches to synthesis is taken. Therefore, a more structured distant-downstream feedback controller that provides scope for scalable synthesis can be useful. One instance of such structured distant-downstream control can be distributed distant-downstream control where only neighboring pools communicate information, reducing the communication overhead. A channel running under this control architecture can have a cascade structure as in Figure 1.5.

1.3.3 Decentralised Distant-Downstream Control

Decentralised distant-downstream control as a special case of distributed distant-downstream control, as shown in Figure 1.6, involves the use of local controller K_i in setting the upstream flow to regulate downstream water-level of pool i to the corresponding reference level, [20, 21].

An approach to the design of decentralised distant-downstream controller is based on each component of the structured controller achieving local control objectives with the spatial interactions, treated as unknown disturbances. In [20,21] local controllers are chosen to be a PI controller and an additional roll-off is introduced to guarantee low gain at wave frequencies. A tuning method of the PI controllers for irrigation channels based on frequency domain techniques such as gain and phase margin analysis are proposed in [34] and [7, chapter 7]. In the latter, H_∞ loop-shaping design is used to tune local controllers. Quantitative feedback control theory (QFT) is utilised in [35] to design decentralised PID controller for irrigation channels.

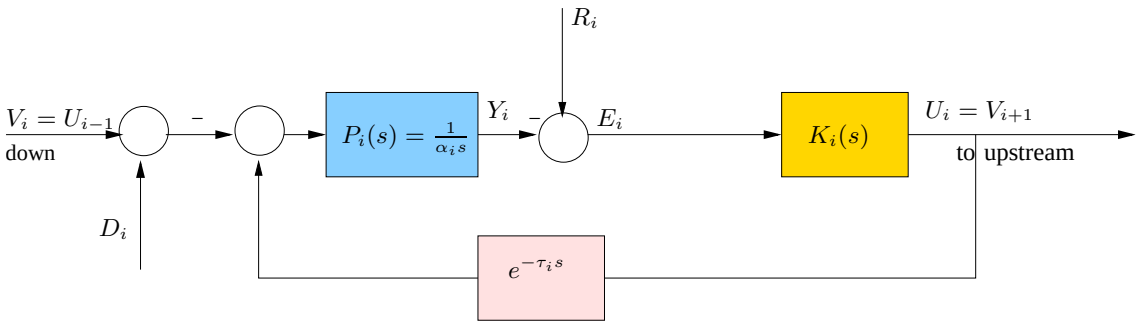

Figure 1.7: Block diagram of a local control loop

A local control block diagram of a purely decentralised control scheme of the structure shown in Figure 1.6 is illustrated in Figure 1.7, where pool model (1.8) is used. Accordingly, the transfer functions associated with the local control objectives are as follows:

$$\begin{aligned} T_{R_i \to E_i}(s) &= \frac{1}{1 + L_i(s)e^{-\tau_i s}}, \\ T_{D_i \to E_i}(s) &= \frac{P_i(s)}{1 + L_i(s)e^{-\tau_i s}}, \\ T_{U_{i-1} \to U_i}(s) &= \frac{L_i(s)}{1 + L_i(s)e^{-\tau s}}, \end{aligned} \tag{1.9}$$

where $L_i(s) = K_i(s)P_i(s)$. Lets consider each control objective separately.

1)*Steady-state flow matching*. It is required that in steady-state the flow of water entering a pool equals the flows leaving the pool. Therefore, $T_{U_{i-1} \to U_i}(0) = 1$ is needed.

2)*Water level tracking*. Usually $r_i(t)$ is a piecewise constant signal. Assuming closed-loop stability and applying the Final Value Theorem [36], for a constant reference input, yield the following expression for the steady-state water-level error:

$$\lim_{t \to \infty} e_i(t) = \lim_{s \to 0} sE_i(s) = \lim_{s \to 0} sT_{R_i \to E_i}(s)\frac{1}{s} = \lim_{s \to 0} \frac{1}{1 + L_i(s)e^{-\tau_i s}},$$

which equals zero provided that the open-loop transfer function $L_i(s)$ contains at least one integrator. Given that $P_i(s)$ contains an integrator and $K_i(0) \neq 0$ to maintain internal stability by avoiding unstable pole zero cancelation between plant and controller [37], water-level regulation

is achieved.

3) *Output disturbance rejection*. Since knowledge of the offtake or downstream flow information is not utilised in design, it is considered as an unknown disturbance to be rejected by control action. Assuming closed-loop stability and applying the Final Value Theorem to $e_i(t)$ in response to a constant disturbance, we get

$$\lim_{t\to\infty} e_i(t) = \lim_{s\to 0} sE_i(s) = \lim_{s\to 0} sT_{D_i\to E_i}(s)\frac{1}{s} = \lim_{s\to 0} \frac{1}{1+L_i(s)}\frac{1}{\alpha_i s}.$$

Hence, at least 2 integrators in $L_i(s)$, i.e. one in $K_i(s)$, are needed to achieve zero steady-state water-level error, i.e. $\lim_{t\to\infty} e_i(t) = 0$.

4) *Stability of the closed-loop*. The two integrators of $L_i(s)$ contribute -180° across all frequencies. Therefore, a phase lead is required, $(1+\phi_i s)$, in the controller to add phase around cross-over frequency, i.e. $\omega_{c,i}$ such that $|L_i(j\omega_{c,i})| = 1$, [21, 27].

5) *Preventing wave dynamics excitation*. In order not to excite wave dynamics which are not accounted for in the pool's integrator-delay model, the loop gain, i.e. $|L_i(j\omega)|$, must be very small around the frequencies of the pool waves. Hence, a low pass filter $\frac{1}{1+\rho_i s}$ is added to the controller.

6) *Accounting for the effect of the delay*. Due to the fact that the delay component $e^{-\tau_i s}$ contributes a phase of $-\tau_i\omega$, cross-over frequency $\omega_{c,i} < \frac{1}{\tau_i}$ is needed for robust stability and ensuring a phase margin of more than 35° [27].

A scalable approach to the design of the decentralised distant-downstream controller is to take $K_i(s) = \frac{\kappa_i(1+\phi_i s)}{s(1+\rho_i s)}$ for the local controllers [20, 21]. But doing this does not directly account for the interaction between the locally controlled pools, which can lead to poor transient propagation characteristics as discussed below. Note that for good water-level regulation and load disturbance rejection large local loop-gain $|L_i(j\omega)|$ is needed at frequencies where $R_i(s)$ and $D_i(s)$ are significant, i.e. low frequencies, see [38, Section 5.5]. For more details of local control loop design refer to [27].

Figure 1.8 shows simulation of an automated irrigation channel of 5 identical pools with specifications as in Table 1.1 operating under decentralised distant-downstream control. It is assumed that an off-take of $17\text{m}^3/\text{min}$ is taken from the most downstream pool of the channel for 1000mins. From the simulations, it can be seen that flow of all the pools equal the offtake flow at steady-state and water-level errors tend to zero at steady-state. However, it can be seen that there is amplifica-

Table 1.1: Pool model and controller parameters

Pool number	Pool Model Parameters		Controller Parameters		
	time-delay τ (mins)	α (m^2)	κ	ρ	ϕ
0,1,2,3,4	16	43806	7.72	15.2	128

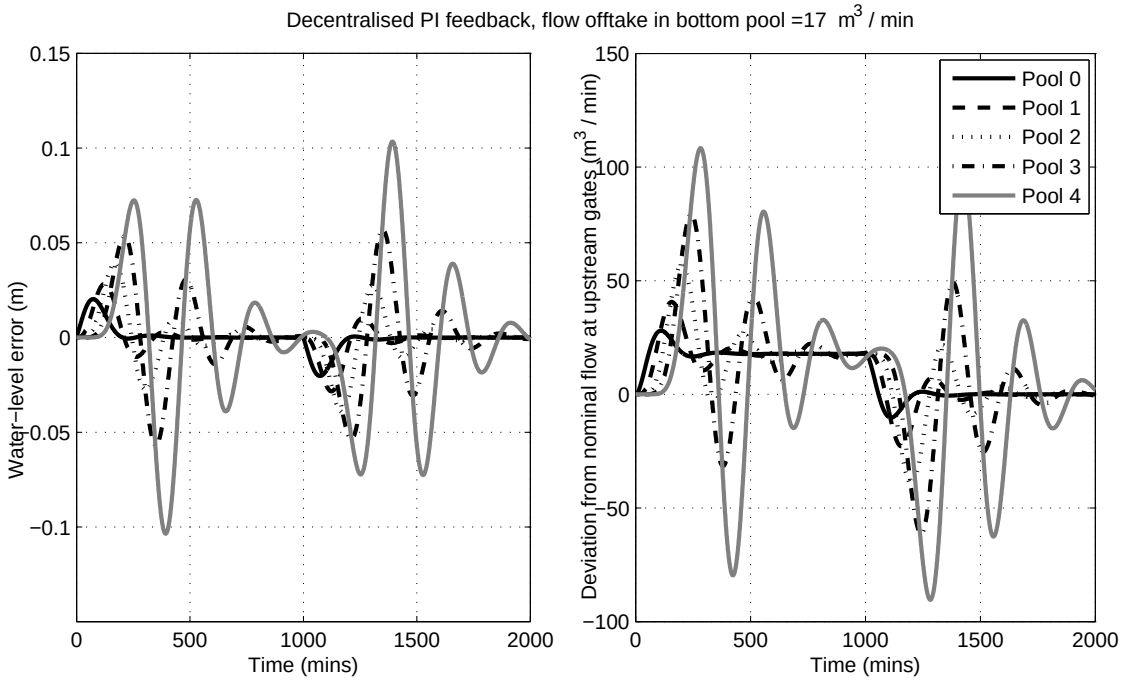

Figure 1.8: Simulations of a channel with decentralised controller.

tion of the transient flow and water-level error peaks as they propagate upstream. This effect can bring the gates to saturation and cause flooding.

The inevitable flow amplification property of the automated channel with the control structure under consideration is shown as follows:

Theorem 1.1. *Let $K_i(s)$ be any proper rational transfer function such that $K_i(s)$ has a pole at $s = 0$ and the local closed-loop system of Figure 1.7 is internally stable. Then the transfer function corresponding to flow propagation, $T_{U_{i-1}\to U_i}(s)$, satisfies*

$$\int_0^\infty \ln |T_{U_{i-1}\to U_i}(j\omega)| \frac{d\omega}{\omega^2} \geq 0.$$

Thus, there exists an $\hat{\omega} \in [0,\infty)$ such that $|T_{U_{i-1}\to U_i}(j\hat{\omega})| > 1$.

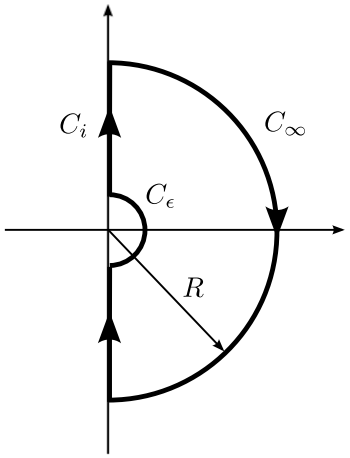

Figure 1.9: Nyquist contour

Proof. The proof follows in the same line of argument as [21,27,39] applied within the context of a homogenous channel to establish a similar result for $T_{E_i \to E_{i+1}}$ which equals $T_{U_{i-1} \to U_i}$ in this case.

Due to $|e^{-j\tau_i\omega}| = 1$,

$$|T_{U_{i-1}\to U_i}(j\omega)| = \Big|\frac{L_i(j\omega)}{1+L_i(j\omega)e^{-j\tau_i\omega}}\Big| = \Big|\frac{L_i(j\omega)e^{-j\tau_i\omega}}{1+L_i(j\omega)e^{-j\tau_i\omega}}\Big|, \tag{1.10}$$

for all $\omega \in \mathbb{R}$. Define

$$Q(s) := \frac{1}{s^2}\ln\Big(\frac{L_i(s)e^{-\tau_i s}}{1+L_i(s)e^{-\tau_i s}}\Big).$$

Applying the Cauchy's Theorem to integral of $Q(s)$ along the Nyquist contour shown in Figure 1.9 , it follows that

$$\oint_C Q(s)ds = 0 = \int_{C_i} Q(s)ds + \int_{C_\varepsilon} Q(s)ds + \int_{C_\infty} Q(s)ds, \tag{1.11}$$

where C_i is the imaginary axis excluding the part due to identation C_ε. The last two terms on the right hand side of (1.11) are evaluated separately:

Dividing the numerator and denominator of the term inside ln in $Q(s)$ by $L_i(s)e^{-\tau_i s}$, and noting

that $L_i(s)$ contains two integrators, we have

$$\begin{aligned}
\int_{C_\varepsilon} Q(s)ds &= \int_{C_\varepsilon} \ln\Big(\frac{1}{1+L_i^{-1}(s)e^{\tau_i s}}\Big)\frac{1}{(s-0)^{1+1}}ds \\
&= \lim_{z\to 0} -2\pi j \frac{d}{dz}(\ln(1+L_i^{-1}(z)e^{\tau_i z}))(\text{ by the Residue Theorem}) \\
&= -2\pi j \lim_{z\to 0} \frac{\frac{d}{dz}(1+L_i^{-1}(z)e^{\tau_i z})}{(1+L_i^{-1}(z)e^{\tau_i z})} \\
&= -2\pi j \lim_{z\to 0} \frac{\frac{dL_i^{-1}(z)}{dz}e^{\tau_i z}+\tau_i L_i^{-1}(z)e^{\tau_i z}}{1+L_i^{-1}(z)e^{\tau_i z}} \\
&= -2\pi j \lim_{z\to 0} \frac{\frac{L_i^{-1}(z)-L_i^{-1}(0)}{z}e^{\tau_i z}}{1+L_i^{-1}(z)e^{\tau_i z}} \\
&= -2\pi j \lim_{z\to 0} \frac{L_i^{-1}e^{\tau_i z}}{z(1+L_i^{-1}(z)e^{\tau_i z})} \\
&= -2\pi j \lim_{z\to 0} \frac{1}{zL_i(z)} \\
&= 0.
\end{aligned}$$

Moreover,

$$\int_{C_\infty} Q(s)ds = \int_{C_\infty} \frac{\ln(L_i(s)e^{-\tau_i s}) - \ln(1+L_i(s)e^{-\tau_i s})}{s^2}ds,$$

whereby $s = Re^{j\theta}$, it follows that

$$\int_{C_\infty} Q(s)ds = j\lim_{R\to\infty}\int_{\frac{\pi}{2}}^{-\frac{\pi}{2}} \frac{\ln(L_i(Re^{j\theta})) - \tau_i Re^{j\theta} - \ln(1+L_i(Re^{j\theta})e^{-R\tau_i e^{j\theta}})}{Re^{j\theta}}d\theta. \tag{1.12}$$

Due to the two integrators in $L_i(s)$, when $R\to\infty$, $L_i(Re^{j\theta})$ can be approximated by $\frac{c}{(Re^{j\theta})^2}$, where c is a constant. Hence, each term of the right hand side of (1.12) can be calculated as follows:

- $j\lim_{R\to\infty}\int_{\frac{\pi}{2}}^{-\frac{\pi}{2}} \frac{\ln(L_i(Re^{j\theta}))}{Re^{j\theta}}d\theta = 0.$

- $j\lim_{R\to\infty}\int_{\frac{\pi}{2}}^{-\frac{\pi}{2}} \frac{-\tau_i Re^{j\theta}}{Re^{j\theta}}d\theta = j\pi\tau_i.$

- Using the fact that $\lim_{|x|\to 0} \ln(1+x) = x$, we get

$$\begin{aligned} & j \lim_{R\to\infty} \int_{\frac{\pi}{2}}^{-\frac{\pi}{2}} \frac{-\ln(1+L_i(Re^{j\theta})e^{-R\tau_i e^{j\theta}})}{Re^{j\theta}} d\theta \\ =& j \lim_{R\to\infty} \int_{\frac{\pi}{2}}^{-\frac{\pi}{2}} \frac{-L_i(Re^{j\theta})e^{-R\tau_i e^{j\theta}}}{Re^{j\theta}} d\theta \\ =& 0 \end{aligned}$$

Therefore, $\int_{C_\infty} Q(s)ds = j\pi\tau_i$.

Then, it follows from (1.11) that $\int_{C_i} Q(s)ds = -j\pi\tau_i$, which yields

$$\int_0^\infty \ln\Big|\frac{L_i(j\omega)e^{-j\tau_i\omega}}{1+L_i(j\omega)e^{-j\tau_i\omega}}\Big|\frac{d\omega}{\omega^2} = \int_0^\infty \ln|T_{U_{i-1}\to U_i}(j\omega)|\frac{d\omega}{\omega^2} = \frac{\pi\tau_i}{2} \geq 0. \tag{1.13}$$

Since with this choice of the controller, $L_i(s)$ is strictly proper,

$$\ln|T_{U_{i-1}\to U_i}(j\omega)| < 0$$

at high frequencies. Hence, from (1.13), there exists an $\hat{\omega}$ such that $|T_{U_{i-1}\to U_i}(j\hat{\omega})| > 1$ as claimed.

□

The Theorem proves amplification of flow peaks along a channel since $|T_{U_{i-1}\to U_i}(j\omega)| > 1$ corresponds to amplification of a component of the transient response to a change in operating conditions, as it propagates towards upstream [39, 40]. Note that if $|T_{U_{i-1}\to U_i}(j\omega)|$ are identical for all pools, the maximum amplification of the flow peaks will be observed. The same effect is appearing in the analysis of vehicle platoons [40–42] for predecessor following and bidirectional control schemes where two integrators are required in the control loop to achieve zero steady-state relative positioning errors of the vehicles in response to disturbance. Avoiding such behaviour of an automated channel is the focus of this thesis.

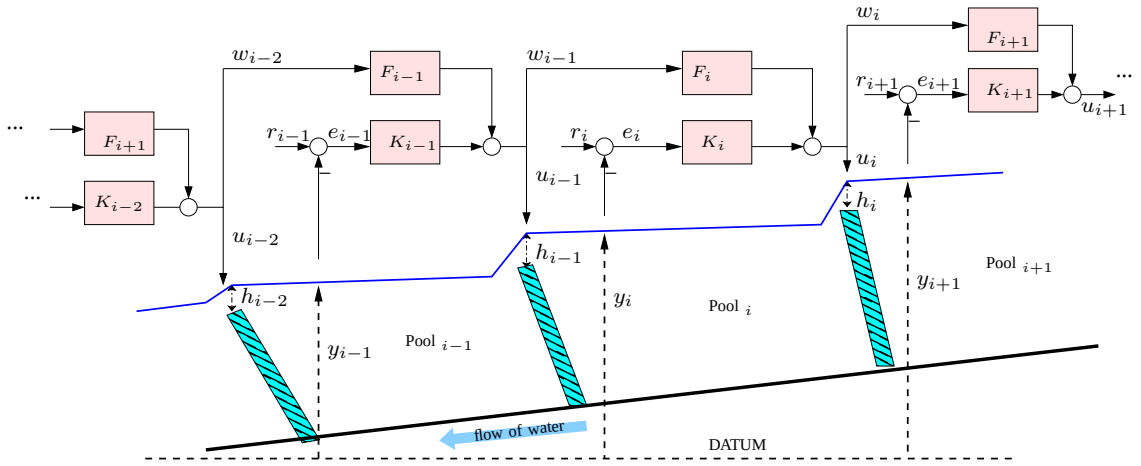

Figure 1.10: Decentralised feedback with flow to flow feedforward control scheme of a channel.

1.3.4 Decentralised Feedback With Flow-to-Flow Feedforward Distant-Downstream Control

The offtake and flow over the downstream gate was considered as an unknown disturbance in the design approach chosen for decentralised feedback distant-downstream control. Motivated by the information available from downstream flow load, the decentralised feedback with flow-to-flow feedforward distant-downstream control structure as in Figure 1.10 has been made available to adjust the flow into a pool accordingly. Indeed, the feedforaward path adds an extra degree of freedom to deal with the spatial propagation of the flow peaks towards upstream of the channel [21]. One approach to design such controller is to design the local feedback controllers as described above, followed by the selection of a simple stable transfer function for $F_i(s)$. An instance of such control structure is [43], where the feedforward path is considered to equal the unity instead of noncausal inverse of the pure delay to decouple the effect of downstream flow.

Figure 1.11 shows simulations of the channel of Table 1.1 with the feedforward path chosen to be $F(s) = 0.7$. As can be seen, local control objectives including steady-state flow matching and water-level regulation are satisfied and spatial propagation of transients performance has improved compared to purely decentralised distant-downstream control. However, there is propagation of flow peaks towards upstream of the channel.

The feedforward path, $F_i(s)$, cannot be used to decouple the effect of downstream flow, since it will have to contain the non-causal inverse of the delay component. In addition, it is not possible

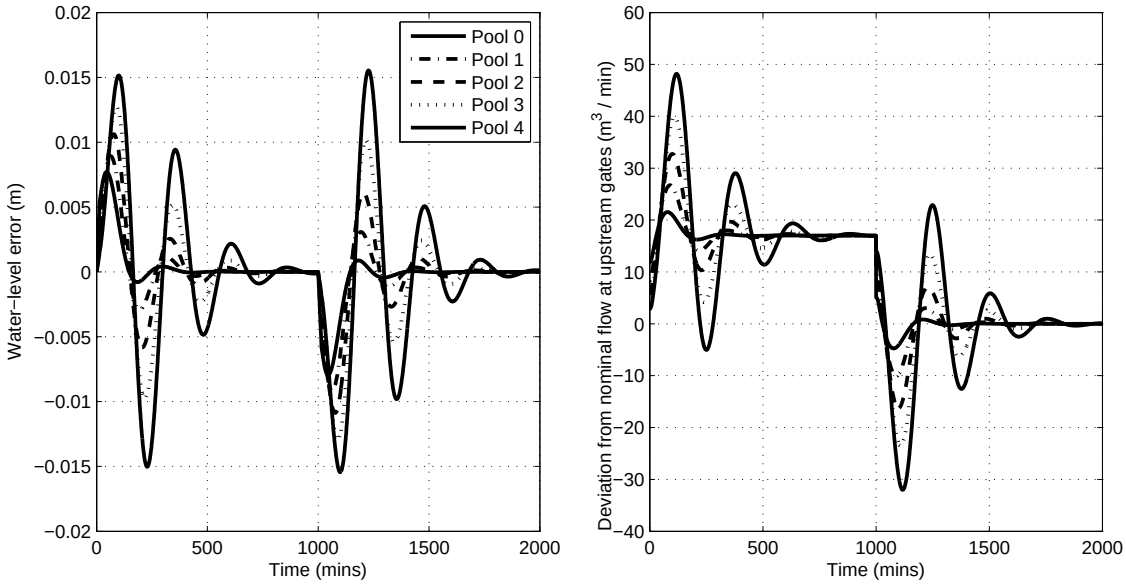

Figure 1.11: Simulations of a channel with decentralised feedback and constant flow-to-flow feedforward, $F_i(s) = 0.7$.

to arbitrarily set $F_i(s)$ to enforce $T_{U_{i-1}\to U_i}(s)$ to be a specific transfer function that prevents amplification of flow peaks along the channel. To see this, following a similar procedure to [27, 39] the inevitable amplification of flow peaks can be proved:

Theorem 1.2. *Let $K_i(s)$ be any proper rational transfer function such that $K_i(s)$ has a pole at $s = 0$ and the local closed-loop system of Figure 1.10 is internally stable. Then, there exists an $\hat{\omega} \in [0, \infty)$ such that the transfer function corresponding to flow propagation satisfies $|T_{U_{i-1}\to U_i}(j\hat{\omega})| > 1$.*

Proof. Note that $T_{U_{i-1}\to U_i}$ is a stable transfer function and so by definition it will be analytic in a sufficiently small open ball centred at $s = 0$. That is to say that $T_i(s)$ is differentiable and the Taylor series is convergent in the vicinity of $s = 0$. Moreover, with the two integrators in $L_i(s)$, it can be proved that $\frac{dT_{U_{i-1}\to U_i}}{dj\omega}(0) = \tau_i$, see [27]. Taylor expansion of $T_{U_{i-1}\to U_i}(s = j\hat{\omega})$ for small $\hat{\omega} > 0$ gives

$$T_{U_{i-1}\to U_i}(j\hat{\omega}) = T_{U_{i-1}\to U_i}(0) + (j\hat{\omega} - 0)\frac{dT_{U_{i-1}\to U_i}}{dj\omega}(0) + R(j\hat{\omega}),$$

where the remainder can be made small for a suitable choice of $\hat{\omega}$. Due to $T_{U_{i-1}\to U_i}(0) = 1$ and

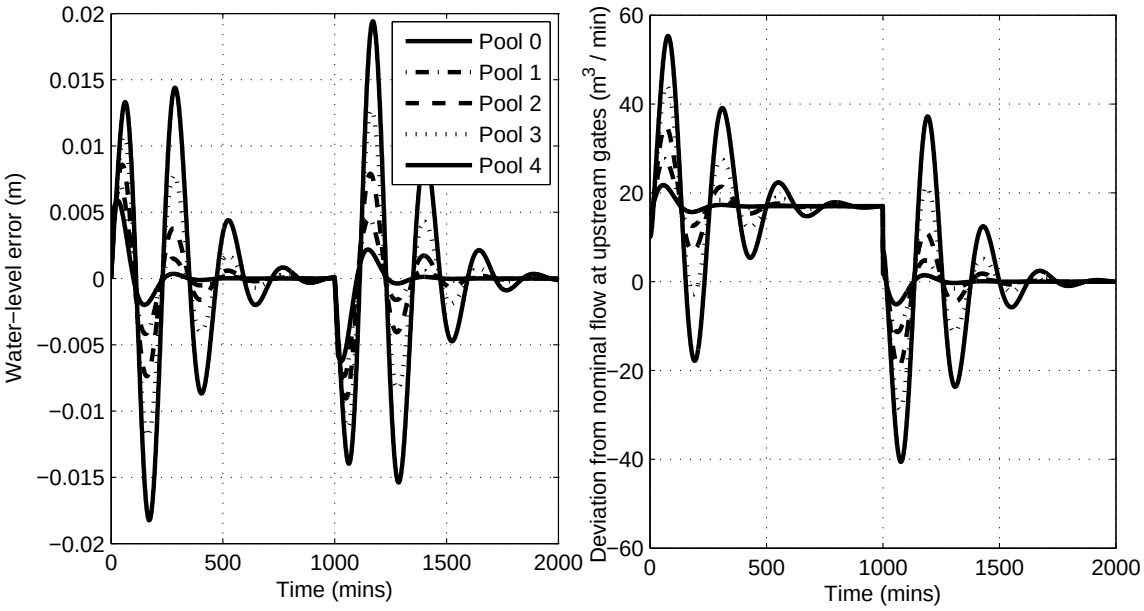

Figure 1.12: Simulations of a channel with decentralised feedback and constant flow-to-flow feedforward, $F_i(s) = 0.9$.

$\frac{dT_{U_{i-1}\to U_i}}{dj\omega}(0) = \tau_i$, it follows that

$$|T_{U_{i-1}\to U_i}(j\hat{\omega})| \approx \sqrt{1+\hat{\omega}^2\tau_i^2} > 1.$$

□

As can be seen from Figure 1.12 choosing a low-pass filter of 0.9 increases the amplification of flow peaks along the channel. So, although including the feedforward path improves flow propagation, it is not systematically dealing with the interaction between pools and flow peak amplification cannot be avoided.

1.3.5 Distributed Distant-Downstream Control Via H_∞ Loop-Shaping

Distributed Distant-Downstream Control with the architecture shown in Figure 1.13 is a generalisation of the decentralised feedback distant-downstream control where there is directed communication between controllers of neighbouring pools.

As discussed in previous section, it is difficult to systematically exploit the downstream infor-

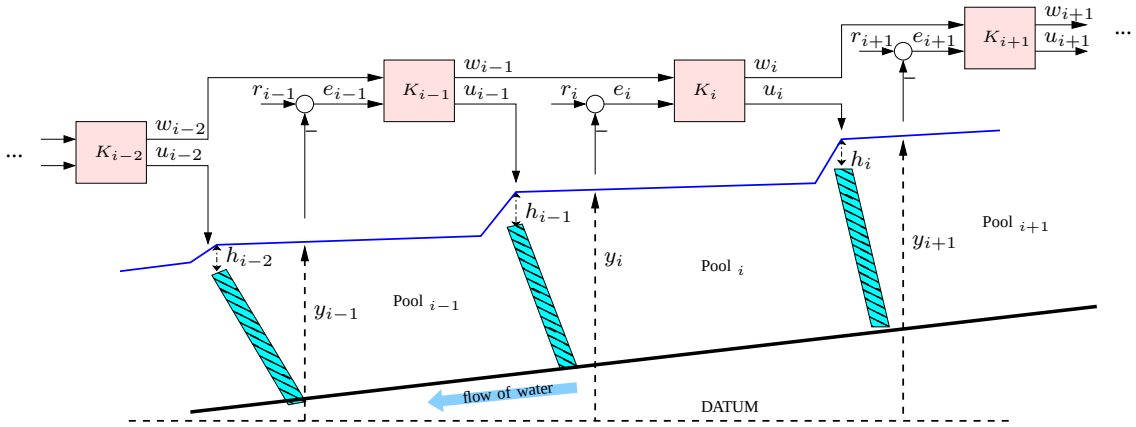

Figure 1.13: Distributed control scheme of an irrigation channel.

mation to deal with spatial propagation of flow transients with the decentralised feedback with flow-to-flow feedforward distant-downstream control [27]. One approach to designing a distributed distant-downstream control to systematically deal with interaction between automated pools and spatial dynamics of channels is a H_∞ loop-shaping based design, [44], which is used for irrigation channels control as in [7, 21, 45]. This method involves two stages. First, loop-shaping weights are scalably designed in view of local control objectives (i.e. local water level regulation, disturbance rejection, and steady-state flow load matching). Design procedure of the loop-shaping weights (e.g. W_i, $i = 0, \cdots$ as shown in Figure 1.14), is similar to the controller design of the decentralised feedback distant-downstream control scheme.

Next step, is a non-scalable synthesis procedure to systematically deal with the interaction between automated pools (i.e. interconnection signals of the cascade in Figure 1.5) via finding $\hat{K}_i$ for all i. In particular, let $n_i := \begin{bmatrix} r_i & d_i & q_i \end{bmatrix}^T$ be the vector of exogenous inputs, $z_i := \begin{bmatrix} (r_i - y_i) & u_i^K \end{bmatrix}^T$ represent performance signals, $\hat{G} = (\hat{G}_0, \cdots, \hat{G}_N)$, and $\hat{K} = (\hat{K}_0, \cdots, \hat{K}_N)$ with respect to Figure 1.14. Define $H(\hat{G}, \hat{K})$ to be the transfer function from input $n := \begin{bmatrix} n_0^T & \cdots & n_N^T \end{bmatrix}^T$ to $z := \begin{bmatrix} z_0^T & \cdots & z_N^T \end{bmatrix}^T$. Then, the second step entails solving the structured optimisation control problem

$$\min_{\hat{K}} \|H(\hat{G}, \hat{K})\|_\infty = \min_{\hat{K}} \sup_{\omega \in \mathbb{R}} \bar{\sigma}(H(\hat{G}, \hat{K})),$$

where $\bar{\sigma}(H)$ denotes maximum singular value of a matrix H, for all the channel via the computa-

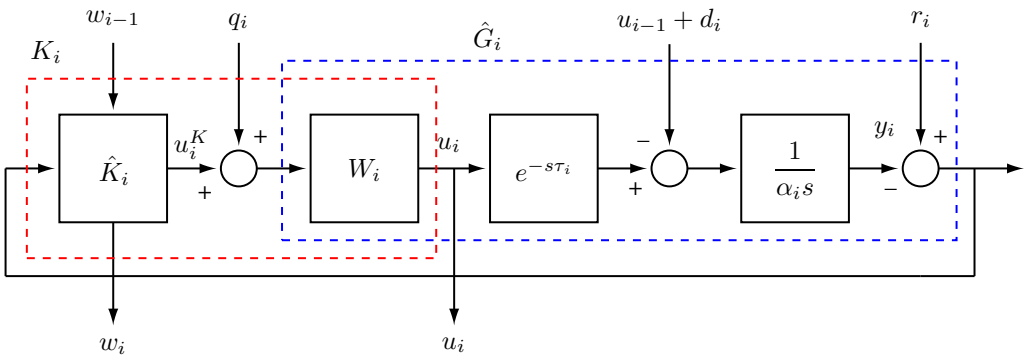

Figure 1.14: Block diagram of a local control system consistent with H_∞ loop-shaping method.

tion techniques described in [46]. Subsequently, the local controller K_i follows from

$$K_i(s) = \begin{bmatrix} I & 0 \\ 0 & W_i \end{bmatrix} \hat{K}_i.$$

Simulation results of 10 identical pools with specifications as in Table 1.1 running under distributed distant-downstream controller designed via H_∞ loop-shaping scheme are plotted in Figure 1.15. An offtake of $17\text{m}^3/\text{min}$ is withdrawn from pool 0 for 1000mins. It can be seen in addition to satisfying local control performance, less amplification of transient flows and water level errors is observed compared to decentralised feedback control or decentralised feedback with flow-to-flow feedforward scheme. Recall that, the cost of this improvement in performance is that synthesis becomes non-scalable (i.e. all components of the controller need to be re-synthesised for any change in plant dynamics). In addition, the flows peaks are still being amplified in the upstream direction, and thus a potential for spatial instability. Therefore, the problem of achieving a channel automation structure that provides non-amplification of flow transients where control design can be carried out in a scalable fashion is still remaining and will be the focus of the current thesis.

1.3.6 Decentralised Feedback With Flow-to-Reference Feedforward Distant Downstream Control

The control structure proposed in this thesis is the local block diagram of a decentralised feedback with flow-to-reference distant downstream control with a PI and a roll-off feedback in Figure 1.16. The addition of the flow-to-reference feedforward path, $F_i(s)$, provides an extra degree

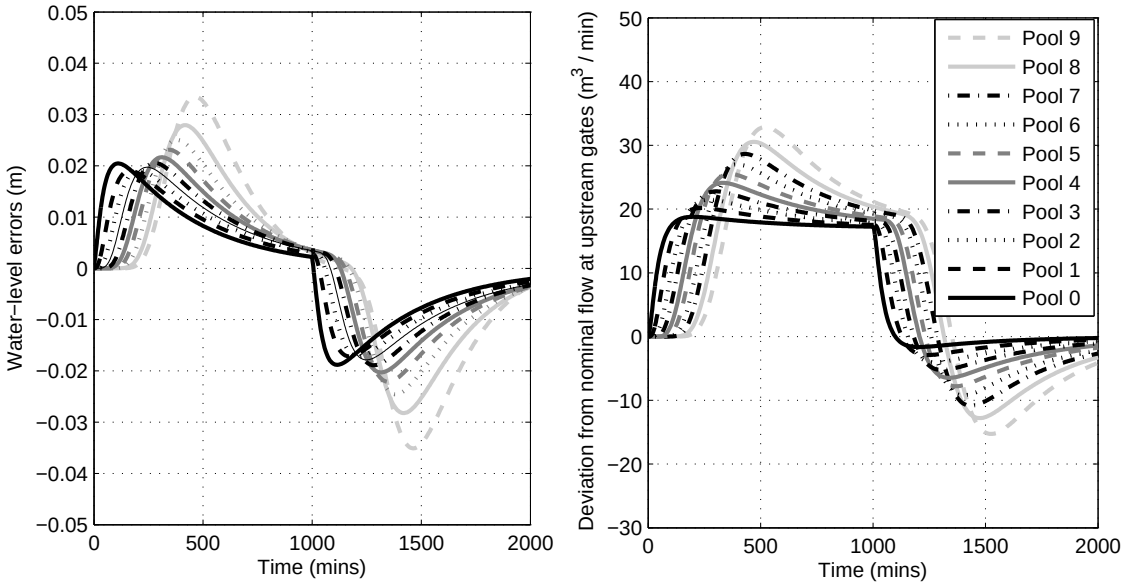

Figure 1.15: Simulations of a channel with distributed control.

of freedom for modifying the flow interactions, $T_{V_i \to U_i}$, characteristic of the purely decentralised distant-downstream scheme. The inclusion of the feedforward path yields a distributed distant-downstream control structure, which also ensures transients propagate in the upstream direction and can be designed in a scalable fashion similar to decentralised distant-downstream control. Furthermore, it has to be designed to maintain the steady-state flow matching property of each pool. For simplicity, by change of variable the references are all considered to be zero;i.e. $r_i = 0$. This new feedforward scheme, discussed in this thesis, can be viewed in terms of non-constant water-level references $R_{\text{i,new}} = R_i - F_i(s)V_i = -F_i(s)V_i$ for a loop with local decentralised PI controller retained to sustain capacity to supply under the power of gravity without steady-state offsets due to the local feedback action alone. The following now holds in the frequency domain:

$$U_i = \frac{L_i(s)}{1 + L_i(s)e^{-\tau_i s}}[(1 - \frac{F_i(s)}{P_i(s)})V_i + D_i], \tag{1.14}$$

where

$$G_i(s) := T_{V_i \to U_i}(s) = \frac{L_i(s)}{1 + L_i(s)e^{-\tau_i s}}(1 - \frac{F_i(s)}{P_i(s)}), \tag{1.15}$$

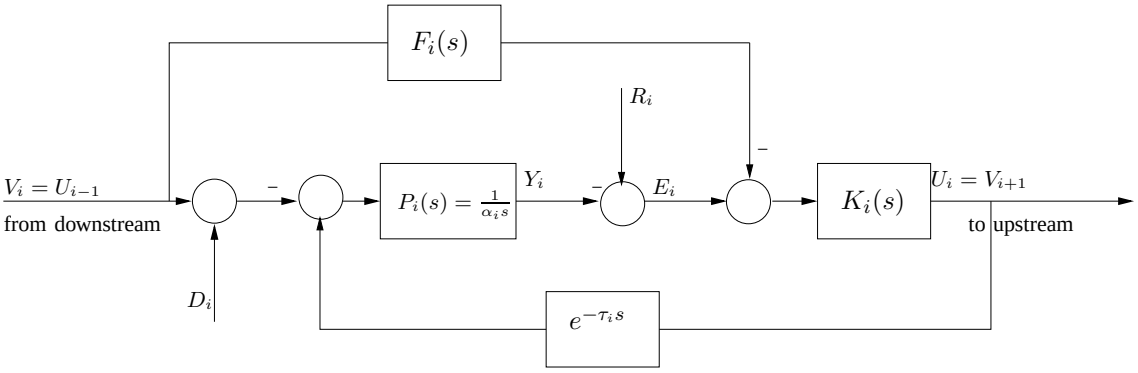

Figure 1.16: Block diagram of a local control loop with a feedforward of the downstream flow

satisfies $G_i(0) = 1$ for steady-state flow matching. As such, it is possible to achieve a desirable $G_i(s)$ for any stable $G_i(s)$ with $G_i(0) = 1$ by appropriate choice of stable

$$F_i(s) = \frac{G_i(s)}{K_i(s)} + P_i(s)(1 - G_i(s)e^{-\tau_i s}), \tag{1.16}$$

provided $K_i(s)$ is the PI with roll-off mentioned in Section 1.3.4. Stability of $F_i(s)$ follows from the stability of both terms on the right hand side of (1.16). The first term is stable by stability of $G_i(s)$ and left half plane zeros of $K_i(s)$; In addition, stability of the second term follows due to $G_i(0) = 1$ and $1 - G_i(s)e^{-\tau_i s}$ having a zero at $s = 0$ which cancels the pole at $s = 0$ in $P_i(s)$ which can be shown by writing the Taylor series of $e^{-\tau_i s}$ around $s = 0$.

In this thesis, zero steady-state water-level error is relaxed to achieve attenuation of transients as they propagate upstream. This introduces a trade-off to be more discussed in section 2.6.

1.4 Summary

Irrigation channels and the need for improved performance of automated channels for sustainable management of water resources is discussed. Different control structures and design approaches for open water irrigation networks are introduced. The properties of different architectures of distant-downstream control are discussed in terms of spatial water flow propagation and scalability of design. Flow transients amplification by existing control structures for automated irrigation channels motivate the thesis focus on spatial stability properties of automated channels and decentralised conditions that imply uniformly bounded water flows across space. In Chapter 2, a flow

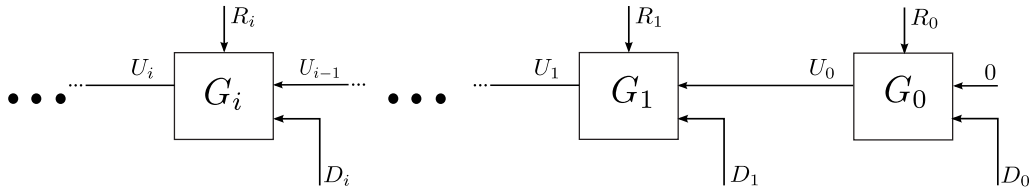

Figure 1.17: Cascade representation of a channel running under decentralised feedback with flow-to-reference distant-downstream control

to reference feedforward scheme is introduced that leads to bounded flows along an automated irrigation channel.

1.5 Thesis Outline

An automated channel with decentralised feedback with or without feedforward (flow-to-flow or flow-to-reference) distant-downstream scheme can be represented by a cascade shown in Figure 1.17. The properties of the subsystems that gives the desirable spatial propagation of the flow peaks along the channel are analysed in this thesis.

Chapter 2: Flow-to-Reference Feedforward Compensator Design for Non-Amplification of Transient Flow Peaks. In this chapter, first, a scalable (sufficient) condition on the flow-to-flow interaction between the automated pools of a channel under distributed distant-downstream control, that ensures a spatially uniform bound on the transient peaks of the flows in response to bounded load variation at the bottom of the channel is identified. Indeed, the conditions introduced ensure non-amplification of transient flow peaks from one pool to an upstream neighbouring pool. On this basis, the flow-to-reference feedforward compensation for each pool, as introduced in Section 1.3.6 is selected to satisfy the corresponding decentralised condition, which relates to the L_∞-to-L_∞ induced norm (i.e. 1-norm of the impulse response) of the flow-to-flow interaction between automated pools. The price to pay is steady-state water-level offsets. This approach is inspired by time headway schemes in vehicle platoons. A design trade-off is identified between steady-state water-level errors and spatial attenuation of water flow peaks, for a particular choice on flow-to-flow interaction between the automated pools along a channel.

Chapter 3: Robustness analysis of a nominally L_∞-to-L_∞ string-stable automated channel.

While the control design process introduced in Chapter 2 nominally achieves L_∞-to-L_∞ string-stability, the robustness of this property to model parameter uncertainty is of practical concern. Robustness of the worst L_∞ to L_∞ induced norm of the automated flow interactions between neighbouring pools is investigated using Linear Matrix Inequalities. While the application of these does not confirm robustness of the string-stability property, the bounds obtained show that the degree to which the property is violated remains mild in the face of substantial uncertainty for a channel under consideration.

Chapter 4: 2-D modeling and analysis of automated irrigation channels. The condition on L_∞ to L_∞ induced norm introduced in Chapter 2 ensures spatially uniform boundedness of the flow interaction signals. Indeed, this is achieved by ensuring transient flow peaks are non-amplified as they propagate from one pool to the next, which is a particularly strong condition. It is also shown that an H_∞ condition on the flow interaction transfer function is necessary for this spatial stability property. In particular, it is of interest to know if it leads to a property of uniform boundedness of flow-interactions without requiring non-amplification between all pools.

Moreover, two-dimensional modeling and analysis are carried out for an automated irrigation channel. Motivated by the finite spatial extent of an irrigation channel, a discrete-discrete 2-D model is introduced for a homogenous automated irrigation channel and analysis conditions implying uniformly boundedness of flow interaction signals are derived. On the other hand, a 2-D discrete-continuous state-space like model for a heterogeneous automated channel represented by a cascade, comprising infinitely many stable sub-systems, is studied in terms of the spatial flow propagation. Lyapunov function based analysis of the 2-D model is used to establish decentralised H_∞ norm based spatial-stability certificates for the sub-systems along the cascade. Collectively, these certificates imply uniformly bounded interconnection signals. This H_∞ norm condition may be more amenable for systematic synthesis than the condition introduced in Chapter 2.

Chapter 5: Conclusion. This chapter contains concluding discussions and future research directions.

This page intentionally left blank.

Chapter 2

Flow-to-Reference Feedforward Compensator Design for Non-Amplification of Transient Flow Peaks

A new distributed distant-downstream controller structure for irrigation channels is studied. The controller ensures upstream propagation of transients, like those considered in Chapter 1, but now in a spatially-stable fashion. This is achieved by foregoing zero steady-state water-level errors in response to step changes in flow offtakes, via a mechanism that adjusts water-level references on the basis of downstream flow load. While structurally different, the approach is inspired by time headway schemes in vehicle platoons. A trade-off between steady-state water-level errors and the spatial attenuation of the water-flow peaks is identified. The design and synthesis procedure can be carried out on a pool by pool basis, building up on the purely decentralised control scheme described in Section 1.3.4.

2.1 Introduction

As discussed in Chapter 1, local control objectives for an irrigation channel, i.e. steady-state flow load matching along the channel and water-level tracking of step references at downstream gate of each pool in presence of offtake disturbances, can be achieved via distributed distant-downstream control schemes that confine transients to spatially propagate in the upstream direction, [7, 21]. Purely decentralised feedback distant-downstream control, the decentralised feedback with flow-to-flow feedforward scheme and H_∞ loop-shaping based distributed distant-downstream control

are possible structures for distant-downstream controllers [21]. As discussed in Chapter 1, these control schemes, result in amplification of the transient flow over gates towards upstream as they propagate along the automated channel. This chapter's focus on bounding flow transients peaks is motivated by the limited authority of the control gates, which saturate in terms of the flow delivered when in the fully open or fully closed position. We use the term "L_∞-to-L_∞ string-stability", which is discussed in Section 2.3, to refer to uniformly bounded water flows towards upstream of an automated channel in response to a constant offtake drawn from a pool. Considering step offtakes in all pools at once does not yield a useful measure of performance since, in this case, the flow over a gate grows linearly with its distance from the bottom pool whenever the flow matching requirement is satisfied in steady-state.

In this chapter, while water-levels are still to be controlled, as these reflect the capacity to locally supply flow under the power of gravity alone, the focus is on flow load matching and on the identification of a control structure for achieving attenuation of transients as they propagate spatially. Ultimately, the latter is accomplished via a feedforward-like adjustment of the local water-level references based on the downstream flow load as set by the downstream controller. The controller ensures upstream propagation of transients, like those considered previously, but now in a spatially stable fashion. This gain comes at the cost of water-level off-sets, which equate to the exploitation of storage in the pools. While structurally different, the modeling style is inspired by the vehicle platoons setup and ideas of time headway, as discussed in [47–49], for example. In that context, string-stability can be achieved by adjustment of the spacing reference, via a modification of the forward path of each local control loop, without changing the closed-loop characteristics. In the irrigation channel context, it is not possible to modify the local control loops in this way as it would require physical modification to the channel infrastructure. In the new set-up introduced, a feedforward-information path provides the extra degree of freedom needed to modify the interaction between neighboring pools under closed-loop control. In the recent work [50], MPC based water-level reference planning is being considered from the perspective of ensuring the satisfaction of operational constraints, given an uncertain load schedule. As such, although the offsets resulting from the feedforward path gives rise to a new trade-off between steady-state water-level errors and the spatial attenuation of the water flow peaks to be considered, the offsets present for constant references is of minor concern as long as the levels remain within

practically acceptable bounds.

Like the decentralised feedback with flow-to-flow feedforward distant-downstream scheme described in [21], the process of designing a controller with the distributed distant-downstream control architecture achieving L_∞-to-L_∞ string-stability introduced here is scalable in the sense that the local components of the distributed controller are chosen on the basis of local pool model parameters alone. In this way, updates of pool dynamics only require update of the local controller components.

This chapter contains an overview of different string-stability notions used in the literature in Section 2.3. In Section 2.4, sufficient conditions on the flow interactions for L_∞-to-L_∞ string-stability is introduced. The design tradeoffs of the proposed method is investigated in Section 2.6. The tradeoff in using a feedback controller in the completely decentralised distant-downstream control scheme that does not include integral action is discussed in Section 2.7. A summary is presented at the end.

2.2 Notation

A transfer function $Q(s)$ and the input-output relation $Y = Q(s)U$, with impulse response $q(t) = \mathscr{L}^{-1}(Q(s))$ in the time domain, where $\mathscr{L}$ denotes the Laplace transform, is called stable if Q is analytic on $Re(s) > -\varepsilon$ for some $\varepsilon > 0$; this is equivalent to bounded-input bounded-output stability in the time domain [51]. For a stable transfer function Q, the following inequalities prove to be useful:

$$\|y\|_\infty \leq \|q(\cdot)\|_1 \|u\|_\infty, \tag{2.1}$$

$$\|y\|_\infty \leq \|Q(j\cdot)\|_2 \|u\|_2, \tag{2.2}$$

$$\|y\|_2 \leq \|Q(j\cdot)\|_\infty \|u\|_2, \tag{2.3}$$

where $\|q(\cdot)\|_1 = \int_0^\infty |q(t)|dt$, $\|Q(j\cdot)\|_2 = (\frac{1}{2\pi}\int_{-\infty}^{\infty} |Q(j\omega)|^2 d\omega)^{\frac{1}{2}}$ is the H_2 norm of Q where $\lim_{s\to\infty} Q(s) = 0$, $\|Q(j\cdot)\|_\infty = \sup_\omega |Q(j\omega)|$ is the H_∞ norm of Q, $\|u\|_\infty = \sup_t |u(t)|$, and $\|u\|_p = (\int_{-\infty}^{\infty} |u(t)|^p dt)^{\frac{1}{p}}$. The L_∞ space is defined to consist of all vector-valued continuous time signals, $x(t) \in \mathbb{R}^n$, for which $\|x\|_\infty < \infty$ and L_2 space consists of those signals with $\|x\|_2 < \infty$. Moreover,

$g(t) \in L_1[0,\infty)$ if $\|g\|_1 < \infty$ and $g(t) = 0$ for $t < 0$.

2.3 Overview of String-Stability

Interests in propagation pattern of disturbances or initial conditions along a chain or string of subsystems is not exclusive to automated irrigation channels. Indeed, a number of research studies are dedicated to this topic in vehicle platoons [52, 53], autonomous intelligent cruise control [54], vehicle formation [55], interval management in aircrafts [56] and supply chain [57, 58], etc. It started with optimal error control of string of vehicles in [59]. Later on, in [60], stability of a string is defined in terms of requiring bounded position error fluctuations, that would also tend to zero in steady-state, in response to bounded initial conditions for all vehicles. Afterwards, more research has been carried out in this field and different types of string-stability can be identified based on different signal measures considered.

2.3.1 Measures of String-Stability

String-stability of a chain of subsystems can be viewed from an input-output perspectives or from autonomous systems view. Consider a string of N identical subsystems interconnected through some physical or communication connections. Moreover, a unidirectional interconnections with communication range of one is considered for simplicity. Then, string-stability can be measured within the following two categories:

- **Autonomous String:**

  Consider a string of subsystems with the dynamics of subsystem i described by

  $$\dot{x}_i(t) = A_i x_i + B_i x_{i-1}, \;\; x_i(0) := x_{i0}, \;\; i = 0, 1, \cdots, N, \tag{2.4}$$

  where x_i is the semi-state, $N \in \mathbb{N}$, and $x_{-1}(.) = 0$.

  The performance of $x_i(t)$ in (2.4) in response to initial conditions, x_{i0}, is of concern for the mentioned string of systems. Therefore, the following measures of performance are

considered:

Definition 2.1 (L_2 **string-stability**). *The origin ($x_i = 0$) of a string of subsystems modeled by (2.4) is said to be L_2 string-stable if $\forall \varepsilon > 0,\ \exists \delta > 0$ s.t. if $|x_{i0}|_2 < \delta$ implies $\|x_i(.)\|_2 < \varepsilon$, for all i where δ is independent of the length of the string.*

Authors of [52, 53] has carried out some analysis of L_2 string-stability of a string interconnection of linear models of vehicles in response to initial conditions.

Definition 2.2 (L_∞ **string-stability**). *The origin ($x_i = 0$) of the string of subsystems modeled by (2.4) is said to be L_∞ string-stable if $\forall \varepsilon > 0,\ \ \exists \delta > 0$ s.t. if $|x_i(0)|_\infty < \delta$ implies $\|x_i(.)\|_\infty < \varepsilon$, for all i where δ is independent of the length of the string, [52, 53].*

Other measures of the boundary conditions and $x_i(t)$ can be used for identifying string-stability.

- **Non-Autonomous String:**

  Consider a string of subsystems with interconnection signal $y_i(t)$ and disturbance $d_0(t)$ and the impulse response $g_i(t)$ for the mapping from $y_{i-1}(t)$ to $y_i(t)$. Therefore, in the frequency domain,

$$\begin{aligned} &Y_i(s) = G_i(s)Y_{i-1}(s),\ \ i = 1,2,\cdots,N, \\ &Y_0(s) = G_0(s)D_0(s) \end{aligned} \tag{2.5}$$

  represents the string, where $G_i(s) = \mathscr{L}(g_i(t))$, $Y_i(s) = \mathscr{L}(y_i(t))$, and $D_0(s) = \mathscr{L}(d_0(t))$ for $i = 0,1,\cdots,N$. Therefore, the following measures of performance are defined for system (2.5) in response to disturbances at the top of the information flow along the string, $d_0(t)$.

  Definition 2.3 (L_2 **string-stability**). *A string of subsystems modeled by (2.5) is said to be L_2 string-stable if $\|y_i\|_2 \leq \|y_{i-1}\|_2$ for all i with $\|d_0(.)\|_2 < \infty$.*

  Due to inequality (2.3) and the fact that $Y_i(s) = \prod_{k=0}^{i} G_k(s)D_0(s)$ for any subsystem, the string of subsystems modeled by (2.5) is L_2 string-stable, as defined above, if $\|G_i(j\cdot)\|_\infty \leq 1$, for all k. Some authors have been interested in L_2 string-stability, mostly in vehicle platoon and formation context. For instance, in [55], authors used the mass-spring-damper

framework as a model for vehicle control and to analyse different string-stability properties of different longitudinal controllers.

Definition 2.4 (L_∞ **string-stability**). *A string of subsystems modeled by (2.5) is said to be L_∞ string-stable if $\|y_i\|_\infty \leq \|y_{i-1}\|_\infty$ for all i with $\|d_0(.)\|_\infty < \infty$.*

Similar to L_2 string-stability, noting $Y_i(s) = \prod_{k=0}^{i} G_k(s)D(s)$ and (2.1), for any subsystem in the string, the string of subsystems modeled by (2.5) is L_∞ string-stable, as defined above, if $\|g_k(.)\|_1 \leq 1$, [55]. Some studies were dedicated to L_∞ string-stability analysis of chains of subsystems. For example, in the context of irrigation channels, the amplification of water levels and flows as they propagate along an irrigation channel have been analysed [21, 39, 61, 62]. Moreover, this property is analysed for automated vehicle strings in [42] or interval management in next generation air transportation systems [56].

L_∞ string-stability is mostly considered as a measure of propagation of the effect of disturbances in vehicle platoons. In [40], it is proved that the predecessor following problem with a constant spacing results in L_∞ string-instability with only relative spacing information available by the follower. Different strategies have been proposed to tackle this issue. One method is communicating extra information from the lead vehicle to all the followers, [40, 63], or the bidirectional control where the information from both adjacent vehicles are exploited by each agent, [42, 64]. Some others have achieved L_∞ string-stability by allowing speed dependent inter-vehicle spacing, [54, 65]. Indeed, the so-called "time headway" policy changes the interaction between two vehicles by modifying the control feedback path [66]. In [67] string-stability is achieved for a string of identical platoons with constant inter-vehicle spacing using non-identical controllers.

Definition 2.5 (**String-stability without overshoot**). *A string of subsystems modeled by (2.5) is said to be string-stable without overshoot if $\|y_i(.)\|_\infty \leq \|y_{i-1}(.)\|_\infty$ with $\|d_0(.)\|_\infty < \infty$, in addition, if y_{i-1} does not change sign, then the y_i always has the same sign as y_{i-1}, [55].*

This type of string-stability is achieved if $\|g_i(.)\|_1 \leq 1$, for all i and $g_i(t) > 0, \forall t > 0$. Indeed by $g_i(t) \geq 0, \forall t \geq 0$, the step response is ensured to be strictly increasing reaching its final value.

This type of string-stability has been used in automation of vehicle platoons. These works include [55, 67, 68], where non-amplification and non-oscillation of the distance errors are guaranteed by imposing positive impulse responses of the interactions transfer functions.

Similar concepts have been used under different terminologies, such as "Bullwhip Effect", in other fields like supply chain and production and inventory control, [57,58]. It is defined as the variance amplification of order quantities observed in supply chains, [69].

In the references mentioned, authors have considered a homogeneous string of subsystems. However, there are others who have investigated the methods of achieving different types of string-stability for heterogenous strings, such as [70, 71] in the field of vehicle platoons or [61] who has studied systematic design of the feedforward path in irrigation channels to improve the propagation of the transients along the channel.

Similar ideas are used in this chapter to achieve L_∞-to-L_∞ string-stability for automated irrigation channels.

2.4 An Approach to Achieving L_∞-to-L_∞ String-Stability

Synthesis of the feedforward path of Figure 1.16 to attenuate flow transients as they propagate upstream is discussed in this section. To this end, $T_{V_i \to U_i}(s)$ is modified. Analysis corresponding to the following definition of L_∞-to-L_∞ string-stability which is weaker than the common definition used for non-autonomous vehicular platoons is carried out first.

Definition 2.6 (L_∞-to-L_∞ **string-stability**). *An irrigation channel operating under the distributed distant-downstream control scheme illustrated in Figure 1.16 is L_∞-to-L_∞ string-stable if there exists an $0 < M < \infty$ such that, with $d_i = 0$ for $i = 1, 2, \ldots$ and d_0 bounded, $\|u_i\|_\infty \leq M\|d_0\|_\infty$ for all $i = 0, 1, 2, \ldots$.*

In the following, $F_i(s)$ is chosen to achieve L_∞-to-L_∞ string-stability in the sense defined above. To this end, using (1.14) and the spatial boundary condition $V_0 = 0$, note that the following holds:

$$U_0 = \frac{L_0(s)}{1 + L_0(s)e^{-\tau_0 s}} D_0, \tag{2.6}$$

$$U_i = G_i(s)V_i \text{ for } i = 1, 2, \ldots, \tag{2.7}$$

whereby

$$U_i = \prod_{k=1}^{i} G_k(s) \frac{L_0(s)}{1+L_0(s)e^{-\tau_0 s}} D_0 \text{ for } i = 1,2,\dots . \tag{2.8}$$

From (2.6), u_0 is bounded since $T_{D_0 \to U_0}(s)$ is designed to be a stable transfer function. For each $i = 1,2,\ldots$, u_i is bounded for a bounded input d_0 if, and only if, $T_{D_0 \to U_i}(s)$ is a stable transfer function. For this to be the case, it is clearly sufficient for $F_i(s)$ to be chosen such that $G_i(s)$ is stable. Indeed, this is also necessary as $L_0(s)\big/(1+L_0(s)e^{-\tau_0 s})$ has no unstable zeros. In view of this, repeated application of (2.1) gives

$$\begin{aligned} \|u_0\|_\infty &\leq \|\mathscr{L}^{-1}(\frac{L_0(s)}{1+L_0(s)e^{-\tau_0 s}})\|_1 \cdot \|d_0\|_\infty, \\ \|u_i\|_\infty &\leq \prod_{k=1}^{i} \|g_k\|_1 \cdot \|\mathscr{L}^{-1}(\frac{L_0(s)}{1+L_0(s)e^{-\tau_0 s}})\|_1 \cdot \|d_0\|_\infty \text{ for } i = 1,2,\dots . \end{aligned} \tag{2.9}$$

As such, we have the following result.

Theorem 2.1. *The distributed distant-downstream control scheme shown in Figure 1.16 is L_∞-to-L_∞ string-stable in the sense of Definition 2.6 if $G_i(s)$ in (1.15) is stable and $\|g_i\|_1 \leq 1$ for $i = 1,2,\dots$.*

In view of Theorem 2.1, ensuring satisfaction of local control objectives and L_∞-to-L_∞ string-stability reduces to deriving an $F_i(s)$ that gives a stable $G_i(s)$ which satisfies $\lim_{s\to 0} G_i(s) = 1$ and $\|g_i\|_1 \leq 1$. There are many possible choices for such a $G_i(s)$, one of which is a constant transfer function of 1; i.e.

$$G_i(s) = (\frac{L_i(s)}{1+L_i(s)e^{-\tau_i s}})(1 - \frac{F_i(s)}{P_i(s)}) = 1.$$

However, inverting over all frequencies in this way will be sensitive to uncertainties, particularly in the high frequency dynamics which have not been modeled here. An alternative is a first-order low pass filter with DC gain 1; i.e.

$$G_i(s) = (\frac{L_i(s)}{1+L_i(s)e^{-\tau_i s}})(1 - \frac{F_i(s)}{P_i(s)}) = \frac{1}{1+T_{c,i}s}, \tag{2.10}$$

for some $T_{c,i} > 0$. The required feedforward transfer function $F_i(s)$ is obtained as

$$F_i(s) = \frac{-1}{K_i(s)(1+T_{c,i}s)} + P_i(s)(1 - \frac{e^{-\tau_i s}}{1+T_{c,i}s}). \tag{2.11}$$

Remark: Note that $F_i(s)$ in (2.11) is stable as discussed in Section 1.3.6 due to stability of $G_i(s)$ and $G_i(0) = 1$.

Remark: If $F_i(s)$ is chosen such that the condition of Theorem 2.1 is satisfied, then it follows that $\|G_i\|_\infty \leq 1$, since $|G_i(j\omega)| \leq \|g_i\|_1 \leq 1$ for all ω. By (2.8) and repeated application of (2.3)

$$\begin{aligned} \|u_0\|_2 &\leq \|\frac{L_0(s)}{1+L_0(s)e^{-\tau_0 s}}\|_\infty \cdot \|d_0\|_2, \\ \|u_i\|_2 &\leq \prod_{k=1}^{i} \|G_k\|_\infty \cdot \|\frac{L_0(s)}{1+L_0(s)e^{-\tau_0 s}}\|_\infty \cdot \|d_0\|_2 \text{ for } i = 1,2,\ldots \end{aligned} \tag{2.12}$$

holds. As such, with $\|G_i\|_\infty \leq 1$, it follows that the controlled channel is also L_2 string stable in the sense of definition 2.3.

Remark: If the proposed feedforward scheme, with $F_i(s)$ as in (2.11), is compared to the decentralised feedback with flow-to-flow feedforward distant-downstream control of Figure 1.10, [21], it can be seen that the first term of the right hand side of (2.11) is equivalent to the flow-to-flow feedforward path, $F_i(s)$, of Figure 1.10. The extra term gives flexibility to deal with the flow amplification property. However, note that with a feedforward path of Figure 1.10, it is not possible to achieve a stable feedforward filter such that $T_{V_i \to U_i} = G_i(s)$ with $\|G_i\|_\infty \leq 1$. It can be shown by noting that

$$G_i(s) = \frac{L_i(s) + F_i(s)}{1 + L_i(s)e^{-\tau_i s}}. \tag{2.13}$$

As such, it is not possible to find a suitable $G_i(s)$, $\|G_i\|_\infty \leq 1$, for any stable $G_i(s)$ with $G_i(0) = 1$ by appropriate choice of stable

$$F_i(s) = G_i(s) - L_i(s)(1 - G_i(s)e^{-\tau_i s}), \tag{2.14}$$

provided $K_i(s)$ is the PI with roll-off mentioned in Section 1.3.4. The first term of $F_i(s)$ is stable by stability of $G_i(s)$; Instability of the second term follows due to $G_i(0) = 1$ and $1 - G_i(s)e^{-\tau_i s}$

having only one zero at $s = 0$ which cancels one pole at $s = 0$ in $L_i(s)$. This can be shown by writing the Taylor series of $e^{-\tau_i s}$ around $s = 0$:

$$L_i(s)(1 - G_i(s)e^{-\tau_i s}) = \frac{\kappa_i(1+\phi_i s)}{\alpha_i s^2(1+\rho_i s)}(1 - G_i(s)\sum_{k=0}^{\infty}\frac{(-\tau_i s)^k}{k!}),$$

which cannot have more than one zero at $s = 0$ due to stability of $G_i(s)$ and $\|G_i\|_\infty \leq 1$. So, $L_i(s)(1 - G_i(s)e^{-\tau_i s})$ has a pole at $s = 0$.

The advantage of the flow-to-reference feedforward scheme is that it is possible to achieve $\|G_i\|_\infty = 1$ with a stable F_i, as this only requires $(1 - G_i(s)e^{-s\tau_i})$ to have one zero at $s = 0$.

Remark: $\|G_i(s)\|_\infty \leq 1$ is a necessary condition for L_∞-to-L_∞ string-stability of an automated irrigation channel with $G_i(s) = G(s)$ for all i. Otherwise, if $\exists\omega_0$ such that $|G_i(j\omega_0)| > 1$, we can show that the channel is not L_∞-to-L_∞ string-stable. Let $u_0(t) = cos(\omega_0 t)$, then response of the ith pool in frequency domain is

$$U_i(s) = G(s)^i U_0(s). \tag{2.15}$$

Therefore, $u_i(t)$ at steady-state, $u_{ss,i}(t)$, equals $a_i \sin(\omega_0 t + \phi_i)$, where

$$\begin{aligned} a_i =& |G(j\omega_0)|^i, \\ \phi_i =& \begin{cases} arcsin(\frac{\mathrm{Re}(G(j\omega_0)^i)}{|G(j\omega_0)|^i|}) & \mathrm{Im}(G(j\omega_0)^i) \leq 0, \\ \pi - arcsin(\frac{\mathrm{Re}(G(j\omega_0)^i)}{|G(j\omega_0)|^i|}), & \mathrm{Im}(G(j\omega_0)^i) > 0. \end{cases} \end{aligned} \tag{2.16}$$

As such, $\sup_{t>0}\lim_{i\to\infty}|u_{ss,i}(t)| = \lim_{i\to\infty} a_i$ which is unbounded. Thus, the conditions for L_∞-to-L_∞ string-stability do not hold.

Remark: If $g_i \in L_1[0,\infty)$ with $g_i(t) \geq 0$ for all $t \in [0,\infty)$ and $G_i(0) = 1$, then $\|g_i\|_1 = \int_0^\infty g_i(t)dt = \lim_{s\to 0}\int_0^\infty g_i(t)e^{-st}dt = G_i(0) = 1$.

Simulation results presented in Figure 2.1 are carried out to illustrate the impact of adding the feedforward path $F_i(s)$ chosen as in (2.11). A channel of 5 identical pools with the specifications as in table 1.1 are used. An off-take of $17\mathrm{m}^3/\mathrm{min}$ is considered to be taken from the most downstream pool of the channel for 1000mins. Flow transients attenuation is reached while having non-zero steady-state water-level errors which can be noticed comparing performance of

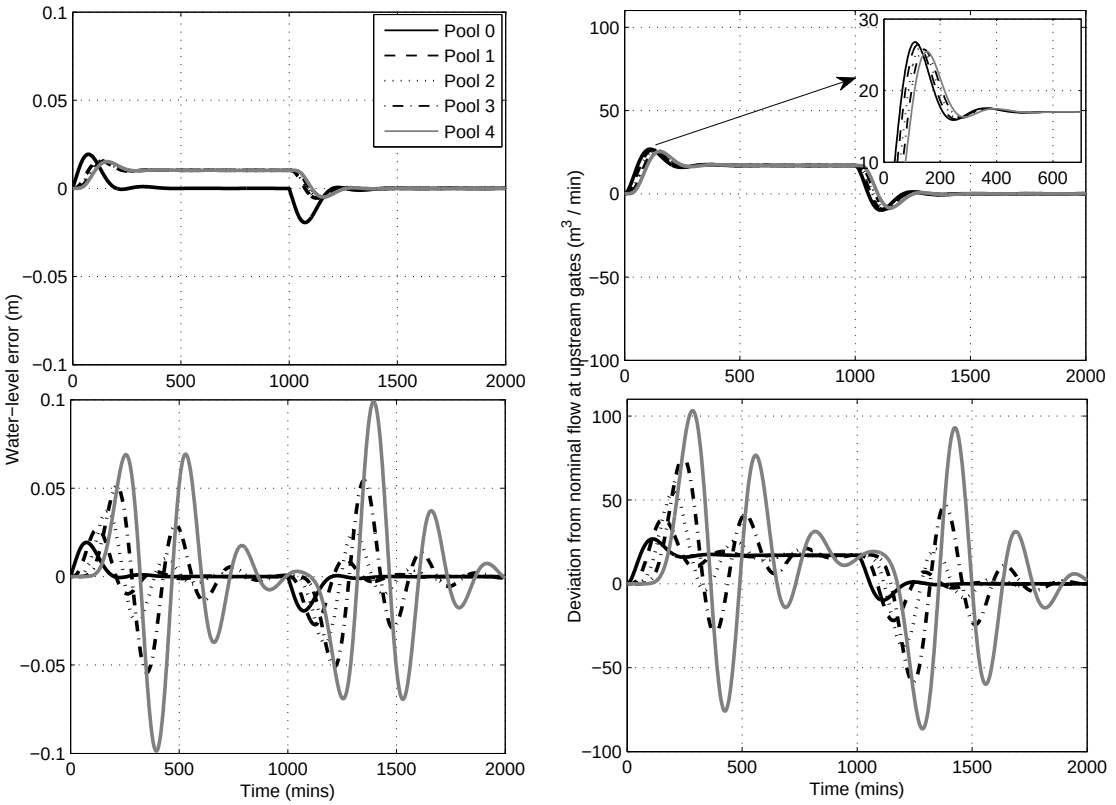

Figure 2.1: Simulations with top plot: $T_{V_i \to V_{i+1}}(s) = \frac{1}{1+T_c s}$, $T_c = 10$, bottom plot: purely decentralised scheme.

the channel under the decentralised feedback distant-downstream control scheme in bottom row of the figure. Indeed, water storage of the pools is exploited to overcome amplification of transients towards upstream. This is a trade-off to be discussed in section 2.6. The roll-off frequency of the low-pass filter $G_i(s)$ is an extra freedom to deal with this trade-off. The nonzero steady-state water levels are acceptable as long as they remain within operational bounds. In fact there are higher level controllers or supervisors to adjust water-level references accordingly.

It should be noted that $F_i(s)$ consists of an infinite dimensional delay component which can be realised with a Pade approximation. It is reasonable to use a rational approximation of the delay transfer function $e^{-\tau_i s}$, provided the error remains sufficiently small up to the loop-gain crossover frequency, as the closed-loop behaviour is insensitive to such modeling uncertainty. For example, the first order Pade approximation $(1 - s\tau_i/2)/(1 + s\tau_i/2)$ is acceptable provided the controller gain and corresponding loop-gain crossover frequency are sufficiently small, which is necessary

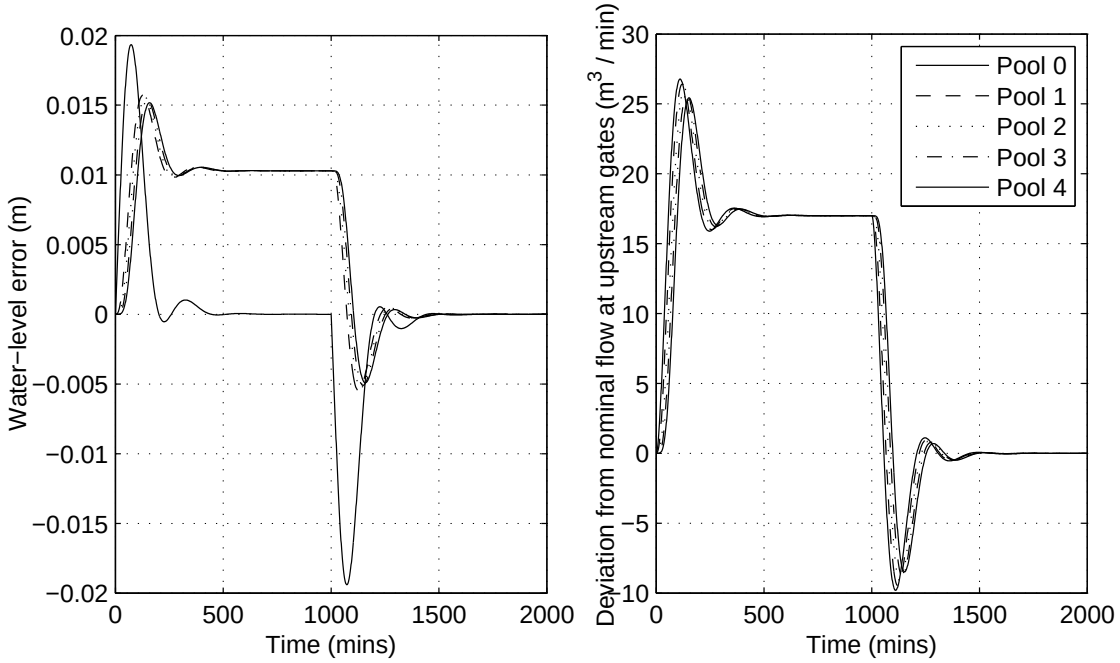

Figure 2.2: Simulations with $T_{V_i \to V_{i+1}}(s) = \frac{1}{1+10s}$ and first order approximation of the delay in $F_i(s)$.

Table 2.1: Pool model and controller parameters

Pool number	Pool Model Parameters			Controller Parameters			
	time-delay τ (mins)	α (m^2)	wave frequency (rad/min)	κ	ρ	ϕ	T_c
0,1,2	16	43806	0.20	7.72	15.2	128	30
3	3	11942	0.74	38.47	3.5	30	10
4	8	22414	0.42	11.44	8.7	77	20

to achieve reasonable control performance and robustness at any rate [27]. Figure 2.2 shows the simulation result carried out for performance comparison when a first order Pade approximation of the delay is used. Comparing Figures 2.1 and 2.2 reveals that such approximation of the delay does not deteriorate performance.

This method is scalable as it uses each pool's data for design of local controllers. Performance of a heterogenous channel of 5 pools with model parameters as in table 2.1 is simulated and illustrated in Figure 2.3. An off-take of $17\text{m}^3/\text{min}$ is drawn from Pool 0 for 1000mins. Water level off-sets depend on pools parameters and $T_{c,i}$ as will be shown in next section. Water flow transients do not get amplified towards upstream of the channel.

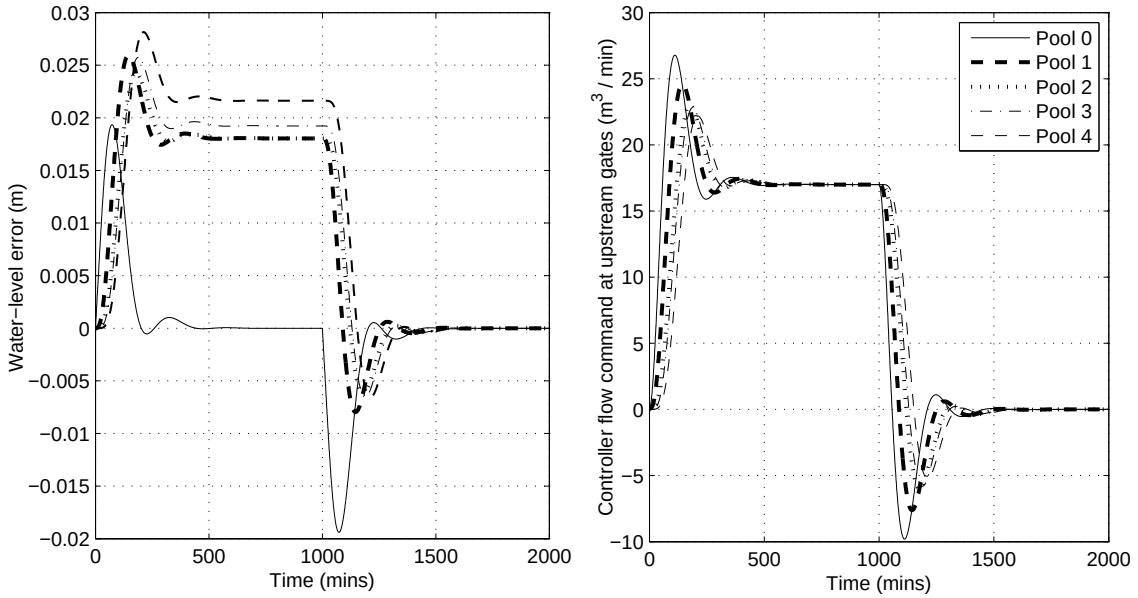

Figure 2.3: Simulations of a heterogenous channel with feedforward scheme.

2.5 Validation of Control Design Approach via Simulation with a PDE Model

To validate the performance of a heterogenous channel controller obtained via the aforementioned design procedure based on the approximate integrator-delay model, simulations of a distributed distant-downstream controller, designed as described in Section 2.4 are carried out, in closed-loop with the corresponding PDE model in Section 1.2.1. Among various methods for approximately solving the Saint-Venant equations, an implicit finite difference scheme known as the Preissmann scheme proves to be consistent, convergent and stable [15]. This scheme involves both spatial and temporal discretisation [1]. The controller designed in continuous time is discretised and the Zero-Order-Hold technique is employed with the sample time of 1 min.

The results are shown in Figure 2.4, which show the downstream water level in each pool and the corresponding inflows, for an off-take flow in pool 0 of 33% of the initial equilibrium channel flow of 70 m3/min, starting at 600 min and stopping at 1000 min. It is apparent that closed-loop water level responses and control flow commands for two models follow similar trajectories, validating use of the integrator-delay model for controller design with the flow-to-reference feed-forward scheme described above. Transients at the start of simulation are due to the effect of the

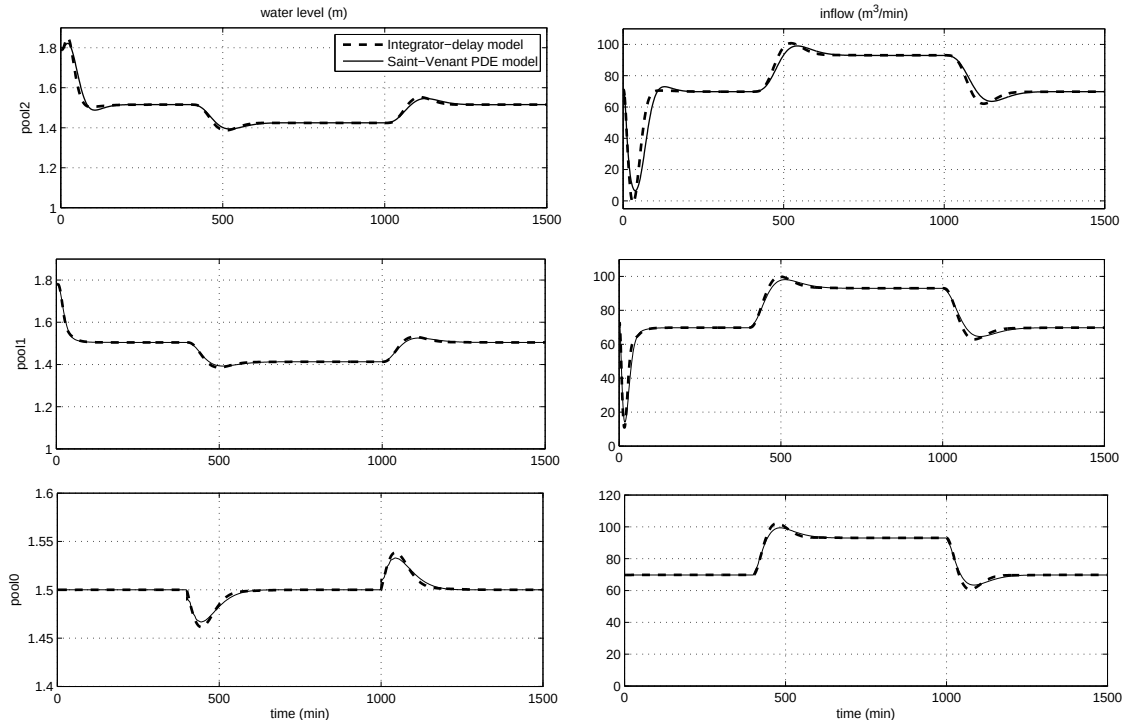

Figure 2.4: Simulations of the closed-loop water levels and flows with flow-to-reference feedforward scheme; dashed line: integrator delay model; solid line: PDE model.

initial equilibrium channel flow input to the feedforward block.

2.6 A Design Trade-Off

As illustrated with simulations of Figure 2.1, by adjusting the water-level references to $R_{\text{new,i}} := R_i - F_i(s)V_i$ via the addition of the feedforward path to the purely decentralised control scheme, L_∞-to-L_∞ string-stability is achieved at the cost of non-zero steady-state water-level errors for step changes in flow load. In this section, we will see how the selected roll-off frequency, $1/T_{c,i}$, of the interconnection dynamics (2.10), gives rise to a trade-off between steady-state water-level errors and the peaks in flow transients.

As shown in Figure 2.1, the response of u_0 to a step change of the off-take d_0 has a peak in the transient component. Note that $u_i,\ i = 0,1,\ldots$ is passed through the low-pass filter, $G_i(s)$, to produce u_{i+1}. Therefore, the lower the bandwidth of $G_i(s)$, larger $T_{c,i}$, the more attenuation of the flow peaks towards upstream of the channel. It can also be seen from the following result which

characterises the effect of $T_{c,i}$ on the flow peaks bounds in response to $d_0 \in L_2 \cap L_\infty$.

Theorem 2.2. *Consider an automated channel operating under a distributed distant-downstream control scheme with the architecture illustrated in Figure 1.16 and $F_i(s)$ set as in (2.11) to yield the flow-to-flow interaction $G_i(s) = \frac{1}{T_{c,i}s+1}$ between neighbouring pools. If $d_0 \in L_2 \cap L_\infty$ and $d_i = 0$ for $i = 1,2,\ldots$, then $\|u_i\|_\infty \leq \beta\sqrt{\frac{1}{2T_{c,i}}}\|d_0\|_2$ for $i = 1,2,\ldots$, where $\beta := \|\frac{L_i(j.)}{1+L_i(j.)e^{-j\tau_i \cdot}}\|_\infty$.*

Proof. According to the relation (2.2), it follows from (2.6) that

$$\|u_1\|_\infty \leq \|\frac{1}{1+jT_{c,1}\omega}\|_2\|u_0\|_2,$$
$$\|u_i\|_\infty \leq \|\frac{1}{1+jT_{c,i}\omega}\|_2\prod_{k=1}^{i-1}\|\frac{1}{1+jT_{c,k}\omega}\|_\infty\|u_0\|_2 \text{ for } i = 2,3\ldots.$$

Noting that $U_0(s) = L_0(s)/(1+L_0(s)e^{-\tau_0 s})D_0(s)$, and $\|\frac{1}{1+jT_{c,i}\omega}\|_\infty = 1$

$$\|u_i\|_\infty \leq \beta\|\frac{1}{1+jT_{c,i}\omega}\|_2\|d_0\|_2 \text{ for } i = 1,2,\ldots$$

where $\beta = \|\frac{L(j\omega)}{1+L(j\omega)e^{-j\tau\omega}}\|_\infty$. Since $\|\frac{1}{(1+jT_{c,i}\omega)}\|_2 = \sqrt{\frac{1}{2T_{c,i}}}$, therefore,

$$\|u_i\|_\infty \leq \beta\sqrt{\frac{1}{2T_{c,i}}}\|d_0\|_2, \tag{2.17}$$

Hence, $u_i(t)$ is uniformly bounded in i for $T_{c,i} > 0$. □

The previous theorem indicates that a larger time-constant $T_{c,i}$ for the flow-to-flow interaction transfer function G_i yields smaller bound on the flow peaks as they propagate. However, as shown next, this also yields larger steady-state water-level errors along the channel, and thus a design trade-off associated with the choice of the time-constant $T_{c,i}$.

Theorem 2.3. *An automated channel operating under a distributed distant-downstream control scheme with the architecture illustrated in Figure 1.16 and $F_i(s)$ set as in (2.11) to yield the flow-to-flow interaction $G_i(s) = \frac{1}{T_{c,i}s+1}$ between neighbouring pools responds to a unit step $d_0(t)$ such*

that

$$\begin{aligned}&\lim_{t\to\infty} e_0(t) = 0,\\ &\lim_{t\to\infty} e_i(t) = \frac{T_{c,i}+\tau_i}{\alpha_i} \textit{ for } i = 1,2,\dots\ .\end{aligned} \tag{2.18}$$

Proof. According to Figure 1.16,

$$E_i = \frac{P_i(s)}{1+L_i(s)e^{-\tau_i s}}[(1+K_i(s)F_i(s)e^{-\tau_i s})V_i + D_i].$$

Note that $v_i(t) = u_{i-1}(t) = d_0(t) + \tilde{v}_i(t)$ due to flow matching property, where $\tilde{v}_i(t)$ is the transient component tending to zero over time. Moreover, considering $D_i = 0$ for $i = 1,2,\dots$ and the integrator of $K_i(s)$ and two integrators of $L_i(s) = P_i(s)K_i(s)$, the steady-state water-level error of pool $i = 1,2,\dots$ is computed as follows

$$\begin{aligned}\lim_{t\to\infty} e_i(t) &= \lim_{s\to 0} sE_i(s)\\ &= \lim_{s\to 0} s\frac{P_i(s)}{1+L_i(s)e^{-\tau_i s}}(1+K_i(s)F_i(s)e^{-\tau_i s})V_i(s)\\ &= 0 + \lim_{s\to 0} s\frac{L_i(s)e^{-\tau_i s}}{1+L_i(s)e^{-\tau_i s}}F_i(s)V_i(s)\\ &= \lim_{s\to 0} s\frac{L_i(s)e^{-\tau_i s}}{1+L_i(s)e^{-\tau_i s}}F_i(s)(\frac{d_0}{s}+\tilde{V}_i(s))\\ &= \lim_{s\to 0} \frac{L_i(s)e^{-\tau_i s}}{1+L_i(s)e^{-\tau_i s}}F_i(s)d_0\\ &= 1\times\lim_{s\to 0} F_i(s)d_0 \qquad (2.19)\\ &= 0 + \lim_{s\to 0} P_i(s)(1-\frac{e^{-\tau_i s}}{1+T_{c,i}s})d_0\\ &= \lim_{s\to 0} \frac{1}{\alpha_i s}\frac{1+T_{c,i}s-e^{-\tau_i s}}{1+T_{c,i}s}d_0\\ &= \lim_{s\to 0} \frac{1}{\alpha_i}\frac{T_{c,i}+\tau_i e^{-\tau_i s}}{1+2T_{c,i}s}d_0\\ &= \frac{T_{c,i}+\tau_i}{\alpha_i}d_0 \text{ for } i = 1,2,\dots, \qquad (2.20)\end{aligned}$$

where $\tilde{V}_i(s)$ is the Laplace transform of $\tilde{v}_i(t)$ with stable singularities and the second last inequality is derived by applying the L'Hospital's rule when $s\to 0$ along the real axis. Recall that $P_i(s) = \frac{1}{\alpha_i s}$.

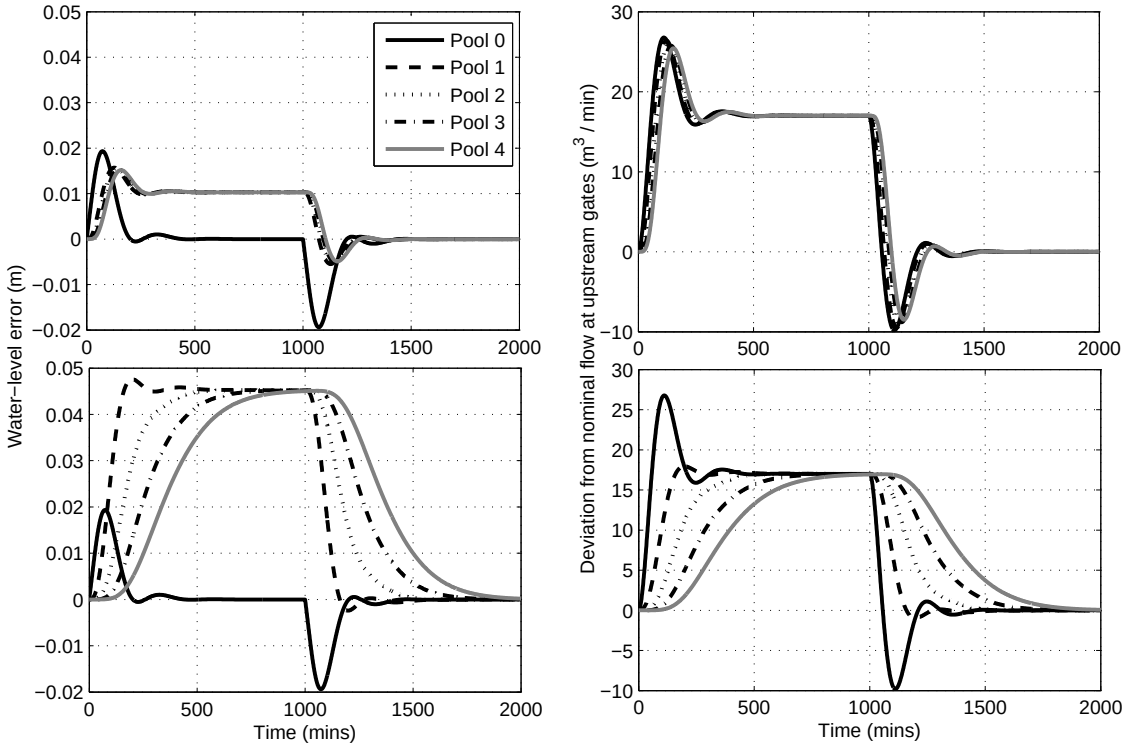

Figure 2.5: Simulations with $T_{V_{f,i}\to V_{f,i+1}}(s) = \frac{1}{1+T_c s}$, top plot: $T_c = 10$, bottom plot: $T_c = 100$.

Steady-state water-level error of the bottom pool, $e_0(t)$, is zero as the feedforward path is not applied, $F_i(s) = 0$. □

Remark: The steady-state water-level error off-sets are proportional to $T_{c,i}$ and decrease with a low-pass filter of a larger bandwidth.

In other words, increasing $T_{c,i}$ results in larger water-level errors and smaller peaks of the flow over gates. This is illustrated via simulations of a channel of Table 1.1 in two cases $T_{c,i} = T_c =$ 10, 100 in Figure 2.5. As plotted, higher attenuation rate of the flow peaks is achieved with a low-pass filter of a smaller cut-off frequency, $\frac{1}{T_c}$, while steady-state water-level errors are increased.

Although flow transients attenuation due to flow offtake disturbances are desired, water-levels are also important as they are considered as a proxy to provide flow at supply points. Therefore, even though transients are attenuated with the non-constant level reference scheme introduced, water-level errors should be taken into consideration at steady-state since a non-zero error means water storage of pool is utilised.

Lemma 2.1. *It is not possible to choose $F_i(s)$ such that zero steady-state water-level errors is achieved in response to a step offtake d_0.*

Proof. According to (2.19), for zero steady-state water-level errors,

$$\lim_{t\to\infty} e_i(t) = \lim_{s\to 0} F_i(s)d_0 = 0 \tag{2.21}$$

has to hold, requiring

$$\lim_{s\to 0} F_i(s) = 0.$$

Since, when applying the Final Value Theorem, the limit is taken along the real axis, then we can apply the L'Hopital's rule for $s = \sigma \in \mathbb{R}$:

$$\begin{aligned}
\lim_{\sigma\to 0} F_i(\sigma) &= \lim_{\sigma\to 0} -\frac{G_i(\sigma)}{K_i(\sigma)} + P({}_i\sigma)(1 - G_i(\sigma)e^{-\tau_i\sigma}) \\
&= \lim_{\sigma\to 0} \frac{1}{\alpha_i\sigma}(1 - G_i(\sigma)e^{-\tau_i\sigma}) \\
&= \lim_{\sigma\to 0} \frac{-\frac{dG_i(\sigma)}{d\sigma}e^{-\tau_i\sigma} + \tau_i G_i(\sigma)e^{-\tau_i\sigma}}{\alpha_i} \\
&= \lim_{\sigma\to 0} \frac{-\frac{dG_i(\sigma)}{d\sigma} + \tau_i G_i(\sigma)}{\alpha_i}.
\end{aligned} \tag{2.22}$$

In order for this to be 0, $\tau_i G_i(0) = \frac{dG_i}{d\sigma}(0)$ is needed. Since $\tau_i G_i(0) > 0$, as implied by $\tau_i > 0$ and $G_i(0) = 1$, $\frac{dG_i}{d\sigma}(0) > 0$ and thus $\exists\sigma_0 > 0$, s.t. $|G(\sigma_0)| > 1$ which implies $\|G(.)\|_\infty > 1$ and the automated channel is string instable in the L_∞-to-L_∞ sense. □

2.7 Decentralised Lead Compensator Distant-Downstream Control

The proposed distributed distant-downstream scheme which is a decentralised feedback with a flow to reference feedforward control with the local control structure of Figure 1.16 and $F_i(s)$ chosen as in (2.11) does not achieve zero steady-state water-level error. Using a completely decentralised feedback controller that does not include an integral action will also yield non-zero steady-state water-level errors in response to a step offtake following the discussion in Section 1.3.4. Therefore, in this section, the performance of decentralised feedback with feedforward control is compared to the completely decentralised feedback distant-downstream scheme.

The design of a feedback control of Figure 1.7 is considered here with the same local control objectives as in Section 1.3.4 without the zero steady-state water-level error requirement. The cross-over frequency, $\omega_{c,i} < \frac{1}{\tau_i}$ needs to hold to avoid poor phase margin due to the phase lag associated with the delay [27]. Local loop-gain $L_i(s) = K_i'(s)P_i(s)$ has an integrator due to $P_i(s)$, thus for robustness to the neglected high frequency wave dynamics, a roll-off is included in the $K_i'(s)$. Around cross-over, phase contribution of $L_i(s)$ is about -90°, not violating closed-loop stability. Therefore, the local controller is picked as

$$K_i' = \frac{\kappa_i'}{1+\rho_i' s}. \tag{2.23}$$

With K_i' in the control loop of purely decentralised scheme, steady-state water-level error in response to a step at $d_0(t)$ and $d_i(t) = 0$ for $i = 1,2,\ldots$ is

$$\begin{aligned}\lim_{t\to\infty} e_i(t) &= \lim_{s\to 0} sE_i(s)\\ &= \lim_{s\to 0} s\frac{P_i(s)}{1+P_i(s)K_i'(s)e^{-\tau_i s}}V_i(s)\\ &= \frac{1}{\kappa_i'}d_0 \text{ for } i = 1,2,\ldots.\end{aligned} \tag{2.24}$$

Therefore, smaller steady-state water-level errors can be achieved by making the gain of the controller larger, however, that implies larger control input values, larger crossover frequency, and larger high frequency magnitudes which reduces robustness to unmodeled wave dynamics.

The flow-to-flow transfer function is

$$\begin{aligned}T_{V_i\to U_i} &= \frac{L_i(s)}{1+L_i(s)e^{-\tau_i s}}\\ &= \frac{\kappa_i'}{\alpha_i s(1+\rho_i' s)+\kappa_i' e^{-\tau_i s}}\end{aligned}$$

for the controller chosen as in (2.23). Although it may be possible to satisfy $\|T_{V_i\to U_i}\|_\infty \leq 1$ with some choice of controller parameters, however, systematically designing controllers that achieve $\|\mathscr{L}^{-1}(T_{V_i\to U_i}(s))\|_1 \leq 1$ is our concern.

A comparison of frequency responses of the open-loop transfer function of Figure 1.7 without the delay component is carried out. A channel with specifications as in Table 1.1 is used here with

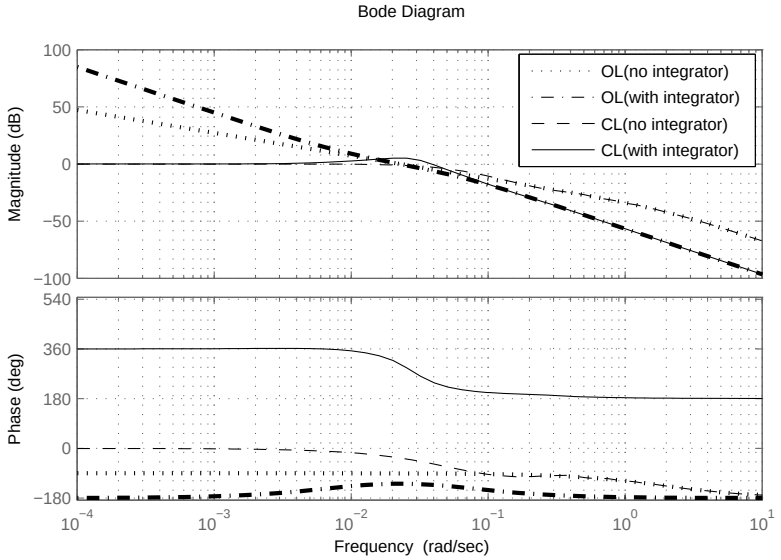

Figure 2.6: Bode plot of open-loop and closed-loop transfer function of the system with and without integrator in the controller($\kappa_i = 1000, \rho_i = 2.2$).

controller parameters designed to yield the required control objectives. The feedback controller of Section 1.3.4 and controller (2.23) are considered for comparison. Corresponding bode plots are shown in Figures 2.6, 2.8, and 2.10. Simulations of the channel with these controllers are plotted in Figures 2.7, 2.9, and 2.11 under an identical scenario to that of Figure 2.5. As can be seen from Figure 2.6, larger high frequency loop gain may be needed to achieve non-amplification of transient flows as shown in Figure 2.7. On the other hand, reducing range of frequencies that the controller magnitude is large, to decrease sensitivity to high frequency uncertainties, by reducing the controller gain κ_i' results in larger steady-state water-level errors according to (2.24). In addition, reducing high frequency gain by increasing ρ_i', results in $\|T_{V_i \to U_i}\|_\infty > 1$ leading to flow amplifications, see Figures 2.8 and 2.9. A non-amplification performance can be achieved by decreasing the controller gain as in Figure 2.11, however, this results in larger water-level offsets. Therefore, there exists a trade-off between flow transients attenuation and steady-state water-level errors.

Hence, reducing steady-state water-level errors is at the price of increasing sensitivity to unmodeled wave dynamics and also amplification of flow transients. The new distributed distant-downstream control structure with a flow-to-reference feedforward path is a systematic method of

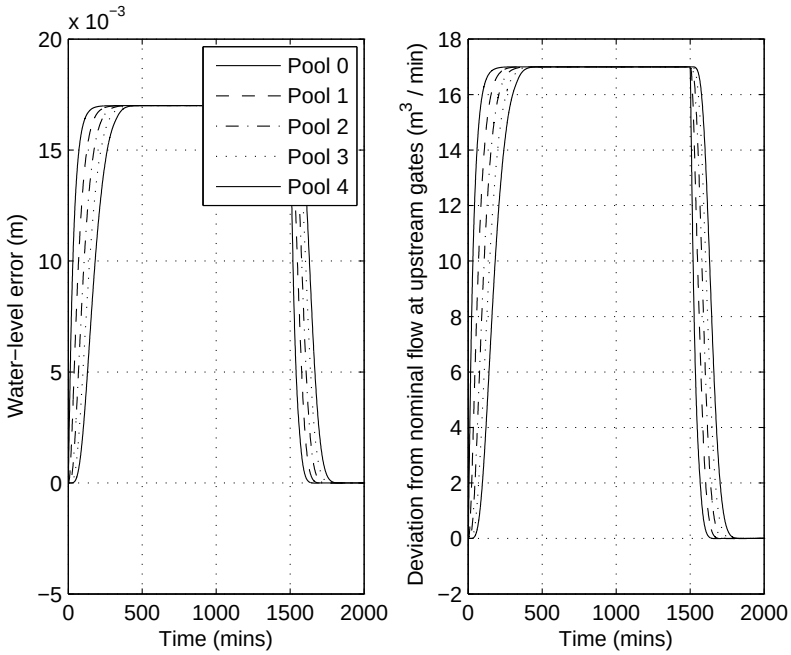

Figure 2.7: Simulation of a channel under completely decentralised control with no integral action($\kappa_i = 1000, \rho_i = 2.2$).

achieving flow transients attenuation, but with non-zero steady-state water-level errors.

2.8 Summary

Attenuation of the effect of flow disturbances propagating along an irrigation channel is gained with the water-level references effectively adjusted on the basis of downstream flow via the feed-forward path. This is achieved at the price of having to exploit water storage in steady-state for step changes in flow load, not just during transients. This shows, if the knowledge of the interaction is used in reference adjustment, performance will improve. In order to accommodate for the case that offtakes are drawn at several points, linear growth of the transients along the string needs to be allowed. This is inevitable due to the steady-state flow matching requirement along the channel. The design method is scalable and allows for pool by pool synthesis in a decentralised fashion. In next chapter, we will analyse robustness of the feedforward scheme to uncertainties in the plant model, particularly to the water transportation delay.

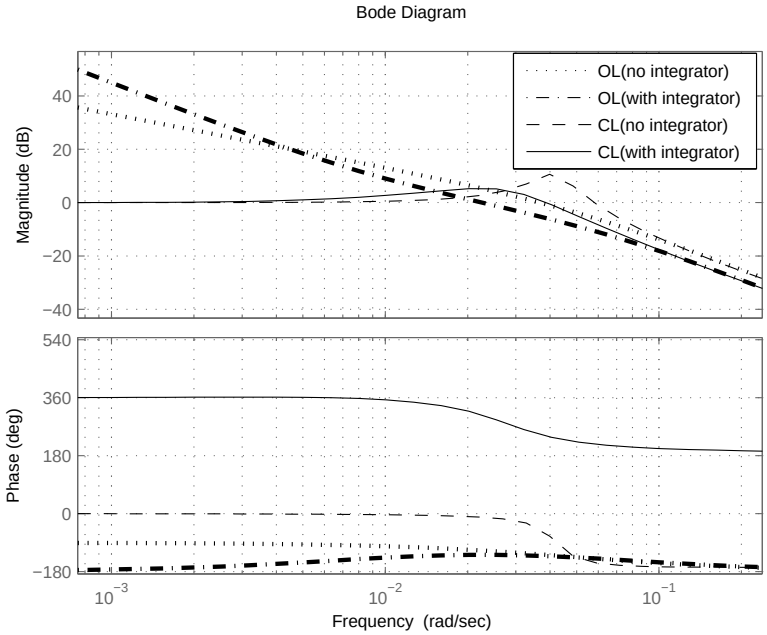

Figure 2.8: Bode plot of open-loop and closed-loop transfer function of the system with and without integrator in the controller($\kappa_i = 1000, \rho_i = 15.2$).

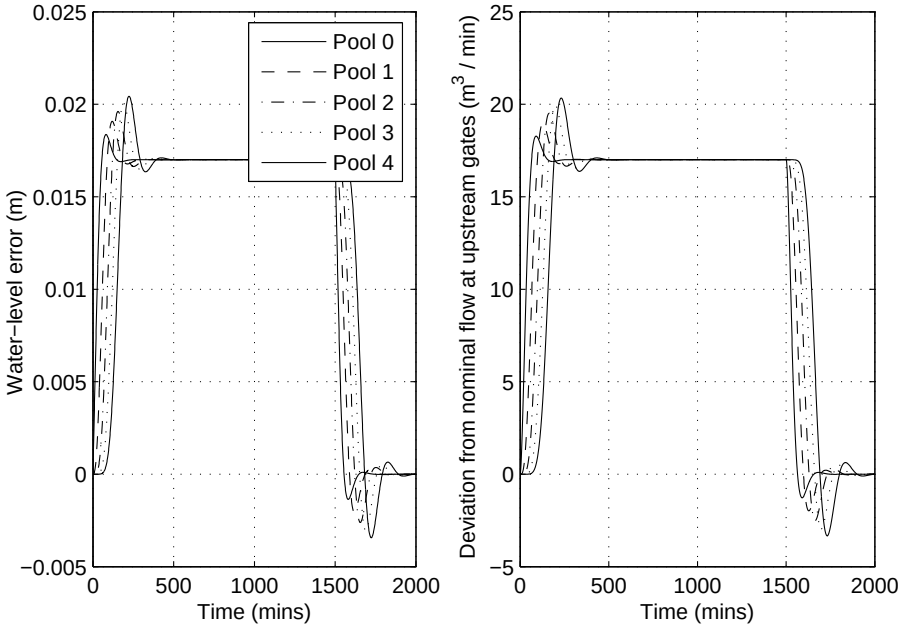

Figure 2.9: Simulation of a channel under completely decentralised control with no integral action($\kappa_i = 1000, \rho_i = 15.2$).

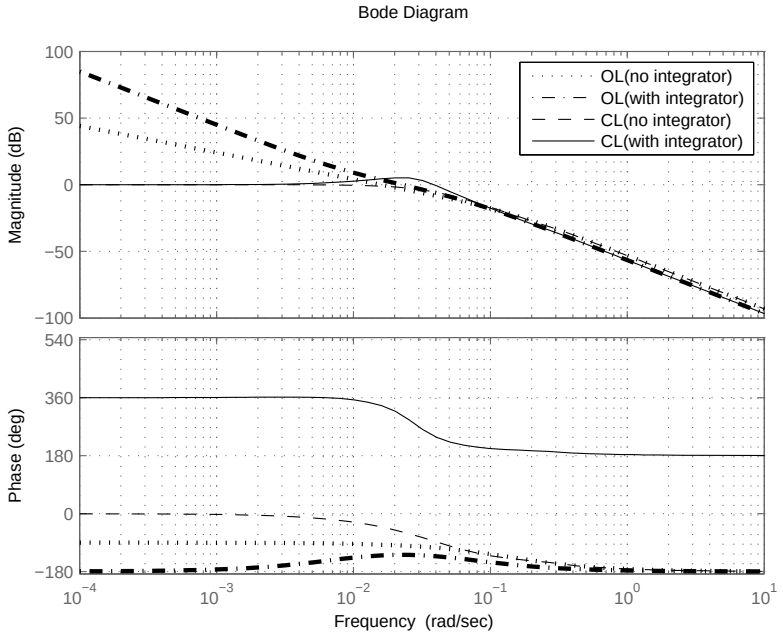

Figure 2.10: Bode plot of open-loop and closed-loop transfer function of the system with and without integrator in the controller($\kappa_i = 700, \rho_i = 5.2$).

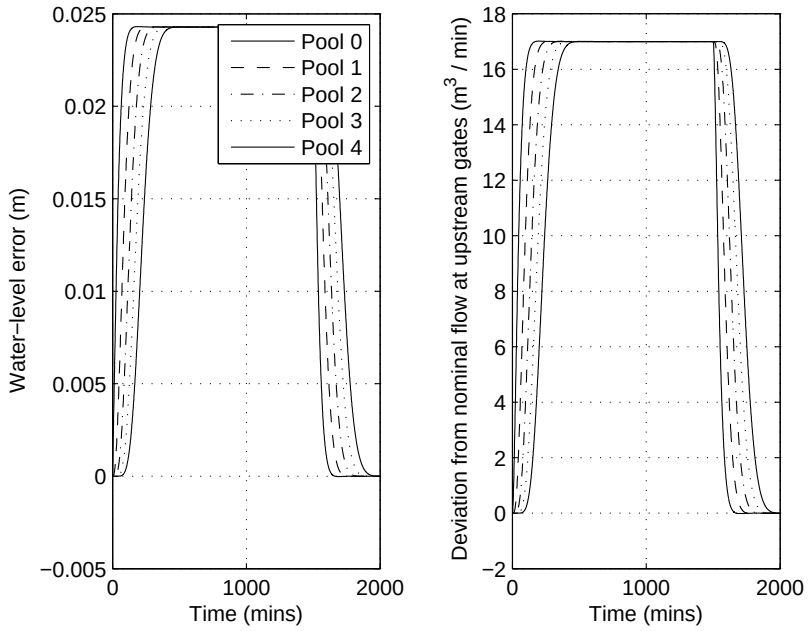

Figure 2.11: Simulation of a channel under completely decentralised control with no integral action($\kappa_i = 700, \rho_i = 5.2$).

This page intentionally left blank.

Chapter 3

Robustness Analysis of a Nominally L_∞-to-L_∞ String-Stable Automated Channel

Robustness of the distributed distant-downstream control architecture for irrigation channels proposed in Chapter 2 is analysed. The robustness of L_∞-to-L_∞ string-stability is investigated via known LMI based analysis conditions for bounding the L_∞-to-L_∞ induced norm of systems with uncertain transfer functions. Application of the conditions, which are only sufficient, does not confirm L_∞-to-L_∞ string-stability robustness for the channel example presented. However, the robust induced-norm bounds obtained for substantial pool-delay parameter uncertainty are such that the degree to which transient flow peaks could be amplified remains reasonable at worst. Illustrative simulations are presented.

3.1 Introduction

In Chapter 2, a nominal spatially-stable propagation of the transient peaks is achieved with a new distributed distant-downstream control architecture at the expense of steady-state water-level error off-sets for step changes in offtake load and constant water-level set-points, [3]. In particular, focusing on the flow interactions between pools, the new scheme involves augmentation of each decentralised local feedback controller with a feedforward path from the downstream flow to the controller input. This translates to an adjustment of the local water-level reference on the basis of downstream flow.

While this design process can nominally achieve peak-to-peak or L_∞-to-L_∞ string-stability that

concerns the spatial propagation of transient flow peaks, the robustness of this property to model parameter uncertainty is of practical concern. Robustness of the peak-to-peak gain of the automated flow interactions between neighbouring pools is investigated here via LMI based analysis conditions from [72] for bounding the L_∞-to-L_∞ induced norm of systems with uncertain transfer functions. While the application of these conditions, which are only sufficient, does not confirm robustness of the L_∞-to-L_∞ string-stability property, the robust induced-norm bounds obtained show that the degree to which the property is violated remains mild in the face of substantial uncertainty. That is, transients may be spatially amplified, but only slightly at worst, compared to other distributed distant-downstream control schemes.

This chapter is organised as follows: Preliminaries including LMI conditions for nominal and robust peak-to-peak performance are introduced in Section 3.3. Section 3.4 introduces robustness analysis techniques for a state-space model with parametric uncertainty. Section 3.5 contains analysis of robustness to uncertainty in pool delay parameter followed by simulations for a channel with uncertainty. A summary of the chapter is presented at the end.

3.2 Notations

Let the L_∞ space consist of all vector-valued continuous time signals, $x(t) \in \mathbb{R}^n$, for which $\|x\|_\infty := \operatorname{ess\,sup}_t \|x(t)\| < \infty$. Then the worst case L_∞ to L_∞ induced norm or peak-to-peak norm of a system M mapping $w(t)$ to $z(t)$ is defined as

$$\|M\|_{p-p} := \sup_{w \in L_\infty} \frac{\|z\|_\infty}{\|w\|_\infty}. \tag{3.1}$$

Two subspaces $\mathbf{X}$ and $\mathbf{Y}$ of a subspace $\mathbf{W}$ are said to be complementary if $\mathbf{X} \cap \mathbf{Y} = \{0\}$ and $\mathbf{X} + \mathbf{Y} = \mathbf{W}$. The latter means that any vector $w \in \mathbf{W}$ can be (uniquely, because $\mathbf{X} \cap \mathbf{Y} = \{0\}$) represented as $w = x + y$, $x \in \mathbf{X}$, $y \in \mathbf{Y}$.

A symmetric $n \times n$ real matrix P is said to be positive (semi-)definite, denoted by $P > (\geq) 0$, if $x^T P x > (\geq) 0$, $\forall x \neq 0$ in $\mathbb{R}^n$ ($\forall x \in \mathbb{R}^n$). P is negative (semi-)definite if $-P$ is positive (semi-)definite. A symmetric $n \times n$ real matrix P is positive definite on a subspace $\mathbf{S}$ if $x^T P x > 0$, $\forall x \neq 0$ in $\mathbf{S}$. The Kernel of a real $m \times n$ matrix P is denoted by $\ker(P) := \{x \in \mathbb{R}^n | Px = 0\}$.

The Schur Complement theorem is defined as follows:

Lemma 3.1. *For any symmetric matrix, H, of the form*

$$H = \begin{bmatrix} A & B \\ B^T & C \end{bmatrix},$$

if C is invertible then the following properties hold:

(i) $H > 0$ *if and only if* $C > 0$ *and* $A - BC^{-1}B^T > 0$.

(ii) *If* $C > 0$, *then* $H \geq 0$ *if and only if* $A - BC^{-1}B^T \geq 0$.

Convex hull of real matrices $\delta_1, \cdots, \delta_H$ *is denoted by* $Co\{\delta_1, \delta_2 \cdots, \delta_H\}$.

3.3 Preliminaries

3.3.1 Nominal Peak-to-Peak Norm Performance

In this section we will be reviewing sufficient conditions guaranteeing L_∞ to L_∞ induced norm of a nominal dynamical system.

Assume the linear time invariant state-space representation of a closed-loop system is

$$M_{22} : \begin{cases} \dot{x}_{\text{cl}} = Ax_{\text{cl}} + B_w w_2 \\ z_2 = C_z x_{\text{cl}} + D_{zw} w_2 \end{cases}, \; x_{\text{cl}}(0) = 0, \tag{3.2}$$

where $x_{\text{cl}} \in \mathbb{R}^n$, $w_2 \in \mathbb{R}^{n_w}$, and $z_2 \in \mathbb{R}^{n_z}$ denote the state vector, exogenous inputs and control performance signal of the closed-loop system, respectively [73]. The system (3.2) is a mapping from $w_2 \in L_\infty$ to $z_2 \in L_\infty$ and we are interested in peak-peak norm, $\|M_{22}\|_{p-p}$.

A non-strict upper bound γ on the L_∞ to L_∞ induced norm can be characterised in terms of the sufficient LMI (linear matrix inequality) conditions in Lemma 3.2 which is established following the analysis technique described in [72] (where the corresponding strict bound result can be found).

Lemma 3.2. *Considering state-space realisation of* M_{22} *in (3.2), if there exists* $X = X^T > 0$, $\lambda > 0$

and $\mu > 0$ *such that*

$$\begin{bmatrix} A^T X + XA + \lambda X & XB \\ B^T X & -\mu I \end{bmatrix} < 0 \text{ and} \tag{3.3}$$

$$\begin{bmatrix} \lambda X & 0 & C^T \\ 0 & (\gamma - \mu) I & D^T \\ C & D & \gamma I \end{bmatrix} \geq 0, \tag{3.4}$$

then the L_∞ *to* L_∞ *induced norm of the system is no larger than* $\gamma > 0$*, i.e.* $\|M_{22}\|_{p-p} \leq \gamma$.

Proof. Considering system (3.2), inequality (3.3) implies

$$\frac{d}{dt} x_{\text{cl}}^T X x_{\text{cl}} + \lambda x_{\text{cl}}^T X x_{\text{cl}} - \mu w_2^T w_2 \leq 0, \ \forall x_{\text{cl}}, w_2.$$

Let $v = \frac{d}{dt}(x_{\text{cl}}^T X x_{\text{cl}}) + \lambda x_{\text{cl}}^T X x_{\text{cl}}$. Then for any $h > 0$,

$$x_{\text{cl}}^T(h) X x_{\text{cl}}(h) = e^{-\lambda h} x_{\text{cl}}^T(0) X x_{\text{cl}}(0) + \int_0^h e^{-\lambda(h-t)} v(t) dt$$

and $v(h) \leq \mu w_2^T(h) w_2(h)$. Thus, using $x(0) = 0$, it follows that

$$x_{\text{cl}}^T(h) X x_{\text{cl}}(h) \leq \mu \int_0^h e^{-\lambda(h-t)} w_2^T(t) w_2(t) dt.$$

Hence,

$$x_{\text{cl}}^T X x_{\text{cl}} \leq \frac{\mu}{\lambda} \|w_2\|_\infty^2. \tag{3.5}$$

The Schur complement applied to (3.4) gives

$$\frac{z_2^T z_2}{\gamma} \leq \lambda x_{\text{cl}}^T X x_{\text{cl}} + w_2^T w_2 (\gamma - \mu),$$

whereby using (3.5) yields

$$\|z_2\|_\infty^2 \leq \gamma^2 \|w_2\|_\infty^2.$$

This is the non-strict bound claimed. □

Modeling of uncertainty follows in next subsection.

3.3.2 Linear Fractional Transformation Based Uncertainty Modeling

To establish L_∞ to L_∞ induced norm performance bounds for parameterically uncertain transfer functions, an LFT (linear fractional transform) modeling framework can be employed [38].

Consider a transfer function

$$M(s) = \begin{bmatrix} M_{11}(s) & M_{12}(s) \\ M_{21}(s) & M_{22}(s) \end{bmatrix}$$

and a $\Delta \in \mathbb{R}^{q_1 \times p_1}$ that represents parametric uncertainty according to the following set of equations

$$\begin{bmatrix} z_1 \\ z_2 \end{bmatrix} = M \begin{bmatrix} w_1 \\ w_2 \end{bmatrix},$$
$$w_1 = \Delta z_1, \tag{3.6}$$

as depicted in Figure 3.1. Then, the transfer function of the upper LFT mapping w_2 to z_2, derived by closing the upper loop of Figure 3.1, is

$$\mathscr{F}_u(M,\Delta) = M_{22} + M_{21}(I - \Delta M_{11})^{-1}\Delta M_{12}, \tag{3.7}$$

given that the inverse $(I - \Delta M_{11})^{-1}$ exists. In fact, M_{22} is the transformation of the nominal mapping (3.2).

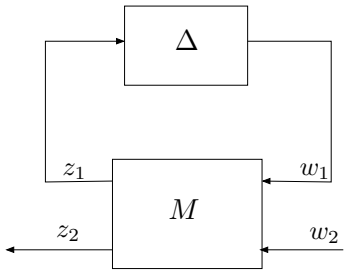

Figure 3.1: Upper LFT representation of $\mathscr{F}_u(M,\Delta)$.

If state-space realisation of $M(s)$ is

$$\left[\begin{array}{c|cc} A & B_1 & B_2 \\ \hline C_1 & D_{11} & D_{12} \\ C_2 & D_{21} & D_{22} \end{array}\right], \tag{3.8}$$

then a state-space realisation of $\mathscr{F}_u(M,\Delta)$ is given by

$$\left[\begin{array}{c|c} A(\Delta) & B(\Delta) \\ \hline C(\Delta) & D(\Delta) \end{array}\right], \tag{3.9}$$

where

$$\begin{aligned} A(\Delta) &:= A + B_1(I-\Delta D_{11})^{-1}\Delta C_1, \\ B(\Delta) &:= B_2 + B_1(I-\Delta D_{11})^{-1}\Delta D_{12}, \\ C(\Delta) &:= C_2 + D_{21}(I-\Delta D_{11})^{-1}\Delta C_1, \text{ and} \\ D(\Delta) &:= D_{22} + D_{21}(I-\Delta D_{11})^{-1}\Delta D_{12}. \end{aligned} \tag{3.10}$$

Definition 3.1. *The LFT representation from w_2 to z_2 in (3.7) is defined to be well-posed if $(I-\Delta M_{11})^{-1}$ exists or $I-\Delta D_{11}$ is non-singular for all $\Delta \in \mathbf{\Delta}$.*

3.3.3 Full Block S-Procedure

The full block S-procedure is a technique that allows to equivalently translate robust performance objectives characterised in terms of a common Lyapunov function into the corresponding analysis test with multipliers [74, 75]. The S-procedure, [76], can be used in similar applications, while introducing some conservatism in general due to the block diagonal structure of multipliers [77] in contrast to full block S-procedure where the full block multipliers are used [75]. LMI conditions for testing robust performance, similar to [75], are used here. These conditions are derived by applying the full block S-procedure to inequalities in terms of rational functions of uncertainties.

The strict version of full block S-procedure of [74, 75] is used here, in addition to non-strict version, which to the best of our knowledge, has not been used in the literature. A prove of this is

proposed in Lemma 3.4.

Let $\mathbf{S} \subset \mathbb{R}^n$ be a subspace, N a fixed symmetric matrix, and $T \in \mathbb{R}^{l\times n}$ a full row rank matrix. For $\boldsymbol{U} \subset \mathbb{R}^{k\times l}$ a compact set of full row rank matrices and $U \in \boldsymbol{U}$ let

$$\mathbf{S}_U := \mathbf{S} \cap \ker(UT) = \{x \in \mathbf{S} | Tx \in \ker(U)\}.$$

In the following, it is assumed that $\boldsymbol{U}$ is such that all subspaces $\mathbf{S}_U$ are complementary to a fixed subspace $\mathbf{S}_0 \subset \mathbf{S}$ that

$$\dim(\mathbf{S}_0) \geq k \text{ and } N \geq 0 \text{ on } \mathbf{S}_0.$$

Lemma 3.3. *[74] The condition*

$$\forall U \in \boldsymbol{U} : \boldsymbol{S}_U \cap \boldsymbol{S}_0 = \{0\},\ N < 0 \text{ on } \boldsymbol{S}_U$$

holds if and only if there exists a symmetric matrix (multiplier) P that satisfies

$$\forall U \in \boldsymbol{U} : \begin{cases} N + T^T P T < 0 \text{ on } \boldsymbol{S} \\ P > 0 \text{ on } \ker(U). \end{cases} \tag{3.11}$$

Lemma 3.4. *The condition*

$$\forall U \in \boldsymbol{U} : \boldsymbol{S}_U \cap \boldsymbol{S}_0 = \{0\},\ N \leq 0 \text{ on } \boldsymbol{S}_U \tag{3.12}$$

holds if and only if there exists a symmetric matrix P that satisfies

$$\forall U \in \boldsymbol{U} : \begin{cases} N + T^T P T \leq 0 \text{ on } \boldsymbol{S} \\ P \geq 0 \text{ on } \ker(U). \end{cases} \tag{3.13}$$

Proof. **Sufficiency**: If condition (3.13) holds then $\forall \hat{x} \in \mathbf{S}_U$ such that

$$\begin{cases} \hat{x}^T N \hat{x} + \hat{x}^T T^T P T \hat{x} \leq 0 \\ \hat{x}^T T^T P T \hat{x} \geq 0, \end{cases} \tag{3.14}$$

It follows that $\hat{x}^T N\hat{x} \leq 0$. Therefore, condition (3.12) holds.

Necessity: Suppose to the contrapositive for all matrices P there exists a $U \in \mathbf{U}$ and an $\hat{x} \in \mathbf{S}_U$ such that

$$\begin{cases} \hat{x}^T N\hat{x} + \hat{x}^T T^T PT\hat{x} > 0 \text{ or} \\ \hat{x}^T T^T PT\hat{x} < 0 \end{cases} \tag{3.15}$$

resulting in 3 cases to be analysed separately.

Case 1 Suppose $\hat{x}^T N\hat{x} + \hat{x}^T T^T PT\hat{x} > 0$ and $\hat{x}^T T^T PT\hat{x} < 0$. It follows that $\exists \hat{x} \in \mathbf{S}_U$ such that $\hat{x}^T N\hat{x} > 0$ which contradicts condition (3.12).

Case 2 Suppose $\hat{x}^T N\hat{x} + \hat{x}^T T^T PT\hat{x} > 0$ and $\hat{x}^T T^T PT\hat{x} \geq 0$. It follows that $\exists \hat{x} \in \mathbf{S}_U$ such that $\hat{x}^T N\hat{x} > 0$ which contradicts condition (3.12).

Case 3 Suppose $\hat{x}^T N\hat{x} + \hat{x}^T T^T PT\hat{x} \leq 0$ and $\hat{x}^T T^T PT\hat{x} < 0$. It follows that $\exists \hat{x} \in \mathbf{S}_U$ such that $\hat{x}^T N\hat{x} > 0$ which contradicts condition (3.12).

Therefore, the result follows as claimed. □

3.4 Robust Performance Analysis

In order to find an upper bound on the L_∞ to L_∞ induced norm of $\mathscr{F}_u(M,\Delta)$ with state-space representation (3.9), Lemma 3.2 and the Schur Complement are applied :

Lemma 3.5. *[75] Given an uncertainty set* $\mathbf{\Delta}$ *of appropriately dimensioned real matrices and a scalar* $\gamma > 0$*, if the interconnection (3.7) is well-posed and* $\exists\, X = X^T,\ \lambda > 0,\ \mu$ *such that*

$$\left[\begin{array}{cc} I & 0 \\ A(\Delta) & B(\Delta) \\ \hline 0 & I \\ C(\Delta) & D(\Delta) \end{array}\right]^T \left[\begin{array}{cc|cc} \lambda X & X & 0 & 0 \\ X & 0 & 0 & 0 \\ \hline 0 & 0 & -\mu I & 0 \\ 0 & 0 & 0 & 0 \end{array}\right] \left[\begin{array}{cc} I & 0 \\ A(\Delta) & B(\Delta) \\ \hline 0 & I \\ C(\Delta) & D(\Delta) \end{array}\right] < 0, \text{ and} \tag{3.16}$$

$$\left[\begin{array}{cc} I & 0 \\ \hline 0 & I \\ C(\Delta) & D(\Delta) \end{array}\right]^T \left[\begin{array}{c|cc} -\lambda X & 0 & 0 \\ \hline 0 & (\mu-\gamma)I & 0 \\ 0 & 0 & \frac{I}{\gamma}I \end{array}\right] \left[\begin{array}{cc} I & 0 \\ \hline 0 & I \\ C(\Delta) & D(\Delta) \end{array}\right] \leq 0, \tag{3.17}$$

for all $\Delta \in \mathbf{\Delta}$*, then the poles of* $A(\Delta)$ *are in the left half plane and* $\|\mathscr{F}_u(M,\Delta)\|_{p-p} \leq \gamma, \ \forall \Delta \in \mathbf{\Delta}$.

Conditions (3.16) and (3.17) involve matrices that are functions of the uncertainty $\Delta \in \mathbf{\Delta}$ which is difficult to verify. Applying the so-called full block *S*-procedure, strict and non-strict versions, equivalent conditions can be derived [74, 75]. Proof of similar conditions can be found in [74, 75].

Lemma 3.6. *Given the set of real matrices* $\mathbf{\Delta}$*, if the interconnection (3.7) is well-posed with all* $\Delta \in \mathbf{\Delta}$ *and* $\exists\, X = X^T,\ \lambda > 0,\ \mu,\ Q_1 = Q_1^T,\ S_1,\ R_1 = R_1^T,\ Q_2 = Q_2^T,\ S_2,\ R_2 = R_2^T,\ \gamma > 0$ *such that*

$$\begin{aligned} &\begin{bmatrix} \Delta \\ I \end{bmatrix}^T \begin{bmatrix} Q_1 & S_1 \\ S_1^T & R_1 \end{bmatrix} \begin{bmatrix} \Delta \\ I \end{bmatrix} > 0, \\ &\begin{bmatrix} \Delta \\ I \end{bmatrix}^T \begin{bmatrix} Q_2 & S_2 \\ S_2^T & R_2 \end{bmatrix} \begin{bmatrix} \Delta \\ I \end{bmatrix} \geq 0, \textit{ for all } \Delta \in \mathbf{\Delta} \end{aligned} \tag{3.18}$$

$$*^T \left[\begin{array}{cc|cc|cc} \lambda X & X & 0 & 0 & 0 & 0 \\ X & 0 & 0 & 0 & 0 & 0 \\ \hline 0 & 0 & Q_1 & S_1 & 0 & 0 \\ 0 & 0 & S_1^T & R_1 & 0 & 0 \\ \hline 0 & 0 & 0 & 0 & -\mu I & 0 \\ 0 & 0 & 0 & 0 & 0 & 0 \end{array}\right] \left[\begin{array}{ccc} I & 0 & 0 \\ A & B_1 & B_2 \\ \hline 0 & I & 0 \\ C_1 & D_{11} & D_{12} \\ \hline 0 & 0 & I \\ C_2 & D_{21} & D_{22} \end{array}\right] < 0, \textit{ and} \tag{3.19}$$

$$*^T \left[\begin{array}{c|cc|cc} -\lambda X & 0 & 0 & 0 & C_2^T \\ \hline 0 & Q_2 & S_2 & 0 & D_{21}^T \\ 0 & S_2^T & R_2 & 0 & 0 \\ \hline 0 & 0 & 0 & (\mu-\gamma)I & D_{22}^T \\ C_2 & D_{21} & 0 & D_{22} & -\gamma I \end{array}\right] \left[\begin{array}{cccc} I & 0 & 0 & 0 \\ \hline 0 & I & 0 & 0 \\ C_1 & D_{11} & D_{12} & 0 \\ \hline 0 & 0 & I & 0 \\ 0 & 0 & 0 & I \end{array}\right] \leq 0, \tag{3.20}$$

then the poles of $A(\Delta)$ lie in the left half plane and $\|\mathscr{F}_u(M,\Delta)\|_{p-p} \leq \gamma$, $\forall \Delta \in \mathbf{\Delta}$.

Conditions in (3.18) involve the uncertainty $\Delta \in \mathbf{\Delta}$, yielding an infinite number of inequalities needed to be checked. Following [74, 75], these can be equivalently converted to tractable conditions by taking $\mathbf{\Delta}$ to be the convex hull of finite number of matrices if $Q_1 \leq 0$ and $Q_2 \leq 0$ is assumed for convexity, introducing conservatism in general [75]:

Lemma 3.7. *Given real matrices $\delta_1, \cdots, \delta_N$, if the interconnection (3.7) is well-posed for all $\Delta = \delta_n$, $n \in \{1,2,\cdots N\}$ and $\exists\, X = X^T$, $\lambda > 0$, μ, $Q_1 = Q_1^T$, S_1, $R_1 = R_1^T$, $Q_2 = Q_2^T$, S_2, $R_2 = R_2^T$, $\gamma > 0$ such that*

$$
\begin{aligned}
&Q_1 \leq 0,\ Q_2 \leq 0,\\
&\begin{bmatrix} \delta_n \\ I \end{bmatrix}^T \begin{bmatrix} Q_1 & S_1 \\ S_1^T & R_1 \end{bmatrix} \begin{bmatrix} \delta_n \\ I \end{bmatrix} > 0,\ \forall\, n \in \{1,2,\cdots N\},\\
&\begin{bmatrix} \delta_n \\ I \end{bmatrix}^T \begin{bmatrix} Q_2 & S_2 \\ S_2^T & R_2 \end{bmatrix} \begin{bmatrix} \delta_n \\ I \end{bmatrix} \geq 0\ \forall\, n \in \{1,2,\cdots N\},
\end{aligned} \tag{3.21}
$$

$$
*^T \left[\begin{array}{cc|cc|cc} \lambda X & X & 0 & 0 & 0 & 0 \\ X & 0 & 0 & 0 & 0 & 0 \\ \hline 0 & 0 & Q_1 & S_1 & 0 & 0 \\ 0 & 0 & S_1^T & R_1 & 0 & 0 \\ \hline 0 & 0 & 0 & 0 & -\mu I & 0 \\ 0 & 0 & 0 & 0 & 0 & 0 \end{array}\right] \left[\begin{array}{ccc} I & 0 & 0 \\ A & B_1 & B_2 \\ \hline 0 & I & 0 \\ C_1 & D_{11} & D_{12} \\ \hline 0 & 0 & I \\ C_2 & D_{21} & D_{22} \end{array}\right] < 0, \tag{3.22}
$$

$$
*^T \left[\begin{array}{c|cc|cc} -\lambda X & 0 & 0 & 0 & C_2^T \\ \hline 0 & Q_2 & S_2 & 0 & D_{21}^T \\ 0 & S_2^T & R_2 & 0 & 0 \\ \hline 0 & 0 & 0 & (\mu-\gamma) I & D_{22}^T \\ C_2 & D_{21} & 0 & D_{22} & -\gamma I \end{array}\right] \left[\begin{array}{cccc} I & 0 & 0 & 0 \\ \hline 0 & I & 0 & 0 \\ C_1 & D_{11} & D_{12} & 0 \\ \hline 0 & 0 & I & 0 \\ 0 & 0 & 0 & I \end{array}\right] \leq 0, \tag{3.23}
$$

then the poles of $A(\Delta)$ *are in the left half plane and* $\|\mathscr{F}_u(M,\Delta)\|_{p-p} \leq \gamma$, $\forall \Delta \in Co\{\delta_1,\ \delta_2,\ \cdots,\ \delta_N\}$.

Lemma follows from a convexity property based on Q_1 and Q_2 where with $Q_1 \leq 0$ and $Q_2 \leq 0$, (3.18) and (3.21) are equivalent. The bilinear term λX in the LMIs above make the conditions non-convex. On the other hand, the problem is a convex problem in γ for a fixed λ. Solving the LMIs for a grid of λ, a value of λ that yields the smallest possible γ can be identified.

3.5 Robustness to Uncertainty in Pool Delay Parameter

To illustrate an example of the robust performance analysis conditions in Section 3.4, within the context of assessing the string-stability robustness of the distributed control architecture shown in Figure 1.16, this section focuses on time-delay parameter uncertainty.

In order to apply the finite-dimensional state-space based conditions of Lemma 3.7, a Padé approximation of the delay element is used to approximate delay terms in $F_i(s)$ and the feedback path in Figure 1.16. The first order Padé approximation $e^{-\tau_i s} \cong \frac{1-\frac{\tau_i}{2}s}{1+\frac{\tau_i}{2}s}$ is reasonable for the delay component in both the plant model and the feedforward filter $F_i(s)$ at low frequencies and suitable as long as the bandwidth of the closed-loop, i.e. cross-over of $L_i(s)$, and that of $G_i(s)$ is set small enough by $K_i(s)$ and $F_i(s)$, respectively [3]. The approximation of the feedforward path filter is denoted by $F_{p,i}(s)$. Using

$$\frac{1-\frac{\tau_i}{2}s}{1+\frac{\tau_i}{2}s} = -1 + \frac{2}{1+\frac{\tau_i}{2}s},$$

the plant model with uncertain parameter $\tau_i = \tau_{0,i} + \delta_{\tau,i}$, where $\delta_{\tau,i} \in \mathbf{\Delta}_i \subset \mathbb{R}$, and $\mathbf{\Delta}_i$ is a closed interval, has the structure shown in Figure 3.2.

With reference to Figure 3.2, an upper LFT representation of $T_{V_i \to U_i}(\delta_{\tau,i})$ is given by $\mathscr{F}_u(M_i, \delta_{\tau,i})$ in accordance with (3.7), where

$$M_i = \begin{bmatrix} M_{11,i} & M_{12,i} \\ M_{21,i} & M_{22,i} \end{bmatrix}, \tag{3.24}$$

with

$$M_{11,i}(s) = -\frac{s}{2(1+\frac{\tau_{0,i}}{2}s)} + \frac{sK_iP_i}{(1+\frac{\tau_{0,i}}{2}s)^2(1+K_iP_i\frac{1-\frac{\tau_{0,i}}{2}s}{1+\frac{\tau_{0,i}}{2}s})}$$

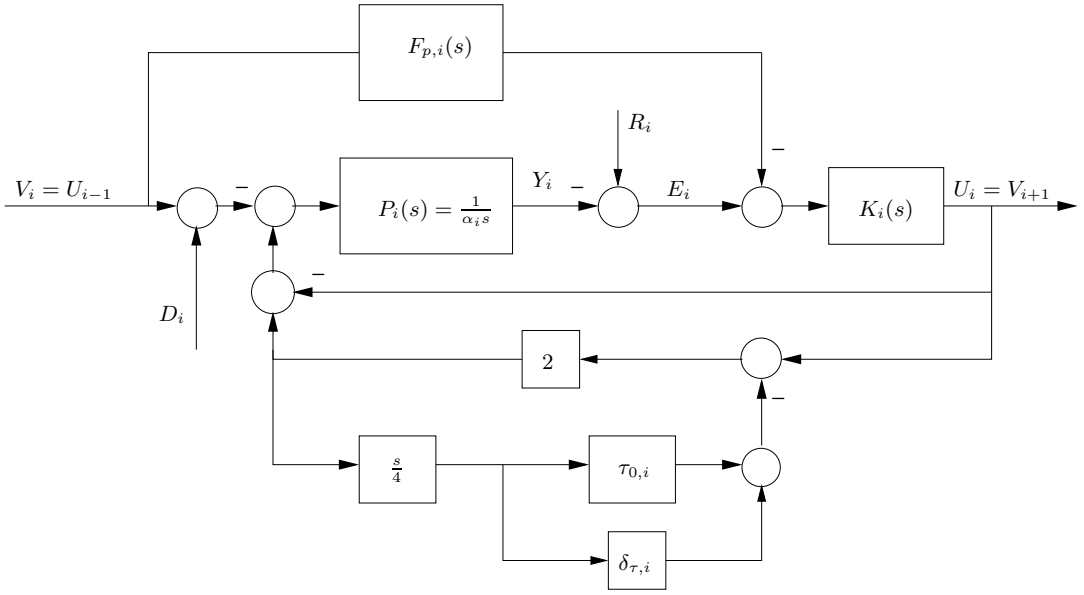

Figure 3.2: Block diagram of a closed-loop with a feedforward of the downstream flow; delay is represented with additive uncertainty.

$$M_{12,i}(s) = \frac{K_i(P_i - F_{p,i})s}{2(1+\frac{\tau_{0,i}}{2}s)(1+K_iP_i\frac{1-\frac{\tau_{0,i}}{2}s}{1+\frac{\tau_{0,i}}{2}s})}$$
$$M_{21,i}(s) = \frac{2K_iP_i}{(1+\frac{\tau_{0,i}}{2}s)(1+K_iP_i\frac{1-\frac{\tau_{0,i}}{2}s}{1+\frac{\tau_{0,i}}{2}s})}$$
$$M_{22,i}(s) = \frac{K_i(P_i - F_{p,i})}{1+K_iP_i\frac{1-\frac{\tau_{0,i}}{2}s}{1+\frac{\tau_{0,i}}{2}s}}.$$

Since $M_{22,i}$ is a SISO transfer function, $\|z_{2,i}\|_\infty$ and $\|w_{2,i}\|_\infty$ represent the supremum on the peak values of the signals. Table 3.1 summarises the smallest achievable γ_i for which the conditions of Lemma 3.7 can be satisfied, given the nominal parameters values specified in Table 1.1 and different uncertainty set ranges. For the identical pools of channel under consideration the flow interactions transfer function, G_i, are considered identical. Since the bound obtained exceeds unity for all cases considered, it is not possible to conclude robustness of the L_∞-to-L_∞ string-stability property. However, it is of note that the bounds are all very close to 1; recall that the gain in transient flow peak as it propagates upstream is bounded as such. The simulations discussed below serve to compare this with the flow peak gain associated with a H_∞ loop-shaping based distributed controller that is designed as described in [21, 45]. The simulations also reveal the

Table 3.1: Bounds on the peak to Peak gain in presence of uncertainty. Parameters are same for all pools.

	τ_i	γ_i	λ_i
$T_{c,i} = 100$	16	1	0.01
	[15,17]	1.0006	0.01
	[14,18]	1.0018	0.01
	[13,19]	1.0042	0.01
	[12,20]	1.008	0.01
$T_{c,i} = 50$	16	1	0.02
	[15,17]	1.0047	0.02
	[14,18]	1.0257	0.019
	[13,19]	1.0632	0.0173
	[12,20]	1.01134	0.0155

conservative nature of the analysis.

Simulations are carried out for a 5-pool channel with model parameters as in Table 1.1, where a flow off-take of $17.7928\frac{\mathrm{m}^3}{\mathrm{min}}$ is drawn for 1000 mins from the most downstream pool. Simulations of a the channel model with nominal delays running under the aforementioned distributed distant-downstream H_∞ loop-shaping based controller are shown in Figure 3.3 for the purpose of comparison. Simulations of channel with uncertainty in the delay parameter equipped with the new decentralised feedback and flow to reference feedforward scheme as described in Chapter 2 are shown in Figures 3.4 and 3.5 for different values of $T_{c,i}$, respectively. Note that for the identical pools under consideration the interactions transfer function, $G_i = 1/(1+T_{c,i}s)$ are designed to be the same. According to Figure 3.3, the peak-to-peak gain of the H_∞ loop-shaping based distributed controller is about 1.15. This is 14% larger than the bound on peak-to-peak gain of the distributed controlled channel under feedforward scheme in the presence of 25% uncertainty in the nominal delay parameter in Table 3.1. The conditions of Lemma 3.7 are only sufficient for L_∞-to-L_∞ string-stability. The bounds on the flow peaks achieved are potentially loose upper bounds. The conservativeness of the method can be seen from the simulations in Figures 3.4 and 3.5 where the flow interactions transfer functions are chosen to be a fast and slow low-pass filter ($T_{c,i} = 10, 100$), respectively. Moreover, simulations are carried out for different uncertainties in the delay parameter. From these, it would appear that the L_∞-to-L_∞ string-stability property is actually robust to delay uncertainty.

According to Table 3.1, if $T_{c,i}$ is chosen large enough, the bound on the peak-to-peak norm

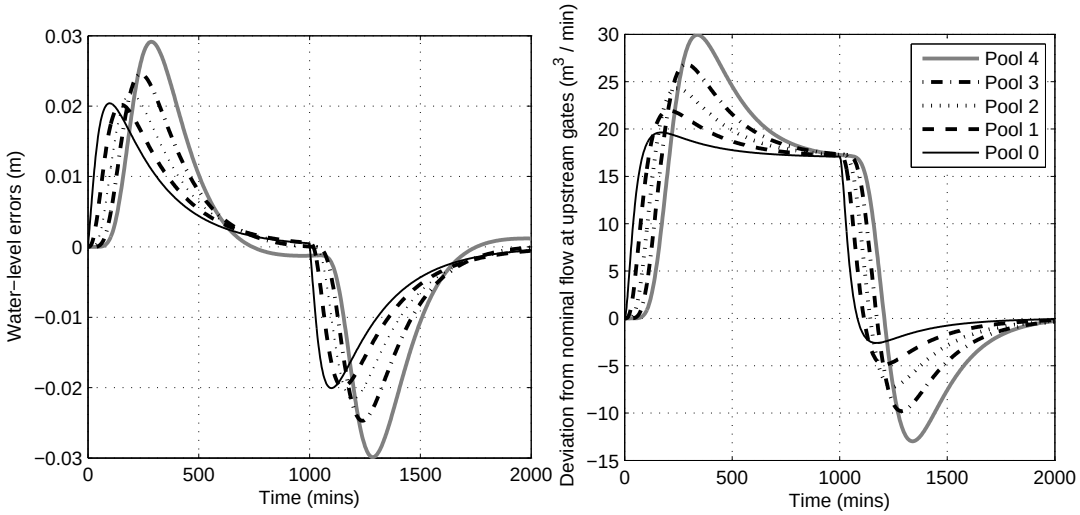

Figure 3.3: Simulations with distributed control scheme.

does not grow much larger than 1. Indeed, $T_{c,i}$ is a design parameter and identifies a trade-off between attenuation of the water flow peaks and steady-state water level errors [3]. Larger $T_{c,i}$ results in smaller bound on the peak-to-peak norms and larger steady-state water-level errors, on the other hand.

3.6 Summary

This chapter provides a framework for robustness analysis of the L_∞-to-L_∞ string-stability of an irrigation channel operating under a distributed distant-downstream control with flow to reference feed-forward scheme via some sufficient LMI conditions. As a sample application, the robustness of the proposed control scheme to delay parameter uncertainty is considered. The framework accommodates for uncertainties of independent or joint model parameters. The results show that the rate of amplification of the water flow peaks of a real channel is reasonably small compared to the previous design schemes of distributed distant-downstream control. It should be noted that the method is scalable spatially and the analysis can be done on a pool by pool basis. It is desirable to derive necessary and sufficient conditions to analyse robustness of the L_∞-to-L_∞ string-stability property of an automated channel.

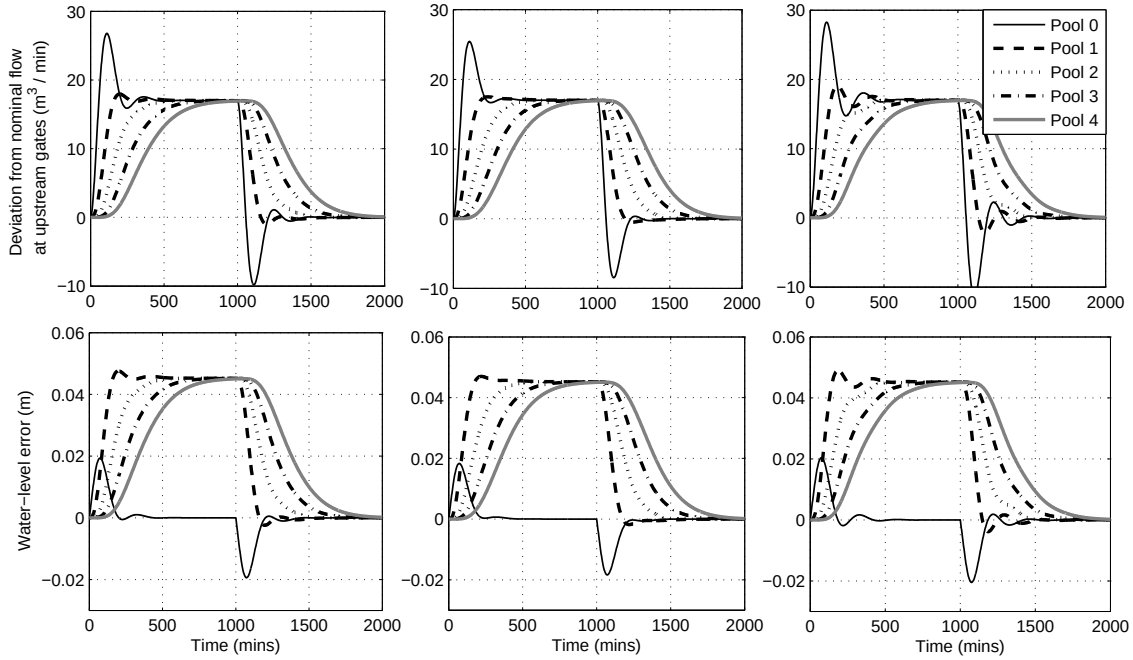

Figure 3.4: Simulations with decentralized feedback and feed-forward scheme, $T_c = 100$. (a)$\tau =$ 16(nominal), (b)$\tau = 13$, (c)$\tau = 19$

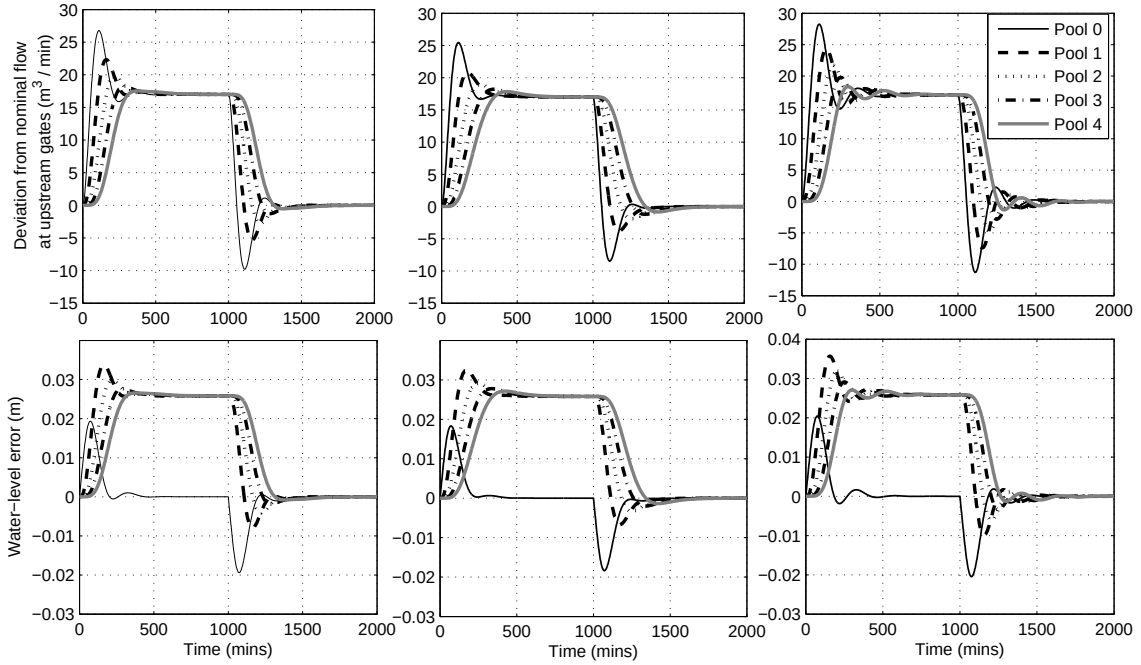

Figure 3.5: Simulations with decentralized feedback and feed-forward scheme, $T_c = 50$. (a)$\tau =$ 16(nominal), (b)$\tau = 13$, (c)$\tau = 19$

This page intentionally left blank.

Chapter 4

A 2-D Modeling and Analysis Framework for Automated Irrigation Channels

Spatially uniform bounded flow peaks along an automated channel is implied by a constraint on the L_∞ to L_∞ induced norm of flow interactions as stated in Chapter 2. This condition, indeed, implies non-amplification of peaks in flow transients as they propagate in the upstream direction. Moreover, it is shown that an H_∞ norm constraint on the flow interactions is a necessary condition for such spatial stability. This chapter considers the question of what type of transient propagation characteristics are implied by this weaker condition. Ultimately, Lyapunov based stability analysis of a 2-D Roesser model is used to show that the collection of decentralized H_∞ norm conditions on each pool imply uniformly bounded flow interactions between the locally controlled pools. However, it does not imply non-amplification of peaks between all pools, as illustrated by example.

4.1 Introduction

In Chapter 2, uniformly bounded in space and time flow interaction signals between pools operating under a new distant-downstream control architecture are achieved by ensuring non-amplification of transient peaks from pool to pool. This is a strong condition, for which a collection of decentralized H_∞ norm conditions is necessary. The nature of flow interaction signals implied by these conditions is studied in this chapter. In particular a 2-D approach, based on Roesser state-space like model, is pursued. To illustrate the modeling approach a homogenous cascade of automated pools is considered first and practical notions of stability are investigated from the perspective of flow interaction signal response to spatial and temporal Roesser model boundary conditions. Ultimately, Lyapunov based analysis of a 2-D Roesser model for a heterogenous cascade is used

to establish sufficiency of decentralised H_∞ norm based certificates that are sufficient for ensuring uniformly bounded interaction signals in response to finite-energy boundary conditions. The analysis is related to work reported in [78, 79], where stability of a homogenous string of vehicle platoons is considered.

The chapter is structured as follows: After introducing notations and preliminary review of the relevant literature, the problem setup for a general heterogeneous cascade is discussed. Strong practical stability and the corresponding conditions are derived for a homogeneous cascade, to illustrate aspects of the modeling approach. String-stability analysis of a heterogeneous cascade is then presented, followed by an application of this within the context of distributed distant-downstream control system design for irrigation channels. Simulation examples are used for comparison.

4.2 Notations and Preliminaries

The symbol $\mathbb{Z}_+$ refers to the subset $\{i \in \mathbb{Z} : i \geq 0\}$ of the integers $\mathbb{Z}$, $\mathbb{R}_+$ denotes the subset $\{t \in \mathbb{R} : t \geq 0\}$ of the real numbers $\mathbb{R}$, and $\mathbb{C}_-$ denotes the subset $\{z \in \mathbb{C} : \Re(z) < 0\}$ of the complex numbers $\mathbb{C} = \{\alpha + j\beta : \alpha, \beta \in \mathbb{R}\}$, where $\Re(z)$ denotes the real part α of $z = \alpha + j\beta$ and $j := \sqrt{-1}$. $\mathbb{F}^{p\times m}$ denotes the linear space p-row-by-m-column matrices with entries in $\mathbb{F} \in \{\mathbb{R}, \mathbb{C}\}$. A superscript $*$ denotes the (complex conjugate) transpose of a matrix or column vector considered as an $n \times 1$ matrix.

Given a vector $x = (x_1, \ldots, x_n)^* \in \mathbb{R}^n$, $|x|_2 := (\sum_{i=1}^n x_i^2)^{\frac{1}{2}}$ and $|x|_\infty := \max\{|x_i| : i = 1, 2, \ldots, n\}$. Note that $|x|_\infty \leq |x|_2 = \sqrt{x^*x}$ for all $x \in \mathbb{R}^n$. Given $A \in \mathbb{R}^{p\times m}$ with elements $a_{ij} \in \mathbb{R}$, $\|A\|_{2\to 2} := \sup_{x\neq 0} |Ax|_2 / |x|_2$ and $\|A\|_{\infty\to\infty} := \sup_{x\neq 0} |Ax|_\infty / |x|_\infty = \max_i \sum_j a_{ij}$. The set of eigenvalues of A is denoted by $\sigma(A) = \{\lambda \in \mathbb{C} \ : \ Ax = \lambda x, \ x \neq 0\}$. Clearly, $\lambda \in \sigma(A) \Leftrightarrow -\lambda \in \sigma(-A)$ and $\lambda \in \sigma(A) \Leftrightarrow (1+\lambda) \in \sigma(I+A)$, where I denotes the identity matrix. The spectral radius of a matrix A is denoted by $\rho(A)$.

A symmetric matrix $P = P^* \in \mathbb{R}^{n\times n}$ has eigenvalues that are real and $\lambda_{\max}(P)$ (resp. $\lambda_{\min}(P)$) denotes the maximum (resp. minimum) eigenvalue. It is said to be positive definite (resp. semi-definite) if $x^*Px \geq cx^*x$ (resp. $x^*Px \geq 0$) for all $x \in \mathbb{R}^n$ and some $c > 0$, which is denoted by $P > 0$ (resp. $P \geq 0$). Also, $P < 0 \Leftrightarrow -P > 0$ and $P \leq 0 \Leftrightarrow -P \geq 0$. Note that $P > 0 \Leftrightarrow \lambda_{\min}(P) > 0$

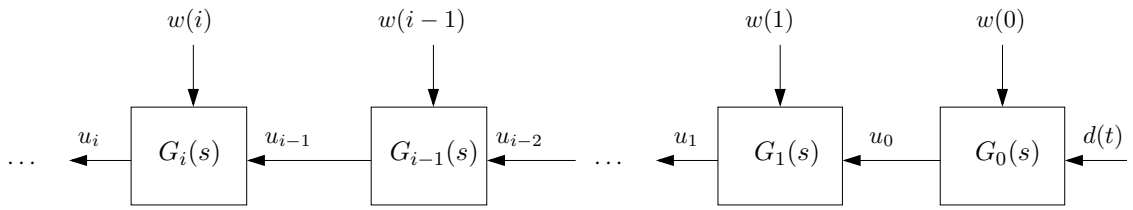

Figure 4.1: Block diagram of cascade of heterogeneous dynamical systems.

and $P < 0 \Leftrightarrow \lambda_{\max}(P) < 0$. The operator $\oplus$ denotes the direct sum of two matrices, i.e., $P_1 \oplus P_2 = diag(P_1, P_2)$.

L_2^n denotes the space of functions $x : \mathbb{R}_+ \to \mathbb{R}^n$ with $\|x\|_2 := (\int_0^\infty |x(t)|_2^2 dt)^{\frac{1}{2}} < \infty$. The space of functions $x : \mathbb{R}_+ \to \mathbb{R}^n$ such that $\|x\|_\infty := \sup_t |x(t)|_\infty < \infty$ is denoted by L_∞^n. Similarly, ℓ_2^n and ℓ_∞^n denote the subspaces of sequences $x : \mathbb{Z}_+ \to \mathbb{R}^n$ such that $\|x\|_2 := (\sum_{i=0}^\infty |x(i)|_2^2)^{\frac{1}{2}} < \infty$ and $\|x\|_\infty := \sup_i |x(i)|_\infty < \infty$, respectively. The dimension n of the function value is often suppressed for convenience.

$X = Ric(A,B,C)$ stands for existence of a $X = X^*$ such that $A^*X + XA + \gamma^{-2}XRX + Q = 0$, where $Q = C^*C$ and $R = BB^*$ are real symmetric $n \times n$ matrices. A solution X of this Riccati equation is stabilising if $\sigma(A + RX) \in \mathbb{C}_-$.

4.3 Problem Setup

An automated irrigation channel operating under a distributed distant-downstream control such as the decentralised feedback with flow-to-reference feedforward control, as discussed in Chapter 1, can be modeled by a cascade of heterogeneous dynamical systems shown in Figure 4.1, where there is a single interconnection signal $u_i(t)$. Subsystems are indexed from right to left, start of the information flow towards the end of the string, with the first subsystem numbered 0. The signals $d(t)$ and $w(i)$ represent spatial and temporal boundary conditions, which correspond to the offtake drawn from pool 0 and $w(i)$ denotes the non-zero initial conditions due to the mismatch between the initialisation of the controllers and initial flows, respectively. According to Figure 1.17, input of the subsystem i is the output of subsystem $i-1$. Therefore, a state-space realisation of $G_i(s)$

denoted by $G_i(s) = \{A(i), B(i), C(i), D(i)\}$ is

$$\begin{aligned} \dot{x}_i(t) &= A(i)x_i(t) + B(i)u_{i-1}(t), \\ u_i(t) &= C(i)x_i(t) + D(i)u_{i-1}(t),\ i = 0,1,2,\cdots, \end{aligned} \tag{4.1}$$

where $x_i(0) = w(i)$ and $u_{-1}(t) = d(t)$ represent the initial condition of each subsystem and source of the chain in Figure 1.17, respectively. Noting that $x_i(t)$ of each subsystem is evolving with time and input of subsystem i, $u_i(t)$, is the output of G_{i-1}, information flow in such strings is in two directions, spatial and temporal, motivating a 2-dimensional representation of the string. In frequency domain

$$\begin{aligned} U_i(s) &= G_i(s)U_{i-1}(s) + \tilde{G}_i(s)w(i),\ i = 1,2,\cdots \\ U_0(s) &= G_0(s)D(s) + \tilde{G}_0(s)w(0), \end{aligned} \tag{4.2}$$

where $\tilde{G}_i(s) = C(i)(sI - A(i))^{-1}$.

In the case of a homogenous cascade, $G_i(s) = G(s)\ \forall i \geq 0$, taking the Z-transform (spatially) with $d(t) = 0$ yields:

$$U(s,z) = \frac{\tilde{G}(s)}{1 - z^{-1}G(s)}W(z)$$

with $W(z) := \sum_{k=0}^{\infty} w(k)z^{-k}$, where due to steady-state interconnection signals' matching requirement, i.e. $G(0) = 1$, the corresponding transfer function has a pole at $(s = 0, z = 1)$ and, according to [80, Theorem 1], the system is not BIBO stable, and $u_i(t)$ does not remain bounded. Similarly, if $w(i) = 0$

$$U_i(s) = G^i(s)G(s)D(s),\ i = 0,2,\cdots.$$

Taking the Z-transform yields

$$U(s,z) = \frac{G(s)}{1 - z^{-1}G(s)}D(s),$$

which is unstable due to the pole at $(s = 0, z = 1)$. Therefore, the cascade can not be BIBO stable

motivating considering a weaker notion of stability [80–83].

4.4 2D Analysis of a Homogenous Channel Under Decentralised Distant-Downstream Control

To illustrate the scope for analysis via the 2-D state-space like Roesser model, consider in this section a homogenous cascade. For a corresponding spatially and temporally homogeneous irrigation channel, measures of performance are defined which relate to notions of strong practical stability and disturbance attenuation and noting that BIBO stability does not hold because of the non-essential singularity on the boundary. Motivated by the finite spatial extent of an irrigation channel, the notion of strong practical stability is introduced for Roesser models, building on work for so-called repetitive systems [84]. This notion is stronger than practical stability defined for n-dimensional systems in [83, 85], but weaker than the conventional notion of asymptotic stability [86]. The analysis carried out in [84, 87] include computational tests that lead to control law design. These are extended to disturbance attenuation measures for discrete linear repetitive systems in [88].

4.4.1 A Discrete-Discrete 2-D Roesser Model

With reference to Figure 1.2 and the integrator-delay model (1.7) of an irrigation channel, where the pools are indexed such that pool $i+1$ is upstream relative to pool i, a discrete-discrete Roesser model is derived.

Discretising dynamics of pool i in (1.7) yields:

$$\begin{aligned}
&y(i,j+1) = y(i,j) + T\left(c_{\mathrm{in}_i} z_1(i,j) - c_{\mathrm{out}_i}\left(u_h(i-1,j) + d_h(i,j)\right)\right)\\
&z_1(i,j+1) = z_2(i,j)\\
&\qquad \vdots\\
&z_{\frac{\tau_i}{T}}(i,j+1) = u_h(i,j),
\end{aligned} \tag{4.3}$$

where T is the sampling time (assumed to be an integer fraction of τ_i), j stands for the j-th time instant, $y(i,j) = y_i(jT)$ and similarly for $u_h(i,j)$, $v_h(i,j)$ and $d_h(i,j)$. This is a 2-dimensional

representation of an irrigation channel, with signals indexed by discrete time and spatial position in the channel. The extent of signals is finite in the spatial dimension, whereas in the temporal dimension the extent of signal is unbounded. Note that under feedback control such that $u_h(i,j)$ only depends on $y(k,l)$ for $k \leq i$ and $l \leq j$, information flow remains directed in both the spatial and temporal dimensions.

Various sate-space forms are available for realising 2-D system models, that exhibit directed information flow in all dimensions; these forms can be converted into each other via straightforward mathematical manipulations. The most popular models are models of linear repetitive systems [89] and those introduced by Roesser and Fornasini-Marchesini, [86, 90–92]. The 2-D model used herein is the discrete-discrete Roesser state-space model involving two independent variables such as spatial and temporal semi-states denoted by $x_s(i,j) \in \mathbb{R}^{n_s}$, and $x_t(i,j) \in \mathbb{R}^{n_t}$, respectively:

$$\begin{bmatrix} x_s(i+1,j) \\ x_t(i,j+1) \end{bmatrix} = \begin{bmatrix} A_{11} & A_{12} \\ A_{21} & A_{22} \end{bmatrix} \begin{bmatrix} x_s(i,j) \\ x_t(i,j) \end{bmatrix} + \begin{bmatrix} B_1 \\ B_2 \end{bmatrix} u(i,j)$$
$$y(i,j) = \begin{bmatrix} C_1 & C_2 \end{bmatrix} \begin{bmatrix} x_t(i,j) \\ x_s(i,j) \end{bmatrix} + D_u u(i,j), \tag{4.4}$$

subject to the boundary conditions defined by $x_s(0,j) = h(j)$ and $x_t(i,0) = v(i)$ for $i,j \in \mathbb{Z}_+$ and $u_h(i,j) \in \mathbb{R}^{n_{u_h}+n_{d_h}}$ containing the control input and disturbance signals. This model was first introduced for an image processing application, [90]. Then, it was utilised for modeling other applications such as grid sensor networks [93], long transmission lines [94] or any process that can be modeled by discrete partial differential equations. Roesser model exhibits the quarter-plane causality, in that the semi-states at node (i,j) only depend on the inputs in the rectangle $[0:i) \times [0:j)$ and southwest boundary condition [95]. Bearing in mind (4.3), define

$$x_s(i,j) := u_h(i-1,j) \quad \text{and} \quad x_t(i,j) := \begin{bmatrix} y(i,j) \\ z_1(i,j) \\ \vdots \\ z_{\frac{\tau_i}{T}}(i,j) \end{bmatrix} \tag{4.5}$$

for $i \in \{0,\ldots,N-1\}$ and $j \in \mathbb{Z}_+$, where $x_s(i,j)$ is the spatial semi-state of pool with spatial index i at time index j, which captures the flow out of pool i due to downstream control action and N is the number of pools. As such, the dynamics of an irrigation channel can be represented by the following Roesser model:

$$\begin{bmatrix} x_s(i+1,j) \\ x_t(i,j+1) \end{bmatrix} = \begin{bmatrix} 0 & 0 \\ A_s(i) & A_t(i) \end{bmatrix} \begin{bmatrix} x_s(i,j) \\ x_t(i,j) \end{bmatrix} + \begin{bmatrix} 1 \\ B_u(i) \end{bmatrix} u_h(i,j) + \begin{bmatrix} 0 \\ B_d(i) \end{bmatrix} d_h(i,j),$$
$$y(i,j) = \begin{bmatrix} 0 & C_t \end{bmatrix} \begin{bmatrix} x_s(i,j) \\ x_t(i,j) \end{bmatrix}, \tag{4.6}$$

with boundary conditions $x_s(0,j) = h(j)$ for $j \geq 0$ and $x_t(i,0) = v(i)$ for $i = 0,\ldots N-1$, where

$$A_t(i) := \begin{bmatrix} 1 & Tc_{\text{in}_i} & 0 & \cdots & 0 \\ 0 & 0 & 1 & \ddots & \vdots \\ \vdots & & \ddots & \ddots & 0 \\ & & & & 1 \\ 0 & & \cdots & & 0 \end{bmatrix}, \quad A_s(i) := \begin{bmatrix} -Tc_{\text{out}_i} \\ 0 \\ \vdots \\ 0 \\ 0 \end{bmatrix}$$

$$B_u(i) := \begin{bmatrix} 0 \\ 0 \\ \vdots \\ 0 \\ 1 \end{bmatrix}, \quad B_d(i) = \begin{bmatrix} -Tc_{\text{out}_i} \\ 0 \\ \vdots \\ 0 \\ 0 \end{bmatrix},$$

and $C_t := \begin{bmatrix} 1 & 0 & \cdots & 0 \end{bmatrix}$. As an initial step, it is of interest to gain an understanding of how a spatially-and-temporally homogeneous version of the model (4.6) – i.e. A_s, A_t do not depend on i – performs under static semi-state feedback $u_h(i,j) = \begin{bmatrix} F_s & F_t \end{bmatrix} \begin{bmatrix} x_s(i,j)^T & x_t(i,j)^T \end{bmatrix}^T$. The resulting closed-loop model is

$$\begin{bmatrix} x_s(i+1,j) \\ x_t(i,j+1) \end{bmatrix} = \begin{bmatrix} A_{ss} & A_{st} \\ A_{ts} & A_{tt} \end{bmatrix} \begin{bmatrix} x_s(i,j) \\ x_t(i,j) \end{bmatrix} + \begin{bmatrix} B_s \\ B_t \end{bmatrix} d_h(i,j)$$

$$y(i,j) = \begin{bmatrix} C_s & C_t \end{bmatrix} \begin{bmatrix} x_s(i,j) \\ x_t(i,j) \end{bmatrix}, \tag{4.7}$$

with $A_{ss} := F_s$, $A_{st} := F_t$, $A_{ts} := A_s + B_u F_s$, $A_{tt} := A_t + B_u F_t$, $B_s := 0$, $B_t := B_d$, $C_s := 0$, and boundary conditions $x_s(0,j) = h(j)$ and $x_t(i,0) = v(i)$ for $(i,j) \in \{0,\ldots,N-1\} \times \mathbb{Z}_+$. This model is used for stability and performance analysis [2].

4.4.2 Practical Stability Analysis

For a Roesser model in the form (4.4), internal asymptotic stability implies BIBO stability [86]. Restricting attention to this notion of stability, however, is limiting in terms of what might be otherwise acceptable performance for systems with *finite* spatial extent. Indeed, asymptotic tendency to 0 in each of the dimensions, with the other fixed at an arbitrary finite value, is possible without X_r being zero as $r \to \infty$. This is illustrated in Figure 4.2, which shows the zero-input semi-state response of a simple 2-D Roesser model (not of an irrigation channel) with non-zero boundary conditions. The corresponding concept of strong practical stability, introduced for linear repetitive systems in [84], is developed below for the Roesser model (4.7).

Lemma 4.1. *[2] Suppose the boundary conditions and input for (4.7) are configured such that $x_s(0,j) = 0$, $x_t(i,0) = 0$ and $d_h(i,j) = \tilde{d}(j)$ for $i,j \in \mathbb{Z}_+$, with $|\tilde{d}(j)|$ uniformly bounded. If*

$$\rho(A_{ss}) < 1 \quad \textit{and} \quad \rho(A_{tt} + A_{ts}(I - A_{ss})^{-1} A_{st}) < 1,$$

then $\tilde{s}(j) := \lim_{i\to\infty} x_s(i,j)$ and $\tilde{t}(j) := \lim_{i\to\infty} x_t(i,j)$ both exist for all $j \in \mathbb{Z}_+$, with uniform bound in magnitude.

Proof. This result concerns the spatially asymptotic response. For each $j \in \mathbb{Z}_+$, let

$$s_\lambda(j) := \sum_{i=0}^{\infty} x_s(i,j)\lambda^i, \qquad t_\lambda(j) := \sum_{i=0}^{\infty} x_t(i,j)\lambda^i, \text{ and} \quad d_\lambda(j) := \sum_{i=0}^{\infty} \tilde{d}(j)\lambda^i = \frac{\tilde{d}(j)}{1-\lambda}.$$

These transformed variables are functions of λ defined on a disc, of suitably small radius, centred

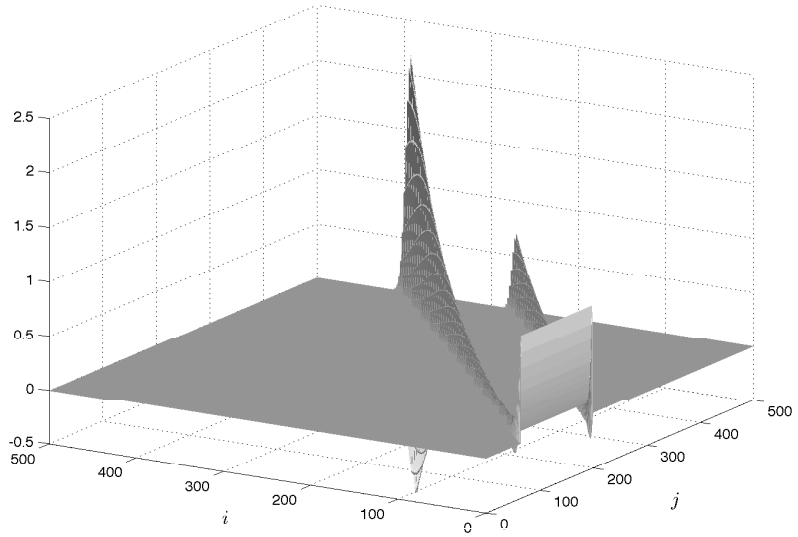

Figure 4.2: Strong practical stability without asymptotic stability: $A_{ss} = 0$; $A_{st} = \sqrt{0.91} = A_{ts}$; $A_{tt} = -0.1$. Non-zero boundary-condition response x_s asymptotically approaches 0 along each dimension, with the other fixed, but not the supremum of the magnitude across the line $r = i + j$ (which diverges) as $r \to \infty$.

at the origin in the complex plane. Applying the transformation to (4.7) yields:

$$\begin{aligned}
\lambda^{-1} s_\lambda(j) &= A_{ss} s_\lambda(j) + A_{st} t_\lambda(j) + B_s \frac{\tilde{d}(j)}{1-\lambda}, \\
t_\lambda(j+1) &= A_{ts} s_\lambda(j) + A_{tt} t_\lambda(j) + B_t \frac{\tilde{d}(j)}{1-\lambda}, \\
y_\lambda(j) &= C_s s_\lambda(j) + C_t t_\lambda(j).
\end{aligned} \tag{4.8}$$

Then

$$\begin{aligned}
s_\lambda(j) &= \lambda(I - \lambda A_{ss})^{-1} A_{st} t_\lambda(j) + \lambda(I - \lambda A_{ss})^{-1} B_s \frac{\tilde{d}(j)}{1-\lambda}, \\
t_\lambda(j+1) &= (\lambda A_{ts}(I - \lambda A_{ss})^{-1} A_{st} + A_{tt}) t_\lambda(j) + (\lambda A_{ts}(I - \lambda A_{ss})^{-1} B_s + B_t) \frac{\tilde{d}(j)}{1-\lambda}, \\
y_\lambda(j) &= C_s s_\lambda(j) + C_t t_\lambda(j).
\end{aligned} \tag{4.9}$$

This constitutes a discrete dynamical system with the state variable $t_\lambda(j)$ and an algebraic equation

for $s_\lambda(j)$. Since the specified boundary conditions imply $t_\lambda(0) = 0$,

$$t_\lambda(j) = \sum_{k=0}^{j-1} [(\lambda A_{ts}(I-\lambda A_{ss})^{-1}A_{st} + A_{tt})^{j-k-1}(\lambda A_{ts}(I-\lambda A_{ss})^{-1}B_s + B_t)\frac{\tilde{d}(k)}{1-\lambda}]. \tag{4.10}$$

In order to apply the final value theorem in the spatial direction, $\frac{1-\lambda}{\lambda}t_\lambda(j)$ needs to be analytic on the unit disc. Since $\rho(A_{ss}) < 1$, $t_\lambda(j)$ is analytic as a function of λ on $|\lambda| < 1$, for any $j \in \mathbb{Z}_+$. In fact, $t_\lambda(j)$ is a rational function with no poles inside or on the unit circle $\mathbb{T} := \{\lambda \in \mathbb{C} : |\lambda| = 1\}$, except one at $\lambda = 1$ due to the input. Therefore, the final value theorem applies to yield

$$\begin{aligned}\lim_{i\to\infty} x_t(i,j) = \tilde{t}(j) &= \lim_{\lambda\to 1}\frac{1-\lambda}{\lambda}t_\lambda(j) \\ &= \sum_{k=0}^{j-1}[(A_{ts}(I-A_{ss})^{-1}A_{st} + A_{tt})^{j-k-1}(A_{ts}(I-A_{ss})^{-1}B_s + B_t)\tilde{d}(k)].\end{aligned} \tag{4.11}$$

Moreover, since $\rho(A_{ts}(I-A_{ss})^{-1}A_{st} + A_{tt}) < 1$ and there exists a $D < \infty$ such that $|\tilde{d}(j)| < D$ $\forall\, j \in \mathbb{Z}_+$, it follows there exists a $T < \infty$ such that $|\tilde{t}(j)| < T\ \forall\, j \in \mathbb{Z}_+$.

Similarly, s_λ is a rational function with no poles inside or on the unit circle $\mathbb{T}$, except at $\lambda = 1$. Applying the final value theorem yields:

$$\begin{aligned}\lim_{i\to\infty} x_s(i,j) = \tilde{s}(j) &= \lim_{\lambda\to 1}\frac{1-\lambda}{\lambda}s_\lambda(j) \\ &= (I-A_{ss})^{-1}A_{st}\tilde{t}(j) + (I-A_{ss})^{-1}B_s\tilde{d}(j)\end{aligned} \tag{4.12}$$

and thus, $\exists S < \infty$ such that $|\tilde{s}(j)| < S\ \forall j \in \mathbb{Z}_+$. □

Corollary 4.1. *When the conditions in Lemma 4.1 hold, the so-called spatial limit profile* $\tilde{y}(j) := \lim_{i\to\infty} y(i,j)$ *exists in accordance with the following stable* 1*-D model:*

$$\begin{aligned}\tilde{t}(j+1) &= (A_{ts}(I-A_{ss})^{-1}A_{st} + A_{tt})\tilde{t}(j) + (A_{ts}(I-A_{ss})^{-1}B_s + B_t)\tilde{d}(j), \\ \tilde{s}(j) &= (I-A_{ss})^{-1}A_{st}\tilde{t}(j) + (I-A_{ss})^{-1}B_s\tilde{d}(j), \\ \tilde{y}(j) &= C_s\tilde{s}(j) + C_t\tilde{t}(j) \\ &= (C_s(I-A_{ss})^{-1}A_{st} + C_t)\tilde{t}(j) + C_s(I-A_{ss})^{-1}B_s\tilde{d}(j),\end{aligned} \tag{4.13}$$

with boundary condition $\tilde{t}(0) = 0$.

Remark: As stated, Lemma 4.1 provides a sufficient condition for the existence of uniform-bounds on the spatially-asymptotic semi-states profiles approached as $i \to \infty$, for a particular configuration of the boundary condition and input. Under the following stabilisability and detectability hypotheses, regarding in particular the model (4.13), the condition in Lemma 4.1 becomes necessary for the analyticity of $t_\lambda(j)$ and $s_\lambda(j)$, the uniform boundedness of the limits in (4.11) and (4.12) and thus, the existence of the uniformly-bounded spatially-asymptotic semi-state profiles:

- $(A_{ss},\, A_{st})$ is stabilisable
- $(A_{ts},\, A_{ss})$ is detectable
- $(A_{ss},\, B_s)$ is stabilisable
- $(A_{ts}(I-A_{ss})^{-1}A_{st}+A_{tt},\, A_{ts}(I-A_{ss})^{-1}B_s+B_t)$ is stabilisable
- $((I-A_{ss})^{-1}A_{st},\, A_{ts}(I-A_{ss})^{-1}A_{st}+A_{tt})$ is detectable.

Remark: The condition in Lemma 4.1 is also sufficient for the existence of spatially-asymptotic semi-state profiles, $\tilde{s}$ and $\tilde{t}$, that are uniformly bounded in magnitude over $j \in \mathbb{Z}_+$, when the input and boundary conditions of (4.7) are configured as follows: $d_h(i,j) = 0$, $x_s(0,j) = \tilde{x}_s(j)$ and $x_t(i,0) = \tilde{x}_t$ for $i, j \in \mathbb{Z}_+$, with $|\tilde{x}_s(j)|$ uniformly bounded. Appropriate stabilisability and detectability hypotheses make the condition necessary.

Lemma 4.2. *Suppose the boundary conditions and input for (4.7) are configured such that* $x_s(0,j) = 0$, $x_t(i,0) = 0$ *and* $d_h(i,j) = \hat{d}(i)$ *for* $i, j \in \mathbb{Z}_+$, *with* $|\hat{d}(i)|$ *uniformly bounded. If*

$$\rho(A_{tt}) < 1 \quad \textit{and} \quad \rho(A_{ss} + A_{st}(I-A_{tt})^{-1}A_{ts}) < 1$$

then $\hat{s}(i) := \lim_{j\to\infty} x_s(i,j)$ *and* $\hat{t}(i) := \lim_{j\to\infty} x_t(i,j)$ *both exist for* $i \in \mathbb{Z}_+$, *with uniform bound in magnitude.*

Proof. The proof involves application of the final value theorem and the transformed variables

$$s_\mu(i) := \sum_{j=0}^{\infty} x_s(i,j)\mu^j, \qquad t_\mu(i) := \sum_{j=0}^{\infty} x_t(i,j)\mu^j, \qquad \text{and} \qquad d_\mu(i) := \sum_{j=0}^{\infty} \hat{d}(i)\mu^j = \frac{\hat{d}(i)}{1-\mu},$$

in a fashion similar to the proof of Lemma 4.1. □

Corollary 4.2. *When the conditions of Lemma 4.1 hold, the temporal limit profile* $\hat{y}(i) := \lim_{j\to\infty} y(i,j)$ *exists in accordance with the following stable 1-D model:*

$$\begin{aligned}
\hat{s}(i+1) &= (A_{ss} + A_{st}(I-A_{tt})^{-1}A_{ts})\hat{s}(i) + (A_{st}(I-A_{tt})^{-1}B_t + B_s)\hat{d}(i),\\
\hat{t}(i) &= (I-A_{tt})^{-1}A_{ts}\hat{s}(i) + (I-A_{tt})^{-1}B_t\hat{d}(i),\\
\hat{y}(i) &= (C_s + C_t(I-A_{tt})^{-1}A_{ts})\hat{s}(i) + C_t(I-A_{tt})^{-1}B_t\hat{d}(i),
\end{aligned} \tag{4.14}$$

with boundary condition $\hat{s}(0) = 0$.

Remark: Under the following stabilisability and detectability hypotheses concerning the model (4.14), the conditions in Lemma 4.2 are also necessary for uniformly-bounded temporal limit profiles:

- $(A_{tt},\, A_{ts})$ is stabilisable
- $(A_{st},\, A_{tt})$ is detectable
- $(A_{tt},\, B_t)$ is stabilisable
- $(A_{st}(I-A_{tt})^{-1}A_{ts} + A_{ss},\, A_{st}(I-A_{tt})^{-1}B_t + B_s)$ is stabilisable
- $((I-A_{tt})^{-1}A_{ts},\, A_{st}(I-A_{tt})^{-1}A_{ts} + A_{ss})$ is detectable.

Remark: The condition in Lemma 4.2 is also sufficient for the existence of temporally-asymptotic semi-state profiles $\hat{s}$ and $\hat{t}$, that are uniformly bounded in magnitude over $i \in \mathbb{Z}_+$, when the input and boundary conditions of (4.7) are configured as follows: $d_h(i,j) = 0$, $x_s(0,j) = \hat{x}_s$ and $x_t(i,0) = \hat{x}_t(i)$ for $i, j \in \mathbb{Z}_+$, with $|\hat{x}_t(i)|$ uniformly bounded. Appropriate stabilisability and detectability hypotheses make the condition necessary.

In view of Lemmas 4.1 and 4.2, the following strong practical internal stability property is defined for the Roesser model (4.7). Note that it is stronger than the usual notion of practical internal stability [83,85], which is typically defined in terms of the weaker requirement of $\rho(A_{ss}) < 1$ and $\rho(A_{tt}) < 1$ alone.

Definition 4.1. *The Roesser model (4.7) is said to have the property of* strong practical internal stability *whenever all of the following hold:*

(a) $\rho(A_{ss}) < 1$,

(b) $\rho(A_{tt}) < 1$,

(c) $\rho(A_{tt} + A_{ts}(I - A_{ss})^{-1}A_{st}) < 1$,

(d) $\rho(A_{ss} + A_{st}(I - A_{tt})^{-1}A_{ts}) < 1$,

Remark: Note that the inverses in (c) and (d) exist provided (a) and (b) hold.

Remark: The strong practical stability notion introduced for irrigation channels turn out not to reflect the desirable string-stability property. Indeed, due to flow matching property in steady-state, it can be seen from (4.14) that $\rho(A_{ss} + A_{st}(I - A_{tt})^{-1}A_{ts}) = 1$ when $\hat{d}(i) = 0$ for $i > 0$. Moreover, the analysis in this section relies on homogeneity of the string of pools. In future, it may be possible to develop new approaches to controller synthesis via more suitable constraints for irrigation channels. In the next section, we will focus on the L_2-to-L_∞ gain from the offtakes to the flow instead of L_∞-to-L_∞ gain, as a weaker notion for string-stability that allows for the analysis to be carried out for a heterogenous channel.

4.5 Analysis of a Heterogenous Channel Under Decentralized Distant-Downstream Control

4.5.1 A Continuous-Discrete 2-D Roesser Model

Performance and spatial stability analysis of an automated irrigation channel operating under distributed distant-downstream control where information flow is directed towards upstream of the channel is carried out via string-stability analysis of the cascade of Figure 1.17. As such, each subsystem represents a mapping from downstream flow to the upstream flow of a pool, i.e. $G_i(s) := T_{U_{i-1} \to U_i}(s)$. Although it is natural to analyse performance in terms of step changes in offtakes and initial conditions, in this section, we consider $d(t) \in L_2 \cap L_\infty$ and $w(i) \in \ell_2$. This assumption is not limiting since, in practice, the offtakes drawn from the channel are taken for a finite time interval and channels are of finite spatial extent. Moreover, effect of only one offtake at

the most downstream pool is analysed, otherwise linear growth of transients must be allowed due to flow matching at steady-state. Considering a state-space realisation of $G_i(s)$ as in (4.1), such a cascade of subsystems can be represented by continuous-discrete Roesser model, as in [96], as follows:

$$\begin{bmatrix} \dot{x}_t(t,i) \\ x_s(t,i+1) \end{bmatrix} = \begin{bmatrix} A(i) & B(i) \\ C(i) & D(i) \end{bmatrix} \begin{bmatrix} x_t(t,i) \\ x_s(t,i) \end{bmatrix}, \quad i \in \mathbb{Z}_+, \tag{4.15}$$

with boundary conditions $x_t(0,.) = w(i) \in \ell_2$ and $x_s(.,0) = d(t) \in L_2 \cap L_\infty$. Linear repetitive systems is an example of such systems [95]. The continuous temporal and discrete spatial semi-states are defined as $x_t(t,i) := x_i(t)$ and $x_s(t,i) := u_{i-1}(t)$. This model will be exploited later in the subsequent Lyapunov based analysis. In the rest of this chapter, a strictly proper $G_i(s)$ for all pools is assumed, i.e. $D(i) = 0, \forall i$. Therefore, the string-stability under consideration follows:

Definition 4.2 (L_2-to-L_∞ **string-stability**). *A cascade of subsystems with the architecture illustrated in Figure 1.17 is L_2-to-L_∞ string-stable if there exists an $0 < M < \infty$ such that, with $d \in L_2 \cap L_\infty$ and $w = \{w(0), w(1), \cdots\} \in \ell_2$, $\|u_i\|_\infty \leq M$ for all $i = 0, 1, 2, \ldots$.*

Now we are in a position to analyse stability of (4.15) with the purpose of deriving conditions that lead to L_2-to-L_∞ string-stability.

4.5.2 L_2-to-L_∞ String-Stability Analysis

Lyapunov analysis is a common way of stability analysis of multi-dimensional systems, [86, 97, 98]. Lyapunov based analysis is carried out here to derive analysis conditions for L_2-to-L_∞ string-stability of the cascade under consideration.

A space dependent positive quadratic 2-D Lyapunov function is used. A non-strict version of Bounded Real Lemma gives conditions on each subsystem of the cascade to imply existence of a 2-D Lyapunov function with negative semi-definite variation. This property of the Lyapunov function is, then, used to derive a bound on the semi-states.

Consider the 2-D Lyapunov function

$$\begin{aligned} V(t,i) &= \begin{bmatrix} x_t(t,i) \\ x_s(t,i) \end{bmatrix}^T P(i) \begin{bmatrix} x_t(t,i) \\ x_s(t,i) \end{bmatrix} \\ &= x_t^T(t,i)P_t(i)x_t(t,i) + x_s^T(t,i)P_s(i)x_s(t,i) \\ &:= V_t(t,i) + V_s(t,i), \end{aligned} \tag{4.16}$$

where $P(i) = P_t(i) \oplus P_s(i) = P^T(i) \geq 0$ is spatially varying matrix.

The variations of $V(t,i)$ along the trajectory of the 2-D system (4.15) is

$$\begin{aligned} \Delta V(t,i) =& \frac{\partial V_t(t,i)}{\partial t} + V_s(t,i+1) - V_s(t,i) \\ =& \dot{x}_t^T(t,i)P_t(i)x_t(t,i) + x_t(t,i)P_t(i)\dot{x}_t(t,i) + x_s^T(t,i+1)P_s(i+1)x_s(t,i+1) \\ & - x_s(t,i)P_s(i)x_s(t,i) \\ =& x(t,i)^T(\tilde{A}^T(i)\tilde{P}_t(i) + \tilde{P}_t(i)\tilde{A}(i) + \tilde{A}^T(i)\tilde{P}_s(i+1)\tilde{A}(i) - \tilde{P}_s(i))x(t,i) \\ =& x^T(t,i)Q(i)x(t,i), \end{aligned}$$

where

$$\begin{aligned} &\tilde{A}(i) := \begin{bmatrix} A(i) & B(i) \\ C(i) & 0 \end{bmatrix}, \ \tilde{P}_t(i) := \begin{bmatrix} P_t(i) & 0 \\ 0 & 0 \end{bmatrix}, \\ &\tilde{P}_s(i) := \begin{bmatrix} 0 & 0 \\ 0 & P_s(i) \end{bmatrix}, \ x(t,i) := \begin{bmatrix} x_t(t,i) \\ x_s(t,i) \end{bmatrix}, \\ &Q := \tilde{A}^T(i)\tilde{P}_t(i) + \tilde{P}_t(i)\tilde{A}(i) + \tilde{A}^T(i)\tilde{P}_s(i+1)\tilde{A}(i) - \tilde{P}_s(i). \end{aligned}$$

Result of Lemma 4.3, as can be found in [78], will be used later to show bounded energy of semi-states.

Lemma 4.3. *Consider function $V(t,i) = V_t(t,i) + V_s(t,i)$ of the form shown in (4.16) with $V_t(t,i) \geq 0$, $V_s(t,i) \geq 0$. If $\Delta V(t,i) = \frac{\partial V_t(t,i)}{\partial t} + V_s(t,i+1) - V_s(t,i) \leq 0$, then, $\forall t,i > 0$*

$$\sum_{k=0}^{i} V_t(t,k) \leq \sum_{k=0}^{i} V_t(0,k) + \int_0^t V_s(\tau,0)d\tau, \ \textit{and}$$

$$\int_0^t V_s(\tau,i)d\tau \leq \int_0^t V_s(\tau,0)d\tau + \sum_{k=0}^{i} V_t(0,k). \tag{4.17}$$

Proof. Since $\Delta V(\tau,k) \leq 0$,

$$\sum_{k=0}^{i}\int_0^t \Delta V(\tau,k)d\tau = \sum_{k=0}^{i}(V_t(t,k)-V_t(0,k)) + \int_0^t (V_s(\tau,i)-V_s(\tau,0))d\tau \leq 0.$$

Thus,

$$\sum_{k=0}^{i} V_t(t,k) + \int_0^t V_s(\tau,i)d\tau \leq \sum_{k=0}^{i} V_t(0,k) + \int_0^t V_s(\tau,0)d\tau,$$

whereby the result claimed follows by $V_s(t,i) \geq 0$ and $V_t(t,i) \geq 0$. □

A statement of the Bounded Real Lemma in the required non-strict form derived in Theorem 4.1 could not be found in the literature. It is used later to extract conditions on each subsystem that imply $\Delta V(t,i) \leq 0$.

Theorem 4.1. *Let $G(s) = C(sI-A)^{-1}B$ be a state-space realization of a strictly-proper matrix transfer function, with $A \in \mathbb{R}^{n\times n}$ Hurwitz (i.e. $\sigma(A) \subset \mathbb{C}_-$), $0 < \gamma \in \mathbb{R}$. The following are equivalent:*

(i) $\|G\|_\infty := \sup_{\Re(s)>0}\|G(s)\|_{2\to 2} = \sup_{\omega\in\mathbb{R}}\|G(j\omega)\|_{2\to 2} \leq \gamma$;

(ii) *there exists a unique real matrix $X = X^* \geq 0$ such that $X = Ric(A,B,C)$ and $\sigma(A+BB^*X) \subset \mathbb{C}_- \cup j\mathbb{R}$.*

Proof. $\|G(.)\|_\infty \leq \gamma$ is equivalent to

$$\begin{aligned}\phi(j\omega) :=& I - \gamma^{-2}G^T(-j\omega)G(j\omega)\\ =& \begin{bmatrix}\gamma^{-1}B^*(-j\omega I - A^*)^{-1} & I\end{bmatrix}\begin{bmatrix}-C^*C & 0\\ 0 & I\end{bmatrix}\begin{bmatrix}\gamma^{-1}(j\omega I - A)^{-1}B\\ I\end{bmatrix} \geq 0.\end{aligned} \tag{4.18}$$

Applying [38, Lemma 13.17], $\phi(j\omega) \geq 0$ for all $\omega \geq 0$ is equivalent to existence of a unique real $Y = Y^* \leq 0$ such that

$$A^*Y + YA - \gamma^{-2}YBB^*Y - C^*C = 0, \tag{4.19}$$

and $\sigma(A-\gamma^{-2}BB^*Y)\in\mathbb{C}_-\cup j\mathbb{R}$. By taking $X=-Y$, it follows that existence of $Y\leq 0$ such that (4.19) and $\sigma(A-\gamma^{-2}BB^*Y)\in\mathbb{C}_-\cup j\mathbb{R}$ hold is equivalent to existence of $X\geq 0$ such that

$$A^*X+XA+\gamma^{-2}XBB^*X+C^*C=0 \tag{4.20}$$

and $\sigma(A+\gamma^{-2}BB^*X)\in\mathbb{C}_-\cup j\mathbb{R}$. Therefore, $\|G(.)\|_\infty\leq\gamma$ if and only if $\exists X=Ric(A,B,C)\geq 0$ and $\sigma(A+BB^*X)\in\mathbb{C}_-\cup j\mathbb{R}$.

□

Lemma 4.4. *Consider the 2D system of the form (4.15) with $G_i(s)=C(i)(sI-A(i))^{-1}B(i)$, if $\sigma(A(i))\subset\mathbb{C}_-$for all i, and $\|G_i(.)\|_\infty\leq 1$, $\forall i\in\mathbb{Z}_+$ then $\exists P_t(i)=P_t(i)^T\geq 0$ such that*

$$\Delta V(t,i)=\frac{\partial V_t(t,i)}{\partial t}+V_s(t,i+1)-V_s(t,i)\leq 0, \tag{4.21}$$

where $V(t,i)=V_t(t,i)+V_s(t,i)=x_t(t,i)^TP_t(i)x_t(t,i)+x_s(t,i)^Tx_s(t,i)$ (i.e. P_s equal to the identity).

Proof. According to Theorem 4.1, for a stable transfer function $G_i(s)$ with $\|G_i(.)\|_\infty\leq 1$, and state-space realisation $\{A(i),B(i),C(i),0\}$, $\exists X(i)=X^T(i)\geq 0$ such that

$$X(i)A(i)+A(i)^TX(i)+X(i)B(i)B(i)^TX(i)+C(i)^TC(i)=0. \tag{4.22}$$

Applying the Schur complement to (4.22) gives

$$\begin{bmatrix} X(i)A(i)+A(i)^TX(i)+C(i)^TC(i) & X(i)B(i) \\ B(i)^TX(i) & -1 \end{bmatrix}\leq 0, \tag{4.23}$$

which yields $Q(i)\leq 0$ by defining $P_t(i):=X(i)$ and $P_s(i):=I$ in (4.17). Therefore, it can be concluded that $\Delta V(t,i)=\begin{bmatrix}x_t\\x_s\end{bmatrix}^T Q(i)\begin{bmatrix}x_t\\x_s\end{bmatrix}\leq 0$. □

The following Theorem provides sufficient conditions that ensure uniformly bounded semi-states based on the introduced Lemmas.

Theorem 4.2. *Given $(A(i),B(i),C(i))$ and $D(i)=0$ for $i\in\mathbb{Z}_+$, consider the spatially varying but temporally stationary 2-D Roesser model (4.15) with boundary conditions $x_s(\cdot,0)\in L_2\cap L_\infty$ and $x_t(0,\cdot)\in\ell_2$. If $\|G_i\|_\infty\le 1$ with $G_i(s):=C(i)(sI-A(i))^{-1}B(i)$ for all $i\in\mathbb{Z}_+$, and the following conditions hold on the model data:*

1. *$\sigma(A(i))\subset\mathbb{C}_-$ for all $i\in\mathbb{Z}_+$;*
2. *there exist constants $0<\lambda,k,\lambda_t,\tilde{C},\tilde{B}<\infty$ such that $\|e^{A(i)t}\|_{\infty\to\infty}\le ke^{-\lambda t}$, $\lambda_{max}(X(i))\le\lambda_t$ with $X(i)=Ric(A(i),B(i),C(i))\ge 0$ such that $\sigma(A(i)+B(i)B(i)^*X(i))\subset\mathbb{C}_-$, $\|B(i)\|_{\infty\to\infty}\le\tilde{B}$ and $\|C(i)\|_{\infty\to\infty}\le\tilde{C}$ for all $i\in\mathbb{Z}_+$.*

then the semi-states remain uniformly bounded in the sense that there exist constants $0<M_{ss}$, $M_{tt}<\infty$ such that $|x_s(t,i)|<M_{ss}$ and $|x_t(t,i)|<M_{tt}$ for all $t>0$ and $i\in\mathbb{Z}_+$.

Proof. Let $X_t:=\sup_i|x_t(0,i)|$, $M_t:=\sum_{k=0}^{i}x_t(0,k)^*x_t(0,k)$, $M_s:=\int_0^t x_s(\tau,0)^*x_s(\tau,0)d\tau$ which are bounded as $x_t(0,.)\in L_2\cap L_\infty$, $x_s(.,0)\in\ell_2$. Since the conditions of Lemma 4.4 hold, with $P_t(i)=X_t(i)$, $P_s=I$ and $V(t,i)=x_t(t,i)^TP_t(i)x_t(t,i)+x_s(t,i)^Tx_s(t,i)$ then $\Delta V(t,i)\le 0\ \forall i$, and we can apply result of Lemma 4.3. As such,

$$\begin{aligned}\int_0^t x_s^*(\tau,i)x_s(\tau,i)d\tau &\le \frac{1}{\lambda_{\min}(P_s)}\int_0^t V_s(\tau,i)d\tau\\ &\le \int_0^t V_s(\tau,0)d\tau+\sum_{k=0}^{i}V_t(0,k)\\ &= \int_0^t x_s^*(\tau,0)P_s(0)x_s(\tau,0)d\tau+\sum_{k=0}^{i}x_t^*(0,k)P_t(k)x_t(0,k)\\ &\le \lambda_{\max}(P_s(0))\|x_s(\cdot,0)\|_2^2+\sup_i\lambda_{\max}(P_t(i))\|x_t(0,\cdot)\|_2^2\\ &= \|x_s(\cdot,0)\|_2^2+\lambda_t\|x_t(0,\cdot)\|_2^2. \end{aligned}\tag{4.24}$$

Now noting that $\|x_s(\cdot,0)\|_2,\|x_t(0,\cdot)\|_2$ are bounded,

$$\begin{aligned}|x_t(t,i)|_\infty &= |x_{t0}(i)e^{A(i)t}+\int_0^t e^{A(i)(t-\tau)}B(i)x_s(\tau,i)d\tau|_\infty\\ &\le |x_{t0}(i)|_\infty ke^{-\lambda t}+k\sup_i\|B(i)\|_{\infty\to\infty}\int_0^t|e^{-\lambda(t-\tau)}||x_s(\tau,i)|_\infty d\tau\\ &\le X_tk+k\tilde{B}\Big(\int_0^t e^{-2\lambda(t-\tau)}d\tau\Big)^{\frac{1}{2}}\Big(\int_0^t|x_s(\tau,i)|_\infty^2d\tau\Big)^{\frac{1}{2}} \end{aligned}\tag{4.25}$$

$$
\begin{aligned}
&\leq X_t k + k\tilde{B}\left(\frac{1-e^{-2\lambda t}}{2\lambda}\right)^{\frac{1}{2}}\left(\int_0^t x_s(\tau,i)^* x_s(\tau,i)d\tau\right)^{\frac{1}{2}} \\
&\leq X_t k + k\tilde{B}\left(\frac{1}{2\lambda}\right)^{\frac{1}{2}}\sqrt{\|x_s(\tau,0)\|_2^2 + \lambda_t \|x_t(0,k)\|_2^2} \qquad (4.26) \\
&\leq X_t k + k\tilde{B}\left(\frac{1}{2\lambda}\right)^{\frac{1}{2}}\sqrt{M_s + \lambda_t M_t} \\
&:= M_{tt}, \forall t, i \qquad (4.27)
\end{aligned}
$$

where, inequality (4.25) follows from the Cauchy Schwartz inequality and (4.26) follows from (4.24). Hence, $\exists M_{tt}\ s.t.\ \|x_t(.,.)\|_\infty < M_{tt}$.

Moreover, according to (4.15), $x_s(t,i+1) = C(i)x_t(t,i)$ holds. Then, it follows that $\|x_s(t,i)\|_\infty \leq \sup_i \|C(i)\|_{\infty\to\infty}\|x_t(t,i-1)\|_\infty \leq \tilde{C}M_{tt} := M_{ss}$. Thus the semi-states are uniformly bounded in i,t as claimed. Note that semi-states grow linearly with $\|x_s(t,0)\|_2$ and $\|x_t(0,i)\|_2$. □

Similar result in the context of irrigation channel follows:

Corollary 4.3. *Consider an automated irrigation channel running under distributed distant- downstream control that can be modeled as (4.15) with an offtake at the bottom pool $d(t) \in L_2 \cap L_\infty$ and pools initial operating conditions $w = \{w(0), w(1), \cdots\} \in \ell_2$. Suppose the following conditions hold on the flow to flow interactions realisation:*

1. *the stable strictly proper flow-to-flow transfer function $T_{V_i \to U_i} = G_i(s)$ has a realisation $\{A(i), B(i), C(i), 0\}$ for all $i \in \mathbb{Z}_+$;*

2. *there exist constants $0 < \lambda, k, \lambda_t, \tilde{C}, \tilde{B} < \infty$ such that $\|e^{A(i)t}\|_{\infty\to\infty} \leq ke^{-\lambda t}$, $\lambda_{max}(X(i)) \leq \lambda_t$ with $X(i) = Ric(A(i), B(i), C(i)) \geq 0$ such that $\sigma(A(i) + B(i)B(i)^* X(i)) \subset \mathbb{C}_-$, $\|B(i)\|_{\infty\to\infty} \leq \tilde{B}$ and $\|C(i)\|_{\infty\to\infty} \leq \tilde{C}$ for all $i \in \mathbb{Z}_+$.*

If $\|G_i\|_\infty \leq 1$ for all $i \in \mathbb{Z}_+$, then the channel is L_2-to-L_∞ string-stable in the sense of Definition 4.2.

Proof. A direct application of Theorem 4.2 to an automated irrigation channel under distributed distant-downstream control architecture modeled as (4.15) gives the result. □

4.5.3 Simulation Examples

For the sake of comparison, in this section three automated channels are compared in terms of response and the analysis conditions. For simplicity, performance of a homogeneous channel is investigated. The first case is a homogeneous channel of pools automated with decentralised feedback distant-downstream control which yields

$$G_1(s) := T_{U_{i-1}\to U_i} = \frac{\frac{1}{\alpha s}K(s)}{1+\frac{1}{\alpha s}K(s)e^{-\tau s}}, \tag{4.28}$$

where $K = \frac{\kappa(1+\phi s)}{s(1+\rho s)}$. The channel under consideration has parameters as in Table 1.1. $G_1(s)$ contains an infinite dimensional delay component, which is approximated by a first order pade as in previous chapters. The transfer function $G_1(s)$ is stable but $\|G_1(.)\|_\infty = 1.8359$. Due to necessity of $\|G_1\|_\infty \leq 1$ for L_∞-to-L_∞ string-stability as stated in Chapter 2, we expect amplification of flow transient peaks toward upstream. Simulation of a channel of pools with the interaction transfer function $G_1(s)$ is shown in Fig. 4.3 where an offtake of 17m^3/min is drawn from the most downstream pool for 1000 mins. As can be seen we face amplification of transient flows towards upstream of the channel.

In another case, an automated channel under the proposed decentralised feedback with flow-to-reference feedforward distant-downstream control scheme in Chapter 2 is considered where the flow to flow interaction transfer function is a low pass filter with $T_c = 40$:

$$G_2(s) := T_{U_{i-1}\to U_i} = \frac{1}{1+40s}, \tag{4.29}$$

which achieves L_∞-to-L_∞ string-stability due to $\|g_2\|_1 \leq 1$. As discussed, with this choice of $G_2(s)$, $\|g_2(.)\|_1 \leq 1 \to \|G_2(.)\|_\infty \leq 1$, which achieves L_∞-to-L_∞ string-stability or non-amplification of transient flows in response to a constant offtake changes. Simulation under same scenario is carried out for a channel of pools with interactions transfer functions equal to $G_2(s)$. The result is plotted in Fig. 4.4 where no amplification is observed as expected.

As an another case, consider the interactions transfer function to be

$$G_3(s) := T_{u_{i-1}\to u_i} = \frac{0.01}{s^2+1.48s+0.01}. \tag{4.30}$$

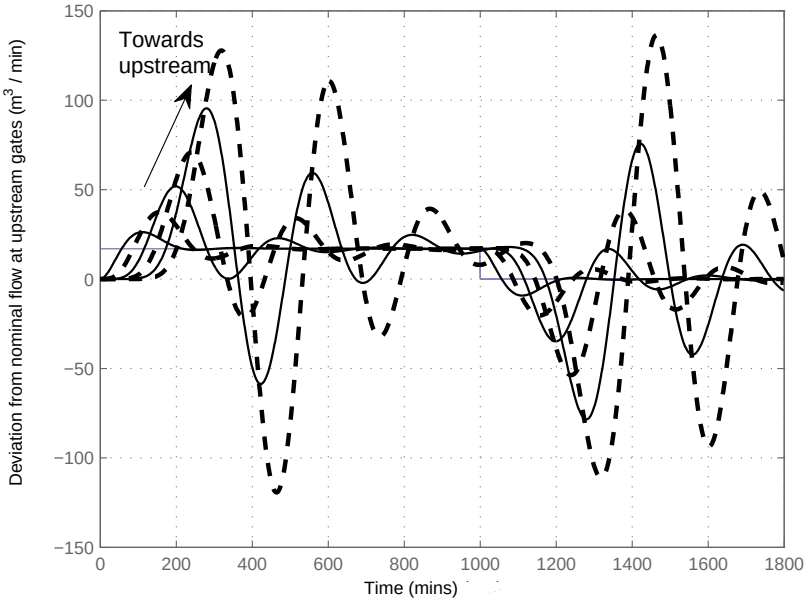

Figure 4.3: Response of a channel with $T_{U_{i-1}\to U_i} = G_1(s)$ to a pulse offtake at bottom pool.

In this case $G_3(s)$ is stable and $\|G_3(.)\|_\infty = 1$. Thus, L_2-to-L_∞ stability can be achieved by Lemma 4.3. The controlled flow responses to a 17m3/min step change in the outflow at the bottom pool are shown in Figures 4.5 and 4.6. It can be seen that, while there is amplification of flow peaks as these propagate along the bottom pools, this does not persist and the peak flows remain uniformly bounded along the channel as expected.

4.6 Summary

The L_2-to-L_∞ string-stability property is defined and analysed for a heterogeneous automated irrigation channel operating under distant-downstream control using 2-D modeling and analysis techniques. Lyapunov based stability analysis is carried out to develop a decentralised string-stability certificate leading to L_2-to-L_∞ string-stability in automated irrigation channels in response to bounded offtakes of finite duration drawn from a pool. The analysis conditions are derived with the aim to find systematic synthesis methods to bound water flows along an automated irrigation channel. It would be of interest to understand if the H_∞ norm condition is necessary for L_2-to-L_∞

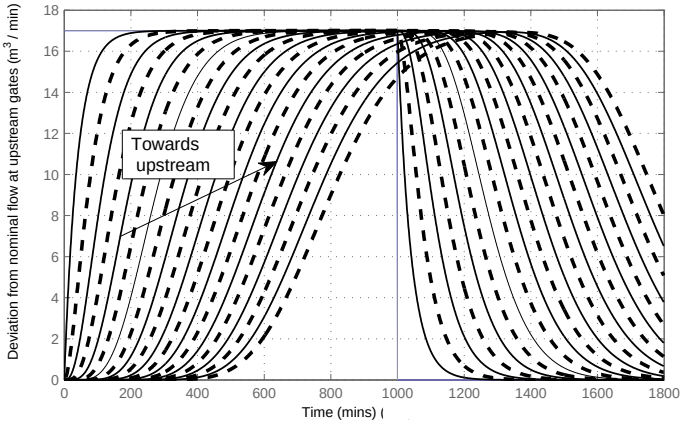

Figure 4.4: Response of a channel with $T_{U_{i-1}\to U_i} = G_2(s)$ to a pulse offtake at bottom pool.

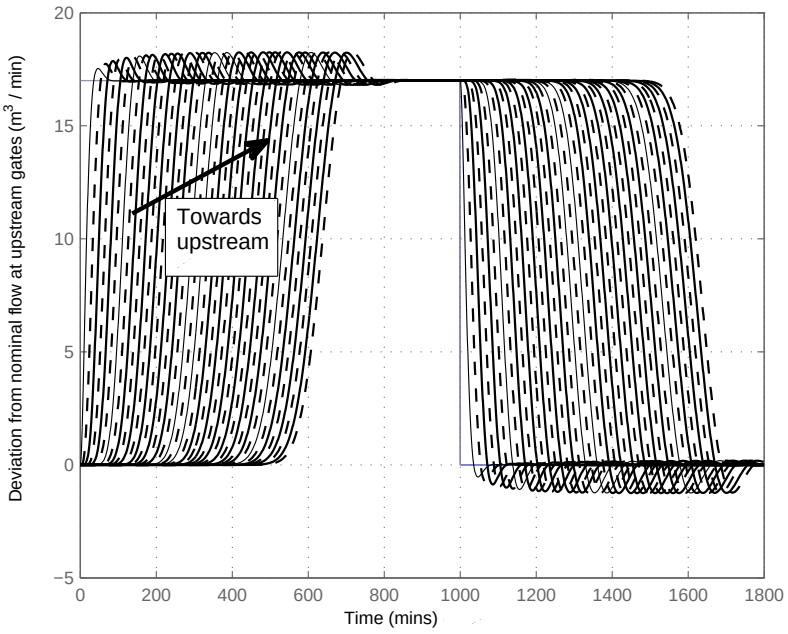

Figure 4.5: Response of a channel with $T_{U_{i-1}\to U_i} = G_3(s)$ to a pulse offtake at bottom pool.

stability of homogeneous cascades. The robustness properties of the presented flow-to-reference feedforward approach to satisfying the decentralised string-stability certificate within the context of irrigation channel control system design also requires further investigation.

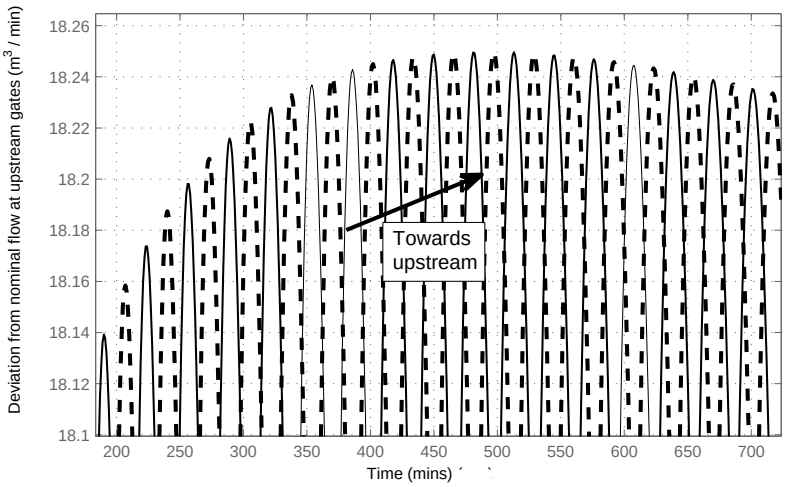

Figure 4.6: Response of a channel with $T_{U_{i-1}\to U_i} = G_3(s)$ to a pulse offtake at bottom pool, closer view.

This page intentionally left blank.

Chapter 5
Conclusion

5.1 Contributions

Aspects of automating the operation of large scale gravity-powered open-water irrigation channels are considered in this thesis. Automation of large scale irrigation channels (e.g. a cascade of pools) under the so-called distributed distant-downstream control architecture has lead to demand driven release of water from resources. This demand driven aspect in turn minimises the water wastage at the end of channels as apposed to conventional manual water delivery operation. Under distant-downstream automatic control, water levels along the channel are regulated as a measure of capacity to provide flow demand. Nevertheless, it has been shown that with the existing distributed distant-downstream control architectures the amplification of load-change induced adjustments of flow along a channel is inevitable. The consequences are the possibility of saturation of flow regulating structures, and poor quality of service to farmers.

In this thesis, such behaviour is avoided by achieving the so-called *string-stability* in terms of channel flows, i.e. by uniformly bounding upstream gate flow values both in time and spatial extent of a channel. To do so, mathematical tools are developed for analysing the propagation of flow adjustments defined by controllers to account for demand variations along an irrigation channel. In particular, the non-amplification of transient flows along the channel is guaranteed by an impulse response constraint on spatial flow interactions. Satisfying such decentralised 1-norm criteria is made possible by introduction of a new distributed distant-downstream control structure in Chapter 2. Namely, the novel *flow-to-reference feedforward scheme* which essentially adjusts water level set-points based on downstream flow demand. However, the price to pay is non-zero water-level errors which reflect the exploitation of the water storages along the channel.

Nonetheless, this is acceptable as long as water-levels remain within pre-specified operational bounds. In addition, a design trade-off has been identified between the magnitude of steady-state water-level errors and the rate of amplification of transient flows peaks.

It should be noted that, the impulse response constraint for string-stability needs time domain mathematical tools which are not suitable for systematic control design. Therefore, weaker decentralised criteria for string-stability of an automated irrigation channel under distributed distant-downstream control is introduced in Chapter 4, which implies existence of uniform bound on flow adjustments along the channel for all times, in response to load changes. This frequency domain constraint on the flow interactions along the channel is more suitable for control analysis and synthesis using existing mathematical tools. Such H_∞ norm constraint is admissible to the introduced distributed distant-downstream control structure and is designed in a decentralised fashion. Motivated by the two-dimensional nature of an automated irrigation channel where information flow is in time and spatial directions, a measure of string-stability is established using two-dimensional modeling and analysis of an automated channel.

Furthermore, a framework is established in Chapter 3 for robustness analysis of string-stability of the distributed distant-downstream control architecture satisfying the 1-norm constraint via linear matrix inequalities. Note that, application of sufficient LMI conditions for L_1 norm robustness analysis does not warrant robustness of the spatial stability of the decentralised feedback with flow-to-reference feedforward control scheme, e.g. to delay parameter uncertainty. Nevertheless, the obtained bound on the amplification rate of transient peaks due to considerable delay parameter uncertainty remains acceptable. Robustness analysis of the H_∞ norm-based criteria is part of the future work.

5.2 Future Research Directions

With the research carried out in this thesis, bounded flow values along an automated irrigation channel are achieved with the introduction of a feedforward path from downstream flow of a pool to adjust water level references while leading to water-level error offset at steady-state. Therefore, the question arises whether with extra information communicated from further downstream pools, zero steady-state water level errors are achievable. While such objective may not be feasible, a

comparison of these seems interesting.

Another approach to achieving zero steady-state water level errors may be to represent an automated channel with a cascade of subsystems where each subsystem is an interconnection of a number of automated pools in itself. Allowing internal pools to have the original decentralised controller and maintain zero steady-state water level errors while still the L_1-norm certificated is required for the cascade of subsystems can improve global flow amplification and water level tracking performance.

Other directions can be followed to remove level steady-state error such as switching between controllers, resetting integrators at required time instances or periodically. However, these methods bring nonlinearity to the system and more complicated tools are required for analysis.

In future, it may be possible to pursue discrete-discrete 2-D model analysis to derive conditions that are more consistent with characteristics of an automated irrigation channel. One other question to investigate is whether continuous-discrete 2-D modeling can be used for synthesis of a controller resulting in smaller steady-state water-level errors using the less conservative H_∞ norm certificate compared to the L_1 norm certificate.

Following the research direction of Chapter 4, it would be of interest to clarify whether H_∞ norm certificate is necessary for L_2-to-L_∞ string-stability of homogeneous automated channels. Moreover, robustness properties of the an L_2-to-L_∞ string-stable automated irrigation channel with a flow-to-reference feedforward scheme designed according to the H_∞ norm certificate can be investigated in future.

This page intentionally left blank.

Bibliography

[1] L. Soltanian, A. Neshastehriz, and M. Cantoni, "Validating an approach to distributed controller synthesis for irrigation channels via simulation with a PDE model," in *Proceedings of the Australian Control Conference*, 2011, pp. 475 – 480.

[2] L. Soltanian and M. Cantoni, "A 2-D Roesser model for automated irrigation channels and tools for practical stability and performance analysis," in *Proceedings of the Australian Control Conference*, 2012, pp. 48–53.

[3] ——, "Achieving string stability in irrigation channels under distributed distant-downstream control," in *Proceedings of the IEEE Conference on Decision and Control*, 2013.

[4] ——, "Robustness analysis of a nominally string-stable irrigation channel control system," in *the 21st International Symposium on Mathematical Theory of Networks and Systems*.

[5] B. Schultz, C. Thatte, and V. Labhsetwar, "Irrigation and drainage. Main contributors to global food production," *Irrigation and Drainage*, vol. 54, no. 3, pp. 263–278, 2005.

[6] ——, "The united nations world water development report 4: Managing water under uncertainty and risk: Executive summary." *UNESCO*, 2012. [Online]. Available: http://unesdoc.unesco.org/images/0021/002171/217175e.pdf

[7] X. Litrico and V. Fromion, *Modeling and control of hydrosystems*. Springer, 2009.

[8] M. E. Jensen, "Design and operation of farm irrigation systems," *The American Society of Agricultural Engineers*, 1980.

[9] A. Clemmens and R. Strand, "Annual reprot of the U.S. water conservation laboratory: Irrigation canal automation," 2000. [Online]. Available: http://www.ars.usda.gov/SP2UserFiles/Place/53442000/AnnualReports/AnnualReport2000/2000WaterProjectManagement.pdf

[10] A. Clemmens and J. Replogle, "Control of irrigation canal networks," *Journal of Irrigation and Drainage Engineering*, vol. 115, no. 1, pp. 96–110, 1989.

[11] J. A. Cunge, F. M. Holly, and A. Verwey, *Practical Aspects of Computational River Hydraulics*. Pitman Advanced Publishing Program, 1980.

[12] M. H. Chaudhry, *Open-Channel Flow*. Prentice Hall, 1993.

[13] S. K. Ooi, M. Krutzen, and E. Weyer, "On physical and data driven modelling of irrigation channels," *Control Engineering Practice*, vol. 13, no. 4, pp. 461–471, 2005.

[14] W. Graf and M. Altinakar, *Fluvial Hydraulics: Flow and transport processes in channels of simple geometry*. John Wiley & Sons, 1998.

[15] A. O. Akan, *Open Channel Hydraulics*. Butterworth-Heinemann, 2011.

[16] E. Weyer, "System identification of an open water channel," *Control Engineering Practice*, vol. 9, no. 12, pp. 1289–1299, 2001.

[17] I. Mareels, E. Weyer, S. K. Ooi, M. Cantoni, Y. Li, and G. Nair, "Systems engineering for irrigation systems: Successes and challenges," *Annual Reviews in Control*, vol. 29, no. 2, pp. 191–204, 2005.

[18] P. Malaterre, "Control of irrigation canals: Why and how?" in *Numerical Modelling of Hydrodynamics for Water Resources: Proceedings of the Conference on Numerical Modelling of Hydrodynamic Systems (Zaragoza, Spain, 18-21 June 2007)*, 2007, p. 271.

[19] J. Schuurmans, O. H. Bosgra, and R. Brouwer, "Open-channel flow model approximation for controller design," *Applied mathematical modelling*, vol. 19, pp. 525–530, 1995.

[20] E. Weyer, "Decentralised PI control of an open water channel," in *Proceedings of the 15th IFAC world congress*, 2002.

[21] M. Cantoni, E. Weyer, Y. Li, S. Ooi, I. Mareels, and M. Ryan, "Control of large-scale irrigation networks," *Proceedings of the IEEE*, vol. 95, pp. 75–91, 2007.

[22] I. Mareels, E. Weyer, S. K. Ooi, M. Cantoni, Y. Li, and G. Nair, "System engineering for irrigation: Successes and challenges," *Annual Reviews in Control*, vol. 29, no. 2, pp. 191–204, 2005.

[23] M. Mesarovic, D. Macko, and Y. Takahara, "Theory of hierarchical, multilevel systems," *New York, London*, 1970.

[24] S. Skogestad, "Control structure design for complete chemical plants," *Computers & Chemical Engineering*, vol. 28, no. 1, pp. 219–234, 2004.

[25] Y. Li, M. Cantoni, and E. Weyer, "Design of a centralized controller for an irrigation channel using H_∞ loop-shaping," in *Proceedings of UKACC Control Conference*, vol. 11, no. 1, 2004, p. 7.

[26] J. M. Reddy, "Design of global control algorithm for irrigation canals," *Journal of Hydraulic Engineering*, vol. 122, no. 9, pp. 503–511, 1996.

[27] Y. Li, "Robust control of open water channels," Ph.D. dissertation, University of Melbourne, Department of Electrical and Electronic Engineering, 2006.

[28] E. Weyer, "LQ control of an irrigation channel," in *Proceedings of 42nd IEEE Conference on Decision and Control*, vol. 1, 2003, pp. 750–755.

[29] A. Garcia, M. Hubbard, and J. J. de Vries, "Open channel transient flow control by discrete time LQR methods," *Automatica*, vol. 28, no. 2, pp. 255–264, 1992.

[30] P. O. Malaterre, "PILOTE: Linear quadratic optimal controller for irrigation canal," *Journal of Irrigation and Drainage Engineering*, vol. 124, pp. 187–194, 1998.

[31] A. Clemmens and J. Schuurmans, "Simple optimal downstream feedback canal controllers: Theory," *Journal of Irrigation and Drainage Engineering*, vol. 130, no. 1, pp. 26–34, 2004.

[32] X. Litrico and V. Fromion, "H_∞ control of an irrigation canal pool with a mixed control politics," *Control Systems Technology, IEEE Transactions on*, vol. 14, no. 1, pp. 99–111, 2006.

[33] ——, "Advanced control politics and optimal performance for an irrigation canal," in *Proceedings of the 2003 European Control Conference*, 2003.

[34] ——, "Tuning of robust distant downstream PI controllers for an irrigation canal pool (i): Theory," *Journal of irrigation and drainage engineering*, vol. 132, no. 4, pp. 359–368, 2006.

[35] O. Balogun, M. Hubbard, and J. DeVries, "Automatic control of canal flow using linear quadratic regulator theory," *Journal of Hydraulic Engineering*, vol. 114, no. 1, pp. 75–102, 1988.

[36] B. Rasof, "The initial-and final-value theorems in laplace transform theory," *Journal of the Franklin Institute*, vol. 274, no. 3, pp. 165–177, 1962.

[37] D. Youla, J. Bongiorno Jr, and C. Lu, "Single-loop feedback-stabilization of linear multivariable dynamical plants," *Automatica*, vol. 10, no. 2, pp. 159–173, 1974.

[38] K. Zhou, J. C. Doyle, K. Glover *et al.*, *Robust and optimal control*. Prentice Hall New Jersey, 1996, vol. 272.

[39] Y. Li, M. Cantoni, and E. Weyer, "On water-level error propagation in controlled irrigation channels," in *Proceedings of the Joint 44th IEEE Conference on Decision and Control and European Control Conference*, 2005, pp. 2101–2106.

[40] P. Seiler, A. Pant, and K. Hedrick, "Disturbance propagation in vehicle strings," *IEEE Transactions on Automatic Control*, vol. 49, no. 10, pp. 1835–1841, 2004.

[41] H. R. Middleton and J. H. Braslavsky, "String instability in classes of linear time invariant formation control with limited communication range," *IEEE Transactions on Automatic Control*, vol. 55, no. 7, pp. 1519–1530, 2010.

[42] P. Barooah and J. P. Hespanha, "Error amplification and disturbance propagation in vehicle strings with decentralized linear control," in *Proceedings of the 44th IEEE Conference on Decision and Control and European Control Conference*, 2005, pp. 4964–4969.

[43] J. Schuurmans, A. Hof, S. Dijkstra, O. Bosgra, and R. Brouwer, "Simple water level controller for irrigation and drainage canals," *Journal of irrigation and drainage engineering*, vol. 125, no. 4, pp. 189–195, 1999.

[44] D. McFarlane and K. Glover, "A loop-shaping design procedure using H_∞ synthesis," *Automatic Control, IEEE Transactions on*, vol. 37, no. 6, pp. 759–769, 1992.

[45] Y. Li and M. Cantoni, "Distributed controller design for open water channels," in *Proceedings of the 17th IFAC World congress*, 2008, pp. 10 033–10 038.

[46] C. Langbort, R. S. Chandra, and R. D'Andrea, "Distributed control design for systems interconnected over an arbitrary graph," *Automatic Control, IEEE Transactions on*, vol. 49, no. 9, pp. 1502–1519, 2004.

[47] S. Darbha, J. K. Hedrick, and P. A. Ioannou, "A comparison of spacing and headway control laws for automatically controlled vehicles," *Vehicle Systems Dynamic*, vol. 23, no. 1, pp. 597–625, 1994.

[48] S. Klinge and R. H. Middleton, "Time headway requirements for string stability of homogeneous linear unidirectionally connected systems," *in Joint 48th IEEE Conference on Decision and Control and 28th Chinese Control Conference*, pp. 1992–1997, December 2009.

[49] M. Sebek and Z. Hurak, "2-D polynomial approach to control of leader following vehicular platoons," *The 18th IFAC World Congress*, pp. 6017–6022, August 28 - September 2 2011.

[50] M. Kearney and M. Cantoni, "MPC-based reference management for automated irrigation channels," *in Proceedings of the Australian Control Conference*, Nov 2012.

[51] J. C. Doyle, B. A. Francis, and A. R. Tannenbaum, *Feedback Control Theory*. Dover Publications, 1992.

[52] D. Swaroop and J. K. Hedrick, "String stability of interconnected systems," *IEEE Transactions on Automatic Control*, vol. 41, pp. 349 – 357, 1996.

[53] S. Klinge and R. H. Middleton, "String stability analysis of homogeneous linear unidirectionally connected systems with nonzero initial conditions," *Proceedings of Joint 48th IEEE Conference on Decision and Control and 28th Chinese Control Conference*, pp. 17–22, 2009.

[54] P. A. Ioannou and C. C. Chien, "Autonomous intelligent cruise control," *IEEE Transactions on Vehicular Technology*, vol. 42, no. 4, pp. 657–672, 1993.

[55] J. Eyre, D. Yanakiec, and I. Kanellakopoulos, "A simplified framework for string stability analysis of automated vehicles," *Vehicle System Dynamics*, vol. 30, pp. 375–405, 1998.

[56] L. A. Weitz, "Investigating String Stability of a Time-History Control Law For Interval Management," *Transportation Research Part C: Emerging Technologies*, vol. 33, pp. 257–271, 2011.

[57] X. Y. Huang, N.-N. Y., and H.-F. G., "An H_∞ control method of the bullwhip effect for a class of supply chain system," *International Journal of Production Research*, vol. 45, pp. 207–226, 2007.

[58] S. Disneya, D. Towilla, and W. Velde, "Variance amplification and the golden ratio in production and inventory control," *International Journal of Production Economics*, vol. 90, pp. 259–309, 2004.

[59] W. Levine and M. Athans, "On the optimal error regulation of a string of moving vehicles," *IEEE Transactions on Automatic Control*, vol. 11, pp. 355 – 361, 1966.

[60] K. Chu, "Decentralized control of high-speed vehicular strings," *Transportation Science*, vol. 8, pp. 361 – 384, 1974.

[61] Y. Li and B. De Schutter, "Offtake feedforward compensator design for an irrigation channel with distributed control," in *Proceedings of American Control Conference (ACC), 2010*, 2010, pp. 3747–3752.

[62] Y. Li and D. S. Bart, "Control of a string of identical pools using non-identical feedback controllers," *IEEE Transactions on Control Systems Technology*, vol. 20, pp. 1638–1646, 2012.

[63] J. K. Hedrick, D. McMahon, V. Narendran, and D. Swaroop, "Longitudinal vehicle controller design for IVHS systems," in *Proceedings of American Control Conference*, 1991, pp. 3107–3112.

[64] L. Peppard, "String stability of relative-motion PID vehicle control systems," *IEEE Transactions on Automatic Control*, vol. 19, pp. 579–581, 1974.

[65] D. V. A. H. G. Swaroop, J. K. Hedrick, C. C. Chien, and P. Ioannou, "A comparision of spacing and headway control laws for automatically controlled vehicles," *Vehicle System Dynamics*, vol. 23, pp. 597–625, 1994.

[66] S. Klinge and R. H. Middleton, "Time headway requirements for string stability of homogeneous linear unidirectionally connected systems," in *Proceedings of Joint 48th IEEE Conference on Decision and Control and 28th Chinese Control Conference*, 2009, pp. 1992–1997.

[67] M. E. Khatir and E. J. Davison, "Decentralized control of a large platoon of vehicles using non-identical controllers," in *Proceedings of the American Control Conference*, vol. 3, 2004, pp. 2769–2776.

[68] S. Sheikholeslam and C. A. Desoer, "Longitudinal control of a platoon of vehicles," in *Proceedings of American Control Conference, 1990*, 1990, pp. 291–296.

[69] J. Dejonckheere, S. M. Disney, M. R. Lambrecht, and D. R. Towill, "Measuring and avoiding the bullwhip effect: A control theoretic approach," *European Journal of Operational Research*, vol. 147, pp. 567–590, 2003.

[70] I. Lestas and G. Vinnicombe, "Scalability in heterogeneous vehicle platoons," in *Proceedings of American Control Conference*, 2007, pp. 4678 – 4683.

[71] E. Shaw and J. K. Hedrick, "String stability analysis for heterogenous vehicle strings," in *Proceedings of American Control Conference*, 2007, pp. 3118 – 3125.

[72] W. C. Scherer and S. Weiland, *Linear Matrix Inequalities in Control*. Lecture Notes, Dutch Institute for Systems and Control, Delft, The Netherlands., 2004.

[73] C. Scherer, P. Gahinet, and M. Chilali, "Multiobjective output-feedback control via LMI optimization," *IEEE Transactions on Automatic Control*, vol. 42, no. 7, pp. 896–911, 1997.

[74] W. C. Scherer, in *A Full Block S-Procedure with Applications*, 1997, pp. 2602–2607.

[75] ——, "Robust mixed control and LPV control with full block scaling," *Advances in LMI Methods in Control, SIAM*, 2000.

[76] S. P. Boyd, L. El Ghaoui, E. Feron, and V. Balakrishnan, *Linear matrix inequalities in system and control theory*. SIAM, 1994, vol. 15.

[77] H. Tokunaga, T. Iwasaki, and S. Hara, "Multi-objective robust control with transient specifications," in *Proceedings of the 35th IEEE Conference on Decision and Control*, vol. 3, 1996, pp. 3482–3483.

[78] S. Knorn, "A two-dimensional systems stability analysis of vehicle platoons," Ph.D. dissertation, National University of Ireland, 2013.

[79] S. Knorn and R. H. Middleton, "Stability of two-dimensional linear systems with singularities on the stability boundary using LMIs," *IEEE Transactions on Automatic Control*, vol. 58, pp. 2579 – 2590, 2013.

[80] D. Goodman, "Some stability properties of two-dimensional linear shift-invariant digital filters," *IEEE Transactions on Circuits and Systems*, vol. 24, no. 4, pp. 201–208, 1977.

[81] E. I. Jury, "Stability of multidimensional scalar and matrix polynomials," *Proceedings of the IEEE*, vol. 66, no. 9, pp. 1018–1047, 1978.

[82] M. Strintzis, "BIBO stability of multidimensional filters with rational spectra," *IEEE Transactions on Acoustics, Speech and Signal Processing*, vol. 25, no. 6, pp. 549–553, 1977.

[83] P. Agothklis and L. Bruton, "Practical-BIBO stability of n dimensional discrete systems," *IEE Proceedings on Electronic Circuits and Systems*, vol. 130, pp. 236–242, 1983.

[84] P. Dabkowski, K. Galkowski, E. Rogers, and A. Kummert, "Strong practical stability and stabilization of discrete linear repetitive processes," *Multidimensional Systems an Signal Processing*, vol. 20, pp. 311–331, 2009.

[85] L. Xu, O. Saito, and K. Abe, "Practical internal stability of n-D discrete dystems," *IEEE Transactions on Automatic Control*, vol. 41, pp. 756–761, 1996.

[86] C. Du and L. Xie, *H_∞ Control and Filtering of Two-Dimensional Systems*. Springer-Verlag, 2002.

[87] P. Dabkowski, K. Galkowski, O. Bachelier, E. Rogers, and J. Lam, "A new approach to strong practical stability and stabilization of discrete linear repetitive processes," in *Proceedings of the 19th International Symposium on Mathematical Theory of Networks and Systems–MTNS*, vol. 5, no. 9, 2010.

[88] P. Dabkowski, K. Galkowski, O. Bachelier, and E. Rogers, "Control of discrete linear repetitive processes using strong practical stability and H_∞ disturbance attenuation," *Systems & Control Letters*, vol. 61, no. 12, pp. 1138–1144, 2012.

[89] E. Rogers, K. Galkowski, and D. H. Owens, *Control systems theory and applications for linear repetitive processes*. Springer, 2007, vol. 349.

[90] R. P. Roesser, "A discrete state-space model for linear image processing," *IEEE Transactions on Automatic Control*, vol. 20, no. 1, pp. 1–10, 1975.

[91] E. Fornasini and G. Marchesini, "State-space realization theory of two-dimensional filters," *IEEE Transactions on Automatic Control*, vol. 21, no. 4, pp. 484–491, 1975.

[92] ——, "Algebraic realization theory of two dimensional filters," *Lecture Notes in Economics and Mathematical Systems, New York, Springer Verlag*, vol. 111, pp. 64–82, 1975.

[93] B. Sumanasena and P. Bauer, "A roesser model based multidimensional systems approach for grid sensor networks," in *Proceedings of Conference on Signals, Systems and Computers (ASILOMAR)*, 2010, pp. 2151–2155.

[94] W. Marszalek, "Two-dimensional state-space discrete models for hyperbolic partial differential equations," *Applied Mathematical Modelling*, vol. 8, pp. 271–295, 1984.

[95] K. Galkowski, E. Rogers, W. Paszke, and D. H. Owens, "Linear repetitive process control theory applied to a physical example," *Applied Mathematics and Computer Science*, vol. 13, no. 1, pp. 87–99, 2003.

[96] Y. Xiao, "Stability test for 2-D continuous-discrete systems," in *Proceedings of the IEEE Conference on Decision and Control*, Dec 2001, pp. 3649–3654.

[97] Agathoklis, "The lyapunov equation for n-dimensional discrete systems," *IEEE Transactions on Circuits And Systems*, vol. 35, no. 4, pp. 448 – 451, 1988.

[98] B. Anderson, P. Agathoklis, E. Jury, and M. Mansour, "Stability and the matrix lyapunov equation for discrete 2-dimensional systems," *Circuits and Systems, IEEE Transactions on*, vol. 33, no. 3, pp. 261–267, 1986.